Fall 11-15-2016

Plant-biocrust interactions mediated by the fungal loop

Eva Dettweiler-Robinson
University of New Mexico

Eva Dettweiler-Robinson
Candidate

Department of Biology
Department

This dissertation is approved, and it is acceptable in quality and form for publication:

Approved by the Dissertation Committee:

Jennifer A. Rudgers, Co- Chairperson

Robert L. Sinsabaugh, Co- Chairperson

D. Lee Taylor

Matthew Bowker

PLANT-BIOCRUST INTERACTIONS MEDIATED BY THE FUNGAL LOOP

By

EVA DETTWEILER-ROBINSON

Bachelor of Arts, Biology, Colgate University, 2005

Master of Science, College of Forest Resources, University of Washington, 2011

DISSERTATION

Submitted in Partial Fulfillment of the
Requirements for the Degree of
Doctor of Philosophy in Biology
The University of New Mexico
Albuquerque, New Mexico

November, 2015

ACKNOWLEDGEMENTS

I acknowledge my co-advisors, Dr. Jenn Rudgers and Dr. Bob Sinsabaugh for pushing me to think critically, constantly seek to improve, and see past my mistakes to what I can meaningfully contribute. I acknowledge my committee members Dr. Lee Taylor and Dr. Matt Bowker for invaluable feedback on this manuscript and many other projects. I appreciate many members of the faculty at University of New Mexico, especially Dr. Marcy Litvak, Dr. Felisa Smith, Dr. Seth Newsome, Dr. Blair Wolf, Dr. Ken Whitney, Dr. Dave Hanson, Dr. Scott Collins, and many others. I appreciate the Rudgers-Whitney and Sinsabaugh lab members, the Center for Stable Isotopes, the Fungal Ecology group, and the STEM-Gateway redesign team. I appreciate financial support for PiBBs, UNM Biology Department, Biology Graduate Student Association, the Sevilleta LTER fellowship, the CSI pilot grant program, the NSF Doctoral Dissertation Improvement Grant program.

I appreciate Ernie Polansky for getting me interested in science in 10th grade by having the nerve to give me a B on a mid-semester report, and then opening up the world once I was ready to see it. I appreciate my parents and sister for emotional support and unpaid labor. I appreciate my partner Aaron for feeding me, laughing with me, and letting me be a little nuts. I appreciate Grace for being silly, elaborately over-dressed, and facing tough questions together. Gina sent me coffee and photos of her beautiful children to keep me uplifted. Karles and Sabrina helped with field work and I can't say for sure, but maybe it contributed to them eventually getting married. And you can't beat the Mediocre Jazz Band and Sweet Jubilee for having a creative outlet that also can give excellent law advice or poster editing. Thank you all so much.

PLANT-BIOCRUST INTERACTIONS MEDIATED BY THE FUNGAL LOOP

by
Eva Dettweiler-Robinson

Bachelor of Arts, Biology, Colgate University, 2005

Master of Science, College of Forest Resources, University of Washington, 2011

Doctor of Philosophy in Biology, University of New Mexico, 2016

ABSTRACT

Plant-microbial interactions influence biogeochemical cycles. Plants and biological soil crusts are primary producers in drylands. Biocrusts include cyanobacteria, lichens, mosses, algae, fungi, bacteria, and archaea on the soil surface, some of which fix atmospheric nitrogen. I investigated controls on biocrust carbon fluxes and their contribution to ecosystem fluxes, the incorporation of plant-derived carbon into biocrusts, and the role of soil fungi in promoting performance of plants and biocrusts. Biocrusts responded to temperature and moisture differently by biome. Biocrusts in grasslands/shrublands contributed >25% of total summertime ecosystem respiration, but biocrusts in savannas/woodlands contributed <1%. Biocrusts contributed <2% to GPP in any biome. To augment their native photosynthesis, biocrusts may include 16% plant-derived carbon. Fungal connections improved plant and biocrust performance and reduced differences in the CN ratio between organisms compared to when connections were impeded. Investigation of interactions among biocrusts, plants, and fungi has improved understanding of resource cycling in drylands.

TABLE OF CONTENTS

Chapter 1: Biocrust contribution to ecosystem respiration exceeds contribution to gross primary production and varies by biome

Eva Dettweiler-Robinson[1], Jenn Rudgers[1], Robert Sinsabaugh[1], Michelle Nuanez[1], Marcy E. Litvak[1]

1. Department of Biology, MSC03 2020, 1 University of New Mexico, Albuquerque, NM 87131-0001

Abstract

Understanding organismal contributions to carbon fluxes enables accurate forecasts for future emission scenarios. In drylands, biological soil crusts (biocrusts) on the soil surface may be active under different climatic conditions than vascular plants and thus have variable contribution to ecosystem carbon fluxes through time. We quantified biocrust fluxes from dryland biomes (grassland, shrubland, savanna, woodland) across summer soil moisture and temperature ranges. We used biocrust cover and meteorological data to estimate the contribution of biocrusts to soil and ecosystem carbon flux measured by eddy covariance. The effects of moisture and temperature on biocrust fluxes and the magnitude of their contribution to ecosystem fluxes differed by biome. Grassland and shrubland biocrust net carbon release peaked at intermediate temperatures and dry-moderate moistures, but savanna and woodland biocrust net release increased to a higher magnitude with warmer summertime temperatures, suggesting they are more sensitive to future warming. Predicted daily biocrust contribution to summer ecosystem respiration was lowest in the woodland (<1%) and highest in the grassland (26%). Biocrust gross photosynthesis was highest at warm, high soil moisture conditions across biomes, but all biocrusts contributed < 2% to daily gross primary productivity. Woodland

and savanna biocrust contribution to gross primary productivity is relatively unresponsive to change in moisture and temperature, but shrubland and grassland contributions vary with soil moisture. Thus, regional differences in biocrust type and cover should be included to predict biocrust contribution to global carbon flux.

Introduction

Dryland ecosystems play a dominant role in global trends and inter-annual variability in atmospheric carbon dioxide (Poulter and others 2014, Ahlstrom and others 2015). Quantifying the carbon stocks and fluxes in these biomes, and determining the processes that regulate them, are crucial to understanding these biomes which cover 45% of the Earth's terrestrial area (Prăvălie 2016). Because drylands are characterized by patchy resources and temporal variability in climate, it is important to understand the role they will play in shaping global carbon source/sink dynamics in the future as climate fluctuates (Frank et al. 2015). Ecosystem carbon budgets integrate photosynthesis and respiration processes and are driven by temperature, moisture, length of the growing season, and belowground resources (Raich and Schlessinger 1992, Friedlingstein and others 2006). However, species and functional group compositions affect the responses to abiotic conditions (Chapin 2003, Lavorel 2013). Quantifying the conditions that affect the size of the contribution of each species or functional group to the ecosystem carbon budget may improve estimates of carbon budgets under future biotic or abiotic conditions.

Biological soil crusts (biocrusts) are important to the function of drylands (Belnap and others 2016). Biocrust communities are ubiquitous components of dryland biomes and consist of primary producers (cyanobacteria, mosses, lichens, algae) and heterotrophs

(fungi, bacteria) living in the top ~5 cm of the soil surface. Current estimates suggest that dryland biocrusts can contribute 1-10 g C m^{-2} y^{-1} (Porada and others 2013), which approximates 1% of the global terrestrial NPP (Elbert and others 2012). However, uncertainties around this number are large due to a lack of direct measurements across a range of biocrust communities and dryland biomes that vary in plant biomass and biocrust cover. Biocrust composition varies among biomes, generally driven by climate (Belnap and others 2016), and these compositional differences contribute to functional differences in carbon cycling at local and even regional scales. For example, gross photosynthesis by light cyanobacterial biocrust is lower than by dark, complex moss/lichen/cyanobacterial biocrusts (Grote and others 2010, Housman and others 2006). Because few multi-biome comparisons using identical methods have been conducted, there is currently poor resolution of biocrust contributions to ecosystem fluxes for different biomes. With changing climate predicted to harm some biocrust communities (Maestre and others 2013, Ferrenberg and others 2015), regional-scale resolution will improve predictions of how changing conditions may influence biocrust carbon exchanges.

Given that temperatures are rising in the western United States (Gutzler and Robbins 2010) and globally, with associated effects on evaporative demand and soil moisture (Cook and others 2014), understanding biocrust carbon flux responses to both moisture and temperature (Grote and others 2010; Maestre and others 2013) will enable more accurate predictions of dryland carbon dynamics under future climate conditions. Many biocrusts show highest carbon uptake at intermediate soil moisture values because low soil moisture does not provide enough time and resources for net carbon uptake

(Cable and Huxman 2004), and high soil moisture may block the diffusion of CO_2 to the soil and reduce photosynthesis (Brostoff and others 2005, Grote and others 2010, Su and others 2012a). Soil moisture is supplied by precipitation, which varies in event size and frequency. In the Chihuahuan desert ecoregion, the precipitation regime is composed of small, frequent rain events, but most of the total precipitation occurs in rare, large events (Petrie and others 2014). If the dominant vegetation cannot respond to small magnitude precipitation events that provide low soil moisture but biocrusts can respond (respire) as soon as they are first wetted, then biocrusts may contribute relatively more to overall ecosystem scale fluxes, specifically respiration, following smaller precipitation inputs than larger ones that provide high soil moisture (Cable and Huxman 2004). Temperature also affects biocrust carbon fluxes because biocrusts have an optimum temperature range for performance (Lange and others 1998, Su and others 2012b), and their respiration generally increases with temperature (Brostoff and others 2005, Housman and others 2006, Grote and others 2010).

In this study, we quantified biocrust carbon fluxes from four dryland biomes across an elevational gradient in central New Mexico and used regression-based modelling to scale up to the ecosystem. We explored 1) the difference in biocrust communities by biome, 2) the relative importance of crust sensitivity to moisture and temperature and whether it is consistent across biomes, 3) the contributions of mature biocrusts to carbon flux in each biome, and 4) the relative importance of moisture and temperature in driving the contribution to total ecosystem fluxes.

Methods

Study Sites. This study was conducted at four biomes in the New Mexico

Elevation Gradient network (Ch. 1 Table 1). The piñon-juniper woodland is dominated by piñon pine (*Pinus edulis* [Engelm]) and one-seed juniper (*Juniperus monosperma* [(Engelm) Sarg]) trees with the C_4 bunchgrass blue grama (*Bouteloua gracilis* [(Willd. ex Kunth) Lag. ex Griffiths]) and biocrusts of lichens (*Collema* spp., *Placidium* sp.), patches of mosses (*Pterygoneurum sp., Bryum* sp.), and cyanobacteria (*Nostoc* sp*., Microcoleus* sp.). The juniper savanna consists of open *J. monosperma* tree canopy with the C_4 bunchgrass black grama (*Bouteloua eriopoda* [(Torr.) Torr.]) dominating the understory. The shrubland is dominated by the shrub creosote (*Larrea tridentata* [(DC.) Coville]) and *B. eriopoda.* Both the savanna and shrubland biomes have patches of cyanobacterial lichens (*Collema* spp.) with cyanobacterial biocrusts (*Microcoleus* sp*., Nostoc* sp.). Vegetation in the grassland is dominated by the C_4 bunchgrasses *B. eriopoda, B. gracilis*, dropseed (*Sporobolus* spp. [R. Br.]), James' galleta (*Pleuraphis jamesii* [Torr.]), and muhly (*Muhlenbergia* spp. [Schreb]) with light cyanobacteria biocrusts (*Microcoleus sp.*). The standing vegetation biomass is highest in the woodland and decreases to the grassland and shrubland (Anderson-Teixeira and others 2011). The savanna is subject to continued cattle grazing which has been shown to decrease the cover and biomass of biocrusts (Williams and others 2008). Disturbance by grazers may also affect the other biomes because there are antelope and oryx at the Sevilleta LTER, and cattle were present at the woodland in the past.

Biocrust type and cover. In each biome, three parallel 50 m transects were placed 15 m apart and were surveyed in October 2012. We recorded the length of the transect that was occupied by different morphogroups of biocrusts at each site. We distinguished between light cyanobacterial, dark cyanobacterial, cyanolichen, mixed lichen, and moss

biocrusts. Morphogroups allow rapid assessment and retain information about site integrity (Read and others 2014).

Biocrust sample collection. We subjectively selected the soil surface with the darkest, most diverse biocrusts in each biome (thus excluding moss-only patches). We moistened the surface with water, pressed a 55 mm-diameter × 12 mm depth petri dish into the biocrust, and removed it with a spatula. We collected 15 samples each from grassland and woodland, and 16 each from savanna and shrubland. Samples were transferred into a new dish such that they were upright and transported to the University of New Mexico where they were stored with ambient light (in window) at 20°C and watered to field capacity once per week.

Gas exchange measurements ex situ. Biocrust samples were pretreated in the 2.2m^3 growth chamber (Conviron, Winnipeg, Manitoba, Canada) at the set air temperature for 3d prior to gas exchange measurements, watered to field capacity each day, and were kept on a 13h light (~2000 μmol m^{-2} s^{-1} photosynthetically active radiation; PAR):11h dark regime, mimicking observed summer conditions. Previous work has found no photoinhibition of cyanobacterial biocrusts with high light intensity (Lange and others 1998) and we observed no light inhibition in a subsample of cyanolichen/lichen biocrusts (Ch. 1 Appendix 1). Humidity was kept at 30%, because average summertime humidity ranged from 30-39% across biomes. Because we sought to measure equilibrium responses rather than instantaneous responses to soil moisture, samples were watered to field capacity at least 1h before measurement to avoid recording the initial burst of respiration upon rewetting (Smith and Molesworth 1973, Cable and Huxman 2004) and to allow activation of the photosystems (Strong and others 2013, Wu

and others 2013). Thus, we may underestimate respiration during the first hour following a precipitation event when we scale up to the ecosystem level (below).

Flux measurements were recorded at up to three moisture values per set temperature, always at the same light level. Soil moisture was recorded as gravimetric water content (GWC), calculated as (weight wet – weight dry)/weight dry. GWC values ranged from air dry (0.012) to the maximum GWC value observed *in situ* in 2012 (0.23). Air temperatures were based on conditions recorded *in situ* from 2009-2011. Fluxes from all samples were measured at 18 C (the 25th percentile of the temperature range) 25 C (close to the mean daytime summer temperature), and 33 C (the 90th percentile of the temperature range). We measured more extensively at the upper range than the lower range because temperatures are expected to increase across these biomes with climate change. The chamber temperature at each set point varied ± 0.1°C s.e. Samples were rested at ambient conditions between set temperatures for >3 weeks (Ch. 1 Appendix 2) to reduce potential legacy effects of biocrusts acclimatizing to antecedent conditions (Hawkes and Keitt 2015).

Gas exchange measurements were made using a portable photosynthesis system (LiCor 6400, LI-COR Biosciences, Lincoln, NE) with a custom clear-top chamber (Barbour and others 2007). CO_2 concentration was fixed at 400 μmol mol^{-1} and flow was fixed at 500 μmol s^{-1}. Samples were allowed to acclimate in the chamber for up to 30 minutes in the light prior to measuring net soil exchange (NSE). A dark cloth was then placed over the chamber and samples were allowed to acclimate to record dark respiration for at least 15 min (DR) until values stabilized. After acclimation, gas exchange measurements were recorded every ten seconds for two minutes, then averaged.

Net uptake was recorded as negative numbers, while net release was recorded as positive numbers. Gross photosynthesis (GP) rates were calculated as NSE - DR.

Eddy flux, soil respiration, and meteorological data in situ. Ecosystem-scale carbon dioxide, water, and energy surface fluxes were measured at 10 Hz using a 3-axis sonic anemometer (CSAT-3, Campbell Scientific, Logan, UT, USA) with an Open Path CO_2/H_2O Gas Analyzer **(**LI-7500, LI-COR Biosciences). Net ecosystem exchange (NEE), ecosystem respiration (RE) and gross primary productivity (GPP) were calculated using methods in Lasslop and others (2010). Thirty minute fluxes were corrected for temperature and moisture variations and gaps were filled as in Anderson-Teixeira and others (2011).

Soil respiration (SR) was measured at the grassland and shrubland biomes. Soil CO_2 concentration were measured using CO_2 solid state sensors (CARBOCAP GMM 221 and GMM 222, Vaisala, Helsinki, Finland), placed in 3 pits at 5, 10, 20, and 50 cm depths. Soil temperature (T107, Campbell Scientific) and volumetric soil moisture (CS616, Campbell Scientific) was measured simultaneously in all pits at all depths. Sensors were installed similarly to Vargas and Allen (2008), using ¾ inch PVC housing and PVC caps sealed with a rubberized sealant to prevent interaction with above ground gasses. Soil CO_2 probes were additionally protected using semi-porous Teflon sleeves (200-07-S-2, International Polymer Engineering, Tempe, AZ, USA).

SR was temperature- and pressure corrected according to manufacturer guidelines. Data filtering and quality analysis was done using R (version 3.2.0, R core team 2015). SR data were smoothed using window size = 10 to maintain diurnal patterns (package RobFilter; Fried and others 2014), and gaps were filled using random forest

modeling (package missForest, Stekhoven 2013). This method has previously been used to fill environmental and flux data (Darrouzet-Nardi and others 2015), and is an effective and accurate imputation technique (Stekhoven and Buhlman 2011). SR data required 23% gap filling. We calculated SR from the soil CO_2 profiles in each pit using the flux gradient method (Vargas & Allen 2008; Vargas et al., 2010). The calculation of surface flux assumes constant production of CO_2 within the soil profile, as well as increasing CO_2 concentration with depth. This assumption was not always met, particularly during periods of rapid increase of CO_2 production, often following precipitation events, and these periods were removed.

Meteorological measurements at all biomes were recorded as 30 minute averages. Air temperature was measured with a temperature and relative humidity probe (HMP45C, Campbell Scientific). Soil moisture at the woodland biome was measured with time domain reflectometry probes (CS-610, Campbell Scientific) and at all other biomes with water content reflectometers (CS-615, Campbell Scientific). Photosynthetically active radiation at each tower site was measured with quantum sensors (Li-190SB, LI-COR Biosciences).

Analysis. All analyses were conducted in R (version 3.3.1; 2016-06-21; R Core Team 2016).

Characterization of biocrust community. We compared total cover across biomes with linear models. We used general linear mixed effect models (R package "nlme", Pinheiro and others 2016) to compare the morphogroup relative cover by site with morphogroup identity as a covariate and transect as a random effect. Post-hoc pairwise comparisons were conducted by comparing least squares means. We assessed

photosynthetic capacity by measuring chlorophyll content (Ch. 1 Appendix 3).

Effect of soil moisture and temperature on biocrust carbon fluxes. We used model selection (Burnham and Anderson 2002) to determine 1) if fluxes differ by biome 2) if temperature and moisture affect fluxes, or 3) if the effect of temperature and moisture are the same or differ by biome. Models for NSE, DR, and GP were run separately. The null model was the intercept-only model with all random effects included. The first candidate model tested for differences among biomes. The second candidate model addressed whether moisture and temperature affect biocrust carbon fluxes. The quadratic effects were included because biocrust fluxes have both moisture and temperature optima (Grote et al. 2010). The third candidate model included pairwise interactions of biome, soil moisture, and temperature linear and quadratic terms. We did not account for other potential forcing on carbon flux, such as wind speed, relative humidity, or short- and long-wave radiation (Porada and others 2013) which affect evaporation rate and thus affect soil available moisture. Moisture and temperature were converted to Z-scores to evaluate them on comparable scales. Sample nested within observation date was treated as a random effect to account for the order of observations. Quantile-quantile plots and histograms of the standardized residuals were visually inspected to assess that the models adequately met assumptions of homogeneity of variance and normality. *AICc* values were used to compare among the candidate models and marginal R^2 was used to assess the amount of variance explained by the fixed effects in each model compared to the null model (Nakagawa and Schielzeth 2013) using the MuMIn package (Bartoń 2015). Because we took a model selection approach, *p*-values of individual terms are not reported. A total of 223 values of NSE and GP and 227 values for DR were included in

model selection.

Controls on biocrust contribution to ecosystem and soil carbon fluxes. We ran the final models with unscaled variables to obtain coefficients in real units. To predict mature biocrust fluxes at the ecosystem scale, we applied the observed *in situ* microclimate data to our modeled *ex situ* response of carbon exchange to air temperature and soil moisture, and scaled the resulting fluxes by the cover of the mature morphotypes from each biome (Sancho and others 2016). When predicted values of DR or GP were the wrong sign, the value was set to zero.

To compare biocrust flux and ecosystem flux, we reduced the annual data to summer of 2012 (April 25-October 2; day of year 115-175) when the average air temperatures were between 18-33°C in all biomes. We excluded 30 minute intervals that were outside that temperature range and that were outside the soil moisture range 0.012 - 0.33 GWC. To ensure that conditions were relatively stable (not warming and becoming brighter in the morning or cooling and becoming darker in the evening), we used 30 minute intervals during the middle of the day for NEE and GPP (12:00 pm to 16:00 pm) when PAR > 1000 μmol m^{-2} s^{-1}. We used 30 minute intervals during the middle of the night for SR and RE (00:00 am to 04:00 am) when PAR < 1 μmol m^{-2} s^{-1} .

We averaged predicted NSE and observed NEE flux values and the proportional contribution of DR to RE, DR to SR, SR to RE, and GP to GPP by day.

We discovered which conditions drove the magnitude of contribution of the biocrusts to the ecosystem flux. We used model selection to assess if there were differences in contribution by biome, if temperature and moisture independently affected the contribution of biocrusts to ecosystem and soil fluxes, and if the effect of moisture

and temperature differed across biomes, as above. A total of 375 values for contribution to RE, 210 values for contribution to SR, and 565 values for contribution to GPP were included in model selection due to differences in number of days that fulfilled the abiotic requirements and missing flux tower data.

Results

Biocrust communities. Biomes differed in total biocrust relative cover and morphogroup composition (Ch. 1 Fig. 1). The shrubland had higher relative cover of biocrusts (>50%) than any other biome, and the grassland and woodland had similarly low relative cover, with ~10% cover ($F_{3,8}$ = 103.7, P < 0.001). The relative cover of morphotypes also differed by biomes (X^2 = 10.90, d.f. = 3, P = 0.01), and although the grassland and woodland did not differ statistically, the woodland had many more dark, complex, mature biocrust components than the grassland.

Abiotic controls on biocrust carbon flux. Biocrusts showed net carbon release under nearly all of the tested temperature and moisture combinations (Ch. 1 Fig. 2). Half of net carbon uptake values (NSE<0) occurred when GWC > 0.16 (Ch. 1 Appendix 4).

Biocrusts fluxes from different biomes responded divergently to soil moisture and air temperature (Ch. 1 Table 2, Ch. 1 Fig. 2, coefficients in Ch. 1 Appendix 4). All biocrusts showed less respiration or increased net uptake in cooler temperatures. Net soil respiration peaked at intermediate temperatures and low-moderate soil moistures in the shrubland and grassland, but net soil respiration at the savanna and woodland biomes peaked at the highest temperatures. Biocrusts at the higher elevation biomes may be acclimated to cooler temperatures because higher elevation biomes experience lower temperatures than the shrubland and grassland. The highest magnitude of dark respiration

was found at moderate soil moistures at the savanna, shrubland, and grassland biome, but the dark respiration of biocrusts at the woodland peaked at high soil moisture and temperature. The highest gross photosynthesis observed occurred in the woodland biome under warm, moist conditions, and high gross photosynthesis at both savanna and shrubland biomes occurred in moderate temperature, moist conditions. The grassland biocrusts took up less than 0.11 μmol CO_2 m^{-2} s^{-1} in any condition tested.

Controls on the contribution of biocrusts to ecosystem and carbon fluxes. We used the relative surface cover of the morphogroup used in the *ex situ* experiment to scale to the whole ecosystem thus we did not capture total biocrust contribution. Mixed lichen biocrusts at the woodland accounted for 1.1% ± 0.36 s.e. relative surface cover. The mature biocrusts from the savanna included cyanolichens with dark cyanobacteria and accounted for 1.7% ± 0.68 s.e. relative surface cover. The mature biocrusts from the shrubland were dark cyanobacteria with few cyanolichens and accounted for 2.6% ± 1.3 s.e. relative cover. Grassland biocrusts were light cyanobacterial biocrusts and accounted for 10.9% ± 0.93 s.e. relative cover.

No biocrusts from any biome were predicted to take up carbon (net soil exchange < 0) in any day during the summer months (Ch. 1 Fig. 3), however, there was net carbon uptake at the ecosystem scale for 57% of summer days in grassland, 80% of days in shrubland, 99% of days in savanna, and 94% of days in woodland. Variations in magnitude of net soil exchange tended to follow the warming and cooling trends (decreased uptake/higher respiration with warmer temperatures, increased uptake/lower respiration with cooler weather), similar to responses at the ecosystem scale as have been presented previously for these sites (Anderson-Teixeira and others 2011).

Biocrusts from different biomes varied in their predicted contribution to ecosystem respiration, soil respiration, and gross primary production (Ch. 1 Table 3, Ch. 1 Fig. 4, coefficients in Ch. 1 Appendix 5). Over summer 2012, biocrusts at the woodland and savanna were predicted to contribute very little to ecosystem respiration (woodland: 0.2% ± 0.03 s.e., savanna: 1.1% ± 0.05 s.e.), but biocrusts at grassland and shrubland were predicted to contribute >20% (grassland: 26.3% ± 2.0 s.e.; shrubland: 23.4% ± 2.6 s.e.). Both shrubland and grassland biocrusts contribute more to ecosystem respiration under dry conditions than intermediate conditions, and grassland contribution is high under high moisture conditions also, though none were observed in summer 2012.

Biocrusts, although only on the top few centimeters of soil, were major components of soil respiration at the shrubland and grassland. Biocrust dark respiration contributed 63.0% ± 2.2 s.e. of grassland soil respiration and 26.4% ± 1.4 s.e. of shrubland soil respiration. Biocrusts contribution generally increased with increasing temperature and moisture at both sites.

Little contribution of biocrust gross photosynthesis to gross primary productivity was predicted (grassland: 2.2% ± 0.40 s.e.; shrubland: 1.4% ± 0.21 s.e.; savanna: 0.03% ± 0.004 s.e.; woodland: 0.14% ± 0.03 s.e.). The grassland and shrubland biocrusts can potentially contribute considerably to carbon uptake under high soil moisture conditions, but these conditions were not observed in summer 2012.

Discussion

Our estimates suggest that biocrusts contribute little (< 2%) to ecosystem GPP at any site, similar to global estimates (Elbert and others 2012). Biocrusts contribute little to ecosystem respiration in biomes with high vegetation biomass, but contribute

considerably (>25%) in grassland and shrubland biomes, especially under dry conditions. By scaling up *ex situ* carbon flux responses of biocrusts to predict the contribution *in situ*, we isolated the activities of the biocrust communities from roots and deeper soil microbial communities, thus improving estimates of biocrust carbon exchanges across abiotic gradients. Regional values for biocrust fluxes are important for accurate large-scale predictions, as fluxes in the savanna and woodland were up to twice the rates of those in shrubland and grassland.

We found differential responses to temperature and moisture of biocrusts from different biomes. Composition of biocrusts may affect these responses. For example, the cyanobacteria at the Sevilleta include both *M. vaginatus* and *M. steenstrupii,* which differ in their responses to temperature (Garcia-Pichel and others 2013). Maestre and others (2013) found that well-developed biocrusts had higher carbon efflux with increased temperatures than light biocrusts, and Zhao and others (2014) found that well-developed biocrusts had higher carbon release than light biocrusts with small rain events. Zelikova and others (2012) found a decrease in photosynthetic capacity and shift from moss to cyanobacteria biocrusts with increased precipitation frequency. At our biomes, the darker, more complex biocrusts characteristic of higher elevations had higher magnitude responses to temperature and moisture than lighter, less complex cyanobacterial biocrusts, suggesting that changing climates may disproportionately affect the higher elevation biocrusts compared to the lower elevation biocrusts, depleting their carbon reserves and potentially changing biocrust composition.

Net flux in biocrusts across all of the biomes was dominated by respiration under most summertime moisture and temperature conditions. Heterotrophic organisms in the

biocrusts respire following even small pulses of water (Xu and others 2004). Additionally, the biocrusts were disturbed when samples were removed from the soil, which could drive high respiration rates (Feng and others 2014). However, because samples were equilibrated to the temperature and provided water for multiple days prior to measurement, the flush of respiration after the first wetting event did not likely account for the high respiration values observed throughout the experiment. To account for the observed, cumulative loss of carbon, we suggest that biocrusts may take up atmospheric carbon during different times of year. Winter or spring precipitation events may be more conducive to net uptake of atmospheric carbon in biocrusts (Darrouzet-Nardi and others 2015) when there is less evaporative demand. Additionally, biocrusts may use organic carbon sources. For example, Green and others (2008) demonstrated that carbon in the form of the amino acid glutamate can be incorporated into biocrusts, suggesting non-atmospheric carbon sources aid some biocrusts.

Both temperature and moisture were important controls on biocrust carbon fluxes and their contributions to ecosystem exchanges. Water is the controlling factor for processes in drylands (Barron-Gafford and others 2013, Chen and others 2016) but its influence is often mediated by other factors, such as temperature (Austin 2011). Reciprocally, biocrusts may be less responsive to temperature if there is insufficient water to activate their metabolism (Wilske and others 2008). This study does not address the precipitation regime (magnitude, frequency) but only the potential carbon flux at a given soil moisture (after the initial respiration). Across our biomes, NEE increased with temperatures greater than 15°C and decreased with soil moisture (Ch. 1 Fig. 3, Anderson-Teixeira and others 2011). However, biocrust carbon fluxes in our study show non-linear

NSE responses to temperature and moisture over the selected ranges, and thus, under some conditions, released carbon when the rest of the ecosystem was taking it up. In the grassland, the biocrusts respired when soil moisture was too low for plants to be active (Collins and others 2008). The shrubland and savanna had similar biocrust morphogroups, but perhaps because the shrubland has lower vegetation biomass, the shrubland biocrusts made a larger relative contribution to respiration. Using the predicted contributions across a range of temperature and moisture conditions, we can estimate the effect of biocrusts on carbon flux as the climate changes: the woodland and savanna biocrust contributions should be relatively robust to increases in temperature and changes in precipitation frequency, whereas shrubland and grassland may contribute more to RE as smaller rain events provide less soil moisture. Predictions of future fluxes would be improved by accounting for the influence of temperature and soil moisture on different communities of plants and biocrusts.

Acknowledgements

Funding for E.D.-R. provided by Sevilleta Long Term Ecological Research (LTER) Summer Fellowship. Funding to M.L provided by National Aeronautics and Space Administration (10-CARBON10-0118), National Science Foundation-LTER (DEB 0217774), and Department of Energy (SC#**:** DE-SC0008088). Austin Dillon assisted with field and lab work. Skyler Hackley and Jonathan Furst maintained eddy flux towers, and Tim Hilton and Greg Maurer processed the fluxes. The Sevilleta LTER and Fish and Wildlife Service, Leroy Humpreys, and Deer Canyon Preserve provided access to biomes.

References

Ahlstrom A, Raupach MR, Schurgers G, Smith B, Arneth A, Jung M, Reichstein M, Canadell JG, Friedlingstein P, Jain AK, Kato E, Poulter B, Sitch S, Stocker BD, Viovy N, Wang YP, Wiltshire A, Zaehle S, Zeng N. 2015. The dominant role of semi-arid ecosystems in the trend and variability of the land CO_2 sink. Science 348:895–9.

Anderson-Teixeira KJ, Delong JP, Fox AM, Brese DA., Litvak ME. 2011. Differential responses of production and respiration to temperature and moisture drive the carbon balance across a climatic gradient in New Mexico. Glob Chang Biol 17:410–24.

Austin AT. 2011. Has water limited our imagination for aridland biogeochemistry? Trends Ecol Evol 26:229–35.

Barbour MM, McDowell NG, Tcherkez G, Bickford CP, Hanson DT. 2007. A new measurement technique reveals rapid post-illumination changes in the carbon isotope composition of leaf-respired CO_2. Plant Cell Environ 30:469–82.

Barron-Gafford GA, Scott RL, Jenerette GD, Hamerlynck EP, Huxman TE. 2013. Landscape and environmental controls over leaf and ecosystem carbon dioxide fluxes under woody plant expansion. J Ecol 101:1471–83.

Bartoń K. 2015. Multi-Model Inference (MuMIn). https://cran.r-project.org/web/packages/MuMIn/MuMIn.pdf

Belnap J, Weber B, Büdel B. 2016. Biological soil crusts as an organizing principle in drylands. Weber B, Büdel B, Belnap J, editors. Biological soil crusts: an organizing principle in drylands. Switzerland: Springer International Publishing. p3–14.

Brostoff WN, Sharifi MR, Rundel PW. 2005. Photosynthesis of cryptobiotic soil crusts in a seasonally inundated system of pans and dunes in the western Mojave Desert, CA: Field studies. Flora 200:592–600.

Burnham KP, Anderson DR. 2002. Model selection and multimodel inference. New York, NY: Springer-Verlag

Cable JM, Huxman TE. 2004. Precipitation pulse size effects on Sonoran Desert soil microbial crusts. Oecologia 141:317–24.

Castle SC, Morrison CD, Barger NN. 2011. Extraction of chlorophyll *a* from biological soil crusts: a comparison of solvents for spectrophotometric determination. Soil Biol Biochem 43:853–6.

Chapin FS. 2003. Effects of plant traits on ecosystem and regional processes: a conceptual framework for predicting the consequences of global change. Ann Bot 91:455–63.

Chen C, Cleverly J, Zhang L, Yu Q, Eamus D. 2016. Modeling seasonal and inter-annual variations in carbon and water fluxes in an arid-zone acacia savanna woodland, 1981–2012. Ecosystems 19:625–44.

Collins SL, Sinsabaugh RL, Crenshaw C, Green L, Porras-Alfaro A, Stursova M, Zeglin LH. 2008. Pulse dynamics and microbial processes in aridland ecosystems. J Ecol 96:413–20.

Cook BI, Smerdon JE, Seager R, Coats S. 2014. Global warming and 21st century drying. Clim Dyn 43:2607–27.

Darrouzet-Nardi A, Reed SC, Grote EE, Belnap J. 2015. Observations of net soil exchange of CO_2 in a dryland show experimental warming increases carbon losses in biocrust soils. Biogeochemistry 126:363–78.

Elbert W, Weber B, Burrows S, Steinkamp J, Büdel B, Andreae MO, Pöschl U. 2012. Contribution of cryptogamic covers to the global cycles of carbon and nitrogen. Nat Geosci 5:459–62.

Ferrenberg S, Reed SC, Belnap J. 2015. Climate change and physical disturbance cause similar community shifts in biological soil crusts. Proc Natl Acad Sci 112:12116–21.

Feng W, Zhang Y, Wu B, Qin S, Lai Z. 2014. Influence of environmental factors on carbon dioxide exchange in biological soil crusts in desert areas. Arid L Res Manag 28:186–96.

Frank D, Reichstein M, Bahn M, Thonicke K, Frank D, Mahecha MD, Smith P, van der Velde M, Vicca S, Babst F, Beer C, Buchmann N, Canadell JG, Ciais P, Cramer W, Ibrom A, Miglietta F, Poulter B, Rammig A, Seneviratne SI, Walz A, Wattenbach M, Zavala MA, Zscheischler J. 2015. Effects of climate extremes on the terrestrial carbon cycle: concepts, processes and potential future impacts. Glob Chang Biol 21:2861–80.

Fried R, Schettlinger K, Borowski M. 2014. Robust Time Series Filters, robfilter. http://www.statistik.tu-dortmund.de/fried.html

Friedlingstein P, Cox P, Betts R, Bopp L, von Bloh W, Brovkin V, Cadule P, Doney S, Eby M, Fung I, Bala G, John J, Jones C, Joos F, Kato T, Kawamiya M, Knorr W, Lindsay K, Matthews H, Raddatz T, Rayner P, Reick C, Roeckner E, Schnitzler K-

G, Schnur R, Strassmann K, Weaver A, Yoshikawa C, Zeng N. 2006. Climate–Carbon Cycle Feedback Analysis: results from the C 4 MIP Model Intercomparison. J Clim 19:3337–53.

Garcia-Pichel F, Loza V, Marusenko Y, Mateo P, Potrafka RM. 2013. Temperature drives the continental-scale distribution of key microbes in topsoil communities. Science 340:1574–7.

Green LE, Porras-Alfaro A, Sinsabaugh RL. 2008. Translocation of nitrogen and carbon integrates biotic crust and grass production in desert grassland. J Ecol 96:1076–85.

Grote EE, Belnap J, Housman DC, Sparks JP. 2010. Carbon exchange in biological soil crust communities under differential temperatures and soil water contents: implications for global change. Glob Chang Biol 16:2763–74.

Gutzler DS, Robbins TO. 2010. Climate variability and projected change in the western United States: regional downscaling and drought statistics. Clim Dyn 37:835–49.

Hawkes C V, Keitt TH. 2015. Resilience vs. historical contingency in microbial responses to environmental change. Ecol Lett 18:612–25.

Housman DC, Powers HH, Collins AD, Belnap J. 2006. Carbon and nitrogen fixation differ between successional stages of biological soil crusts in the Colorado Plateau and Chihuahuan Desert. J Arid Environ 66:620–34.

Lange OL, Belnap J, Reichenberger H. 1998. Photosynthesis of the cyanobacterial soil-crust lichen *Collema tenax* from arid lands in southern Utah, USA: role of water content on light and temperature responses of CO_2 exchange. Funct Ecol 12:195–202.

Lasslop G, Reichstein M, Papale D, Richardson AD, Arneth A, Barr A, Stoy P, Wohlfahrt G. 2010. Separation of net ecosystem exchange into assimilation and respiration using a light response curve approach: critical issues and global evaluation. Glob Chang Biol 16:187–208.

Lavorel S. 2013. Plant functional effects on ecosystem services. J Ecol 101:4–8.

Maestre FT, Escolar C, de Guevara ML, Quero JL, Lazaro R, Delgado-Baquerizo M, Ochoa V, Berdugo M, Gozalo B, Gallardo A. 2013. Changes in biocrust cover drive carbon cycle responses to climate change in drylands. Glob Chang Biol 19:3835–47.

Nakagawa S, Schielzeth H. 2013. A general and simple method for obtaining R^2 from generalized linear mixed-effects models. Methods Ecol Evol 4:133–42.

Petrie MD, Collins SL, Gutzler DS, Moore DM. 2014. Regional trends and local variability in monsoon precipitation in the northern Chihuahuan Desert, USA. J Arid Environ 103:63–70.

Pinheiro J, Bates D, DebRoy S, Sarkar D, R CoreTeam. 2015. nlme: Linear and Nonlinear Mixed Effects Models. http://cran.r-project.org/package=nlme

Porada P, Weber B, Elbert W, Poschl U, Kleidon A. 2013. Estimating global carbon uptake by lichens and bryophytes with a process-based model. Biogeosciences 10:6989–7033.

Poulter B, Frank D, Ciais P, Myneni RB, Andela N, Bi J, Broquet G, Canadell JG, Chevallier F, Liu YY, Running SW, Sitch S, van der Werf GR. 2014. Contribution of semi-arid ecosystems to interannual variability of the global carbon cycle. Nature 509:600–3.

Prăvălie R. 2016. Drylands extent and environmental issues. A global approach. Earth-Science Rev 161:259–78.

R Core Team. 2016. R: a language and environment for statistical computing.

Raich JW, Schlesinger WH. 1992. The global carbon dioxide flux in soil respiration and its relationship to vegetation and climate. Tellus 44B:81–99.

Read CF, Duncan DH, Vesk PA, Elith J. 2014. Biocrust morphogroups provide an effective and rapid assessment tool for drylands. J Appl Ecol 51:1740–9.

Sancho LG, Belnap J, Colesie C, Raggio J, Weber B. 2016. Carbon budgets of biological soil crusts at the micro-, meso-, and global scales. In: Biological soil crusts: an organizing principle in drylands. Switzerland: Springer International Publishing. p287–304.

Smith DC, Molesworth S. 1973. Lichen physiology. XIII. Effects of rewetting dry lichens. New Phytol 72:525–33.

Stekhoven D, Buhlmann P. 2011. MissForest—non-parametric missing value imputation for mixed-type data. Bioinformatics 28:112–8.

Stekhoven DJ. 2013. Nonparametric Missing Value Imputation using Random Forest (missForest). https://github.com/stekhoven/missForest

Strong CL, Bullard JE, Burford MA., McTainsh GH. 2013. Response of cyanobacterial soil crusts to moisture and nutrient availability. Catena 109:195–202.

Su Y, Wu L, Zhang Y. 2012a. Characteristics of carbon flux in two biologically crusted soils in the Gurbantunggut Desert, Northwestern China. Catena 96:41–8.

Su Y, Li X, Qi P-C, Chen Y. 2012b. Carbon exchange responses of cyanobacterial-algal crusts to dehydration, air temperature, and CO_2 concentration. Arid L Res Manag 26:44–58.

Vargas R, Allen MF. 2008. Environmental controls and the influence of vegetation type, fine roots and rhizomorphs on diel and seasonal variation in soil respiration. New Phytol 179:460–71.

Vargas R, Detto M, Baldocchi DD, Allen MF. 2010. Multiscale analysis of temporal variability of soil CO_2 production as influenced by weather and vegetation. Glob Chang Biol 16:1589–605.

Williams WJ, Eldridge DJ, Alchin BM. 2008. Grazing and drought reduce cyanobacterial soil crusts in an Australian Acacia woodland. J Arid Environ 72:1064–75.

Wilske B, Burgheimer J, Karnieli A, Zaady E, Andreae MO, Yakir D, Kesselmeier J. 2008. The CO_2 exchange of biological soil crusts in a semiarid grass-shrubland at the northern transition zone of the Negev desert, Israel. Biogeosciences 5:1411–23.

Wu L, Lan S, Zhang D, Hu C. 2013. Recovery of chlorophyll fluorescence and CO_2 exchange in lichen soil crusts after rehydration. Eur J Soil Biol 55:77–82.

Xu L, Baldocchi DD, Tang J. 2004. How soil moisture, rain pulses, and growth alter the response of ecosystem respiration to temperature. Global Biogeochem Cycles 18:1–10.

Zelikova TJ, Housman DC, Grote EE, Neher DA, Belnap J. 2012. Warming and increased precipitation frequency on the Colorado Plateau: implications for biological soil crusts and soil processes. Plant Soil 355:265–82.

Zhao Y, Li X, Zhang Z, Hu Y, Chen Y. 2014. Biological soil crusts influence carbon release responses following rainfall in a temperate desert, northern China. Ecol Res 29:889–96.

Figures

Chapter 1 Figure 1. Characterization of biocrusts by biome. A) Means ± 95% *CI* of total biocrust relative cover (%) and B) means ± 95% *CI* of relative cover (%) by morphogroup. Different letters show post-hoc differences in least squares means by biome at false discovery rate $P \leq 0.05$.

Chapter 1 Figure 2. Net soil exchange (NSE), dark respiration (DR), and gross photosynthesis (GP) of biocrust samples by soil moisture (gravimetric water content; GWC) and temperature (C) for each biome.

Chapter 1 Figure 3. Average daily net ecosystem exchange (NEE), predicted biocrust net soil exchange (NSE), and air temperature (C) and soil moisture (gravimetric water content, GWC) for summer 2012 for each biome. Splines with spline parameter = 0.33 are displayed for ease of visualization.

Chapter 1 Figure 4. Predicted daily contribution (%) of biocrusts to ecosystem carbon flux by soil moisture (gravimetric water content; GWC) and temperature (C) for each biome with the number of days in 2012 (text) in each temperature × soil moisture combination. Top row: biocrust dark respiration (DR) contribution to ecosystem respiration (RE). Middle row: DR contribution to soil respiration (SR). Bottom row: biocrust gross photosynthesis (GP) contribution to ecosystem gross primary productivity (GPP).

Chapter 1 Figure 1

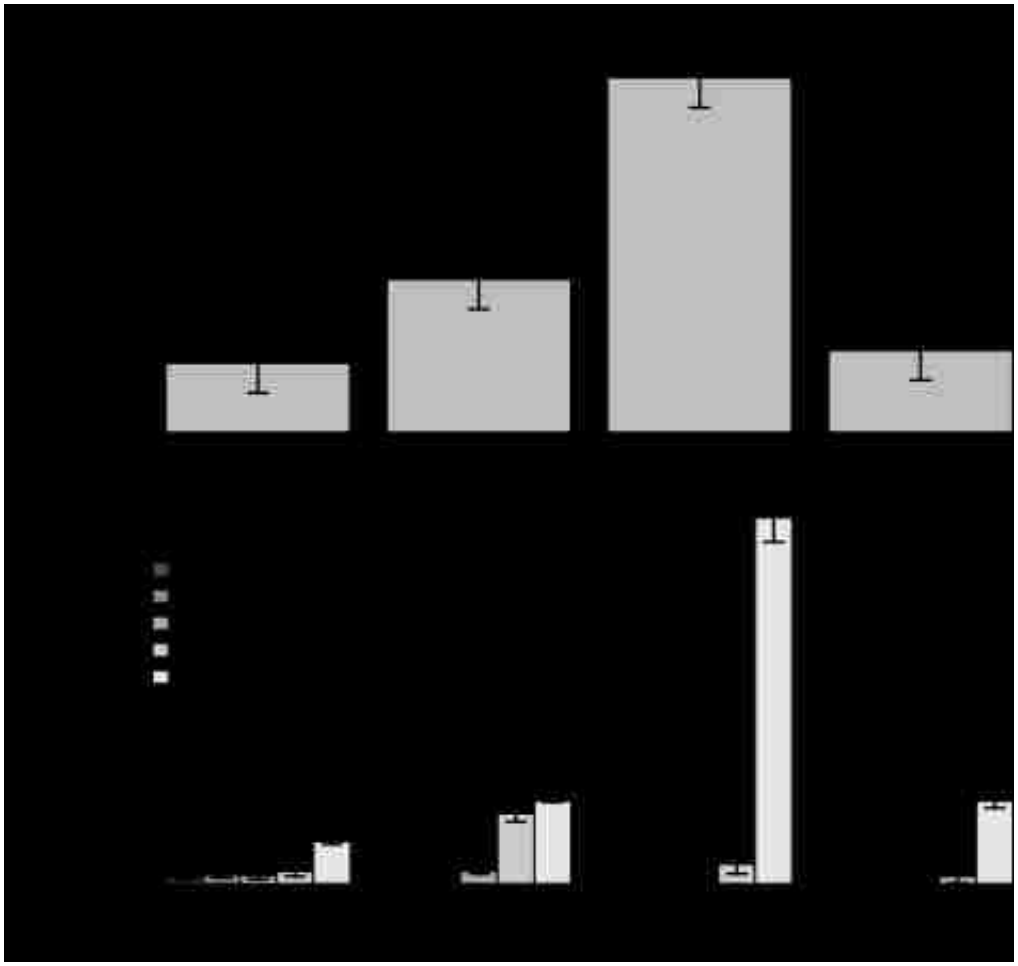

Chapter 1 Figure 2

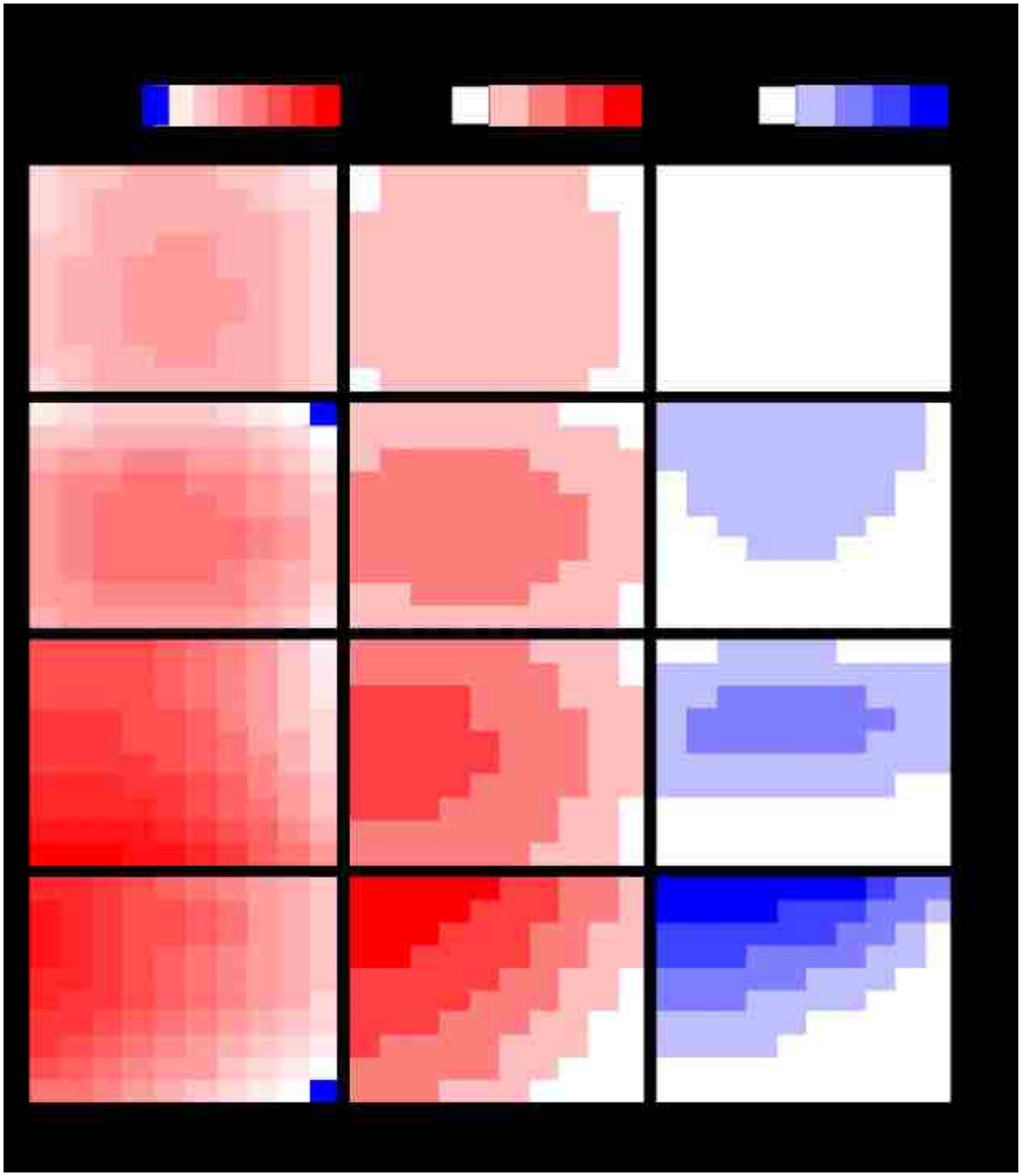

Chapter 1 Figure 3

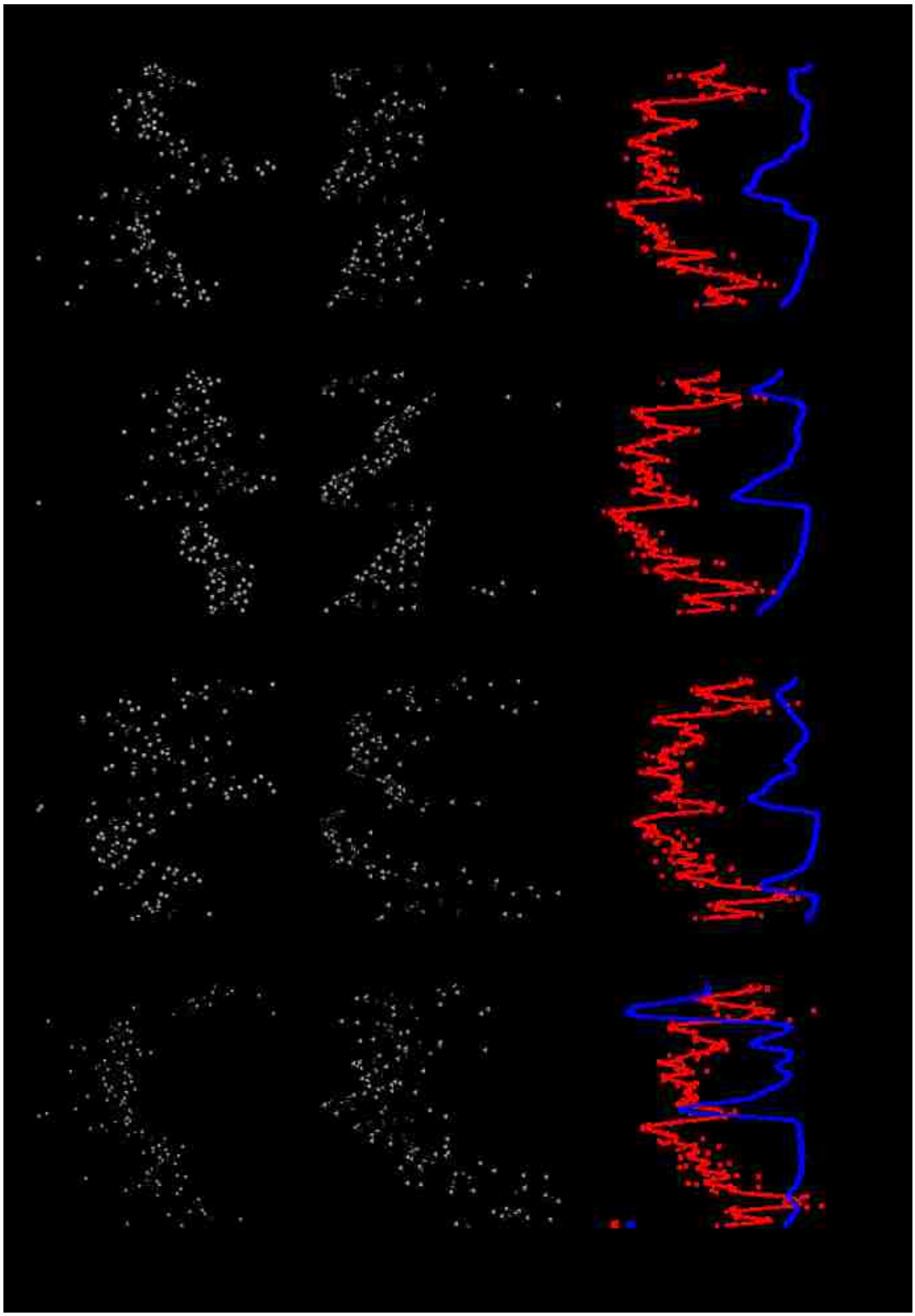

Chapter 1 Figure 4

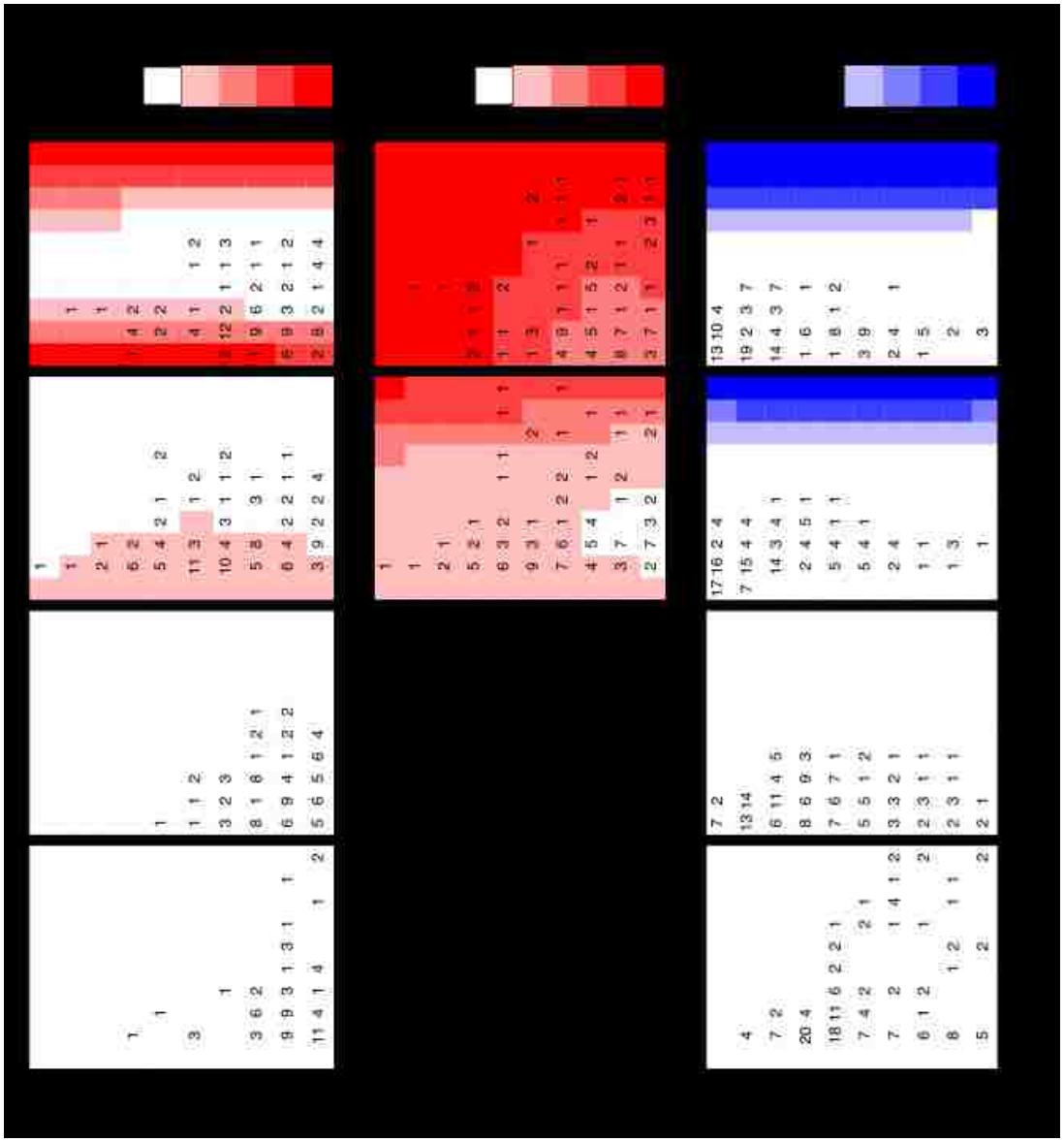

Tables

Chapter 1 Table 1. Geographic data and average abiotic conditions of biomes in the New Mexico Elevation Gradient 2007-2012 (Woodland 2008-2012 only due to missing data). Summer is considered April 25– October 2. Projection system is WGS 84 Web Mercator. MAT: Mean annual air temperature; MST: Mean summer air temperature; TAP: Total annual precipitation; SP: percent of precipitation arriving in summer.

Chapter 1 Table 2. Candidate models for biocrust net soil exchange (NSE), dark respiration (DR), and gross photosynthesis (GP) including combinations of temperature (T; °C) and soil moisture (M; gravimetric water content) with the number of parameters estimated for each model (*k*), *AICc*, log likelihood (*LogLik*) and marginal r^2.

Chapter 1 Table 3. Candidate models for the contribution of biocrust dark respiration to ecosystem respiration (RE) and soil respiration (SR) and biocrust gross photosynthesis to gross primary productivity (GPP) including combinations of temperature (T; °C) and soil moisture (M; gravimetric water content) with the number of parameters estimated for each model (*k*), *AICc*, log likelihood (*LogLik*) and marginal r^2.

Biome	Location, County	Extent in SW US ($\times 10^6$ ha)	Latitude	Longitude	Elevation (m)	MAT (C)	MST (C)	TAP (mm)	SP (%)
Woodland	Heritage Land Conservancy, Torrance	16	34.4384	-106.2377	2126	10.8	18.3	287	60
Savanna	Private property, Torrance	2	34.4255	-105.8615	1926	12.8	20.1	251	67
Shrubland	Sevilleta National Wildlife Refuge, Socorro	85	34.3349	-106.7442	1605	14.3	22.4	194	61
Grassland	Sevilleta National Wildlife Refuge, Socorro	39	34.3623	-106.7019	1596	13.6	22.7	214	63

Chapter 1 Table 2

Flux	Model	*k*	*AICc*	*logLik*	r^2_m
NSE	Null	5	615.0	-302.4	
	Biome	8	600.1	-291.7	0.18
	$M + T + M^2 + T^2$	9	548.6	-264.9	0.18
	Biome × M + Biome × M^2 + Biome × T + Biome × T^2	24	511.6	-228.8	0.35
DR	Null	5	699.5	-344.6	
	Biome	8	670.6	-327.0	0.27
	$M + T + M^2 + T^2$	9	655.8	-318.5	0.21
	Biome × M + Biome × M^2 + Biome × T + Biome × T^2	24	525.7	-235.9	0.44
GP	Null	5	314.7	-152.2	
	Biome	8	304.4	-143.9	0.16
	$M + T + M^2 + T^2$	9	291.5	-136.4	0.07
	Biome × M + Biome × M^2 + Biome × T + Biome × T^2	24	243.9	-94.9	0.35

Chapter 1 Table 3

Flux	Model	*k*	*AICc*	*logLik*	r^2_m
RE	Null	2	1376.3	-686.2	
	Biome	5	1112.6	-551.2	0.51
	$M + T + M^2 + T^2$	6	1331.3	-659.5	0.13
	Biome × M + Biome × M^2 + Biome × T + Biome × T^2	21	1051.4	-503.4	0.61
SR	Null	2	752.8	-374.4	
	Biome	3	649.9	-321.9	0.39
	$M + T + M^2 + T^2$	6	729.9	-358.8	0.14
	Biome × M + Biome × M^2 + Biome × T + Biome × T^2	11	587.4	-282.0	0.57
GPP	Null	2	509.6	-252.8	
	Biome	5	359.0	-174.5	0.24
	$M + T + M^2 + T^2$	6	478.1	-233.0	0.07
	Biome × M + Biome × M^2 + Biome × T + Biome × T^2	21	217.5	-86.9	0.43

Supplementary Material

Chapter 1 Appendix 1. Light response curves for cyanolichen/lichen biocrusts.

We recorded net soil exchange of five biocrust samples with mixed cyanolichens/lichens/ cyanobacteria in the Conviron growth chamber with varying light intensity. We compared the linear, quadratic, and cubic mixed effect of light intensity on net photosynthesis with sample ID as a random effect. AICc values showed that the linear model (k = 4, $AICc$ = 72.4, slope = -0.007) was better than the quadratic (k = 5, $AICc$ = 75.3) or cubic models (k = 6, $AICc$ = 77.5) (Ch. 1 Appendix 1 Fig. 1). There was no evidence of high light intensity inhibiting the biocrusts from shrubland, savanna, and woodland.

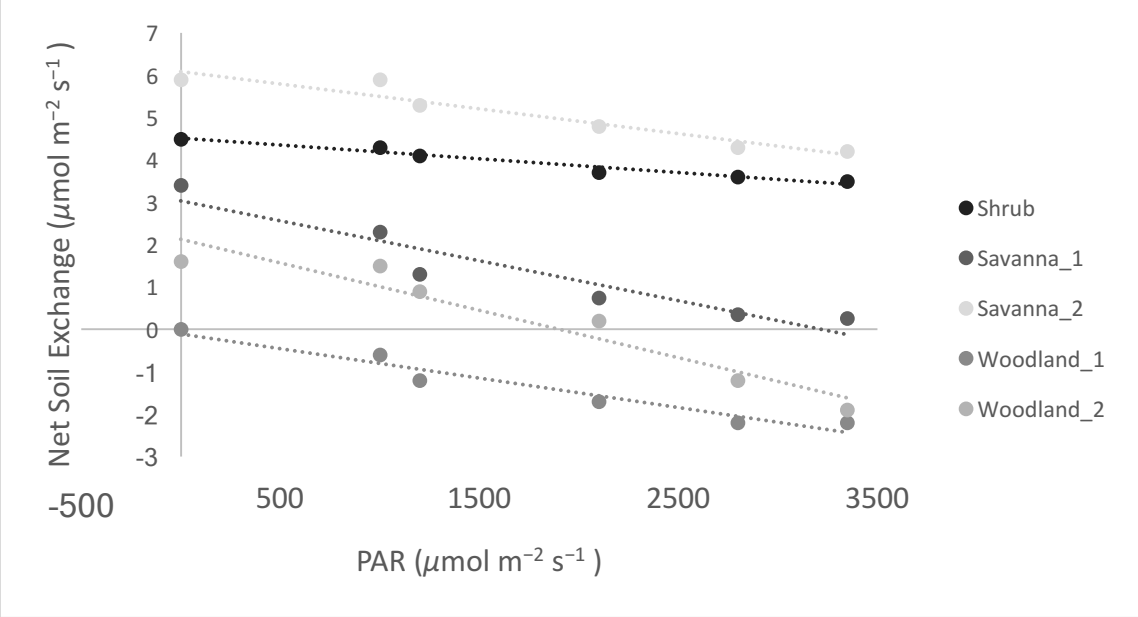

Chapter 1 Appendix 1 Figure 1. Net soil exchange for five biocrust samples tested in the growth chamber tested under varying light intensity.

Chapter 1 Appendix 2. Order *ex situ* measurements for each sample

We collected data from all samples within 9 months. We had initially focused only on biocrust response to soil moisture and so took all measurements at 25C with varying soil moisture, and then later decided to add in the temperature component. Although there may have been effects of long-term storage, the long breaks (>3 weeks, minimum) may have ameliorated potential legacy effects of the tested temperature in different orders (generally 25C, 18C, then 33C) that each sample experienced.

Chapter 1 Appendix 2 Table 1. Sample ID (1-15 or 16 from each biome) and when it was run at each temperature (C).

Biome	T	July 2012	August 2012	February 2013	March 2013
GR	18			1-4, 6-7, 10, 13-14	
	25	10, 11	3, 8-10, 13-14		4-7
	33				1-7, 10, 12-15
Shrubland	18			2-3, 5-12, 15-16	
	25	13-15	1, 3-4, 6, 11-12		7-10
	33				2-3, 5-12, 15-16
Savanna	18			5-8	3-4, 9-12
	25	2, 10-12, 14-17	1, 3-4, 13		5-9
	33				3-12
Woodland	18			6, 9	1-2, 12, 14-15
	25	2, 4-5, 13-15	3, 10-12	6, 9	7-10
	33				1-2, 6-12, 14-15

Chapter 1 Appendix 3. Chlorophyll content of biocrusts and relationship to net soil exchange

Chlorophyll content was determined as a measure of potential photosynthetic capacity. Biocrust samples were collected in June - October 2012. We analyzed 11 replicates from the woodland, savanna, and grassland, and 10 replicates from shrubland. Each sample was ground and passed through a 2 mm mesh, then 1g of each sample was dissolved in 1ml dimethylsulfoxide and left for 72h in the dark at room temperature. (so we captured ~75% of the chlorophyll content; Castle et al. 2011). Absorbance of 280μL supernatant at 665 and 750nm were recorded on a Synergy H1 Hybrid Multi-Mode Microplate Reader (BioTek U.S., Winooski, VT, USA) and chlorophyll *a* concentration (μg soil^{-1}) was calculated according to Castle and others (2011).

We compared chlorophyll content by biome using ANOVA in R. Additionally, we compared the gross photosynthesis to chlorophyll content by biome with analysis of variance using a subset of the samples where GPP was measured at 20 C and soil gravimetric water content was between 0.15 and 0.25 (8 samples from woodland, savanna, and grassland and 6 samples from shrubland).

The chlorophyll content of subjectively collected samples was highest at the woodland and that of the other three biomes were not significantly different ($F_{3,39} = 17.4$, $P < 0.01$, Ch. 1 Appendix 3 Fig. 1). Gross photosynthesis increased with chlorophyll content of the sample (Ch. 1 Appendix 3 Fig. 2, $F_{1,22} = 22.37$, $P < 0.001$). Chlorophyll content was within the range reported for light, intermediate, and dark biocrusts from Utah in Castle and others (2011). However, chlorophyll content at all biomes was lower than light biocrust collected in the Chihuahuan desert and Colorado Plateau desert, which averaged 20mg chlorophyll *a* g^{-1} soil (Grote and others 2010). Although the New Mexico Elevation Gradient is intermediate to the latitude/biomes/abiotic conditions of the Chihuahuan desert and Colorado Plateau, disturbance history may contribute to the low chlorophyll content. The savanna is subject to continued cattle grazing which has been

shown to decrease the cover and biomass of biocrusts (Williams and others 2008). Disturbance by grazers may also affect the other biomes because there are antelope and oryx at the Sevilleta LTER, and cattle were kept at the woodland.

This analysis confirms that the darkness category of biocrust is an appropriate measure of function at these biomes because darker biocrusts have higher chlorophyll content and biocrusts with higher chlorophyll content have higher gross photosynthesis.

Magnitude of biocrust GP increased with chlorophyll content ($F_{1,28}$ = 20.23, P = <0.001). The lower chlorophyll values and disturbance regime may help account for the low predicted biocrust uptake across the biome.

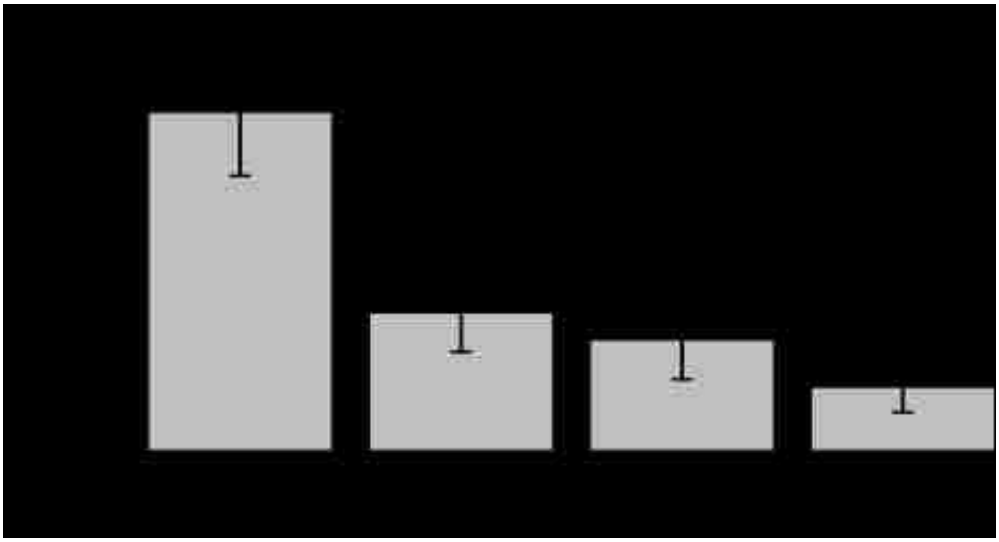

Chapter 1 Appendix 3 Figure 1. Means ± s.e. in biocrust chlorophyll *a* content by biome; letters indicate significantly different means (Tukey's HSD, α = 0.05).

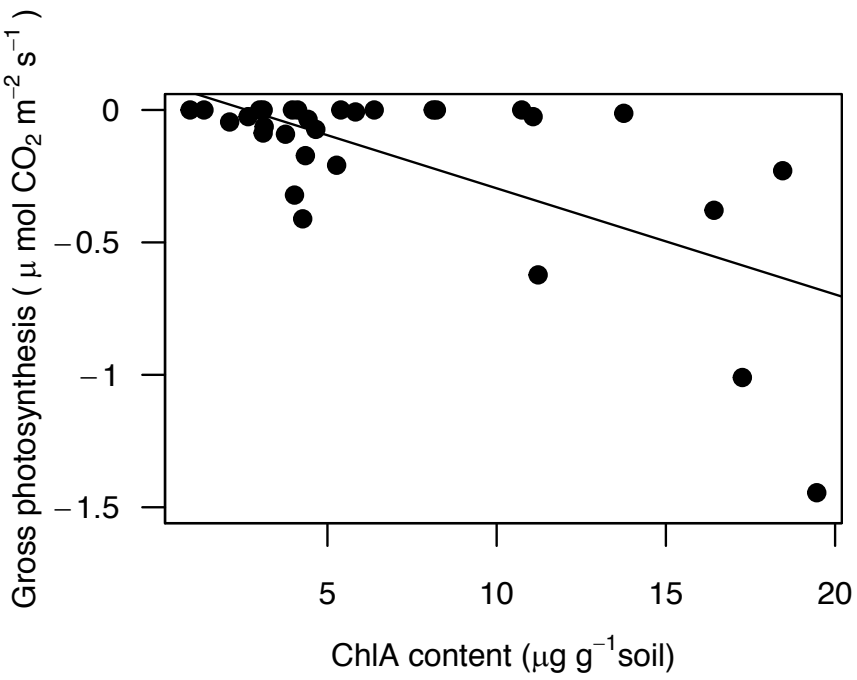

Chapter 1 Appendix 3 Figure 2. Biocrust gross photosynthesis (at 20C with water content between 0.15 and 0.25 GWC) by chlorophyll content from four biomes in New Mexico.

Chapter 1 Appendix 4. Selected model coefficients with s.e. for biocrust fluxes and raw biocrust carbon flux data plotted with predicted response lines for the three set temperatures across the range of soil moisture.

Chapter 1 Appendix 4 Table 1. Least square means ± s.e. coefficients from the best model (via *AICc* selection) for biocrust net soil exchange (NSE), respiration (DR), and gross photosynthesis (GP) for each biome and slopes for each unscaled abiotic predictor. Means and standard deviations of air temperature (C) and soil moisture (gravimetric water content) were 27.3C ± 6.1 and 0.13 ± 0.05 for NSE and GP and 27.3 ± 6.0 and 0.13 ± 0.05 respectively.

Term	Site	NSE	DR	GP
Site	Grassland	0.80 ± 0.15	1.00 ± 0.17	-0.04 ± 0.10
	Shrubland	1.03 ± 0.14	1.52 ± 0.16	-0.29 ± 0.10
	Savanna	1.69 ± 0.15	2.05 ± 0.17	-0.38 ± 0.11
	Woodland	1.63 ± 0.16	2.38 ± 0.18	-0.60 ± 0.11
Soil Moisture	Grassland	3.72 ± 6.80	5.77 ± 6.16	-0.21 ± 3.94
	Shrubland	16.26 ± 7.84	21.40 ± 7.47	-4.65 ± 4.57
	Savanna	-10.06 ± 9.26	14.96 ± 8.59	-25.75 ± 4.96
	Woodland	14.92 ± 12.93	13.27 ± 12.51	-3.00 ± 7.13
Soil Moisture^2	Grassland	-19.47 ± 25.5	-26.66 ± 23.43	0.38 ± 14.68
	Shrubland	-81.18 ± 28.76	-97.11 ± 27.38	10.97 ± 16.76
	Savanna	24.85 ± 34.04	-61.42 ± 31.30	88.79 ± 18.27
	Woodland	-43.63 ± 46.08	-6.84 ± 44.6	-18.72 ± 25.49
Temperature	Grassland	0.38 ± 0.23	0.33 ± 0.22	-0.06 ± 0.09
	Shrubland	0.52 ± 0.22	0.49 ± 0.22	-0.16 ± 0.10
	Savanna	0.52 ± 0.27	0.55 ± 0.27	-0.10 ± 0.10

Term	Site	NSE	DR	GP
	Woodland	0.24 ± 0.33	0.57 ± 0.33	-0.26 ± 0.12
Temperature^2	Grassland	-0.01 ± 0.00	-0.01 ± 0.00	0.00 ± 0.00
	Shrubland	-0.01 ± 0.00	-0.01 ± 0.00	0.00 ± 0.00
	Savanna	-0.01 ± 0.00	-0.01 ± 0.00	0.00 ± 0.00
	Woodland	-0.00 ± 0.01	-0.01 ± 0.01	0.00 ± 0.00

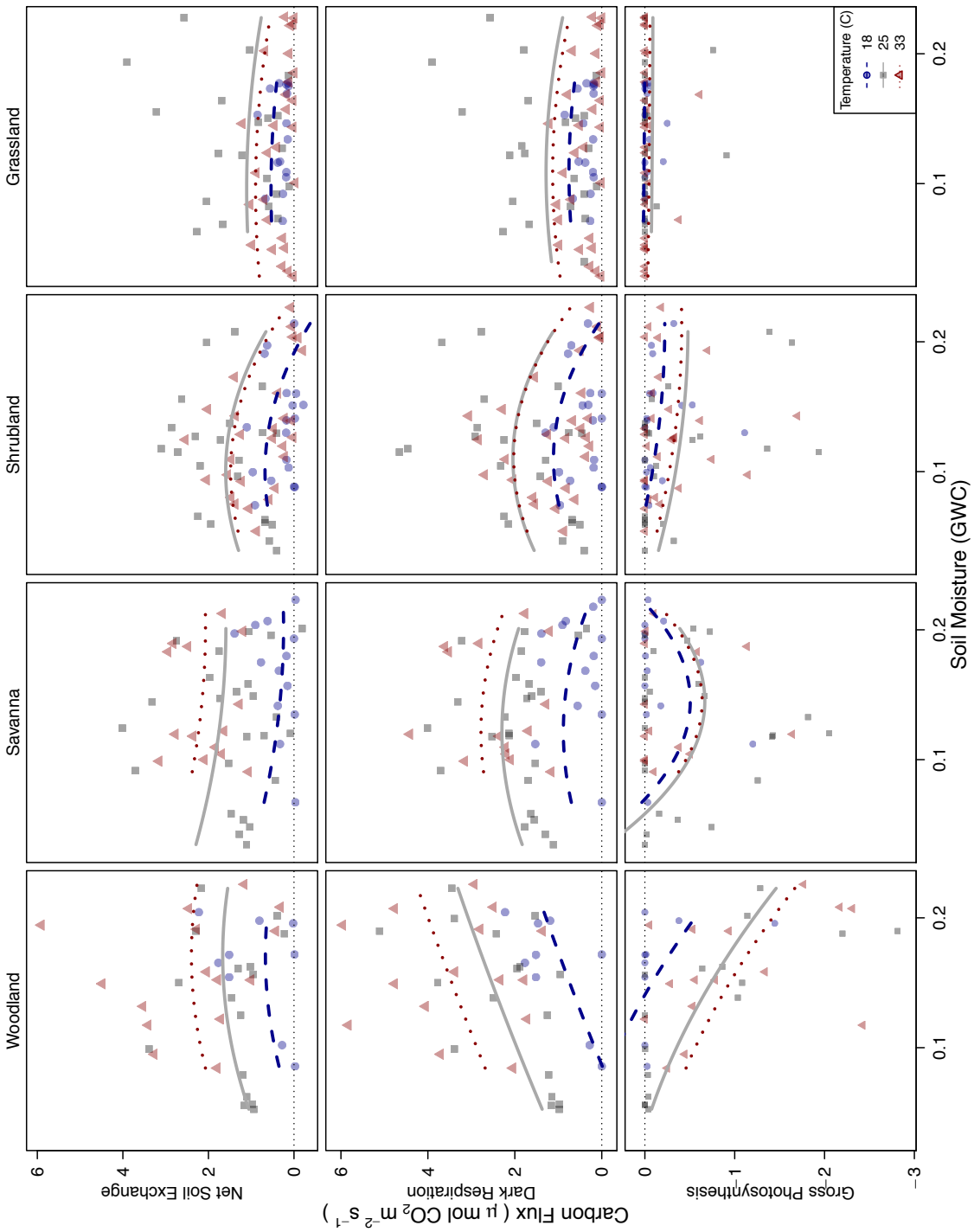

Chapter 1 Appendix 4 Figure 1. Net soil exchange (NSE), dark respiration (DR), and gross photosynthesis (GP) of biocrust samples by soil moisture (gravimetric water content; GWC) for each biome. Point color and type show set air temperatures (C). Lines show predicted responses at the set air temperatures across the observed range of soil moisture.

Chapter 1 Appendix 5. Least Square means ± s.e. of means for logit transformed proportion contributed of biocrusts dark respiration to ecosystem respiration (RE) and soil respiration (SR), and gross photosynthesis to ecosystem gross primary productivity (GPP) for each biome and slopes for each scaled abiotic predictor. Mean and standard deviation of air temperature (C) and soil moisture (gravimetric water content) for RE were 20.2 ± 1.7, 0.06 ± 0.02 for RE and SR and 26.9C ± 3.7 and 0.06 ± 0.03, for NSE, respectively.

Term	Site	RE	SR	GPP
Site	Grassland	-1.19 ± 0.09	0.94 ± 0.10	-3.08 ± 0.05
	Shrubland	-1.33 ± 0.11	-1.00 ± 0.10	-3.09 ± 0.06
	Savanna	-3.29 ± 0.16		-3.63 ± 0.05
	Woodland	-3.55 ± 0.15		-3.62 ± 0.04
Soil Moisture	Grassland	-1.00 ± 0.13	0.35 ± 0.12	-0.36 ± 0.04
	Shrubland	-0.50 ± 0.20	0.04 ± 0.20	-0.19 ± 0.06
	Savanna	-0.05 ± 0.12		0.03 ± 0.04
	Woodland	0.05 ± 0.22		0.06 ± 0.04
Soil Moisture^2	Grassland	0.47 ± 0.13	0.18 ± 0.10	0.51 ± 0.07
	Shrubland	-0.05 ± 0.12	0.30 ± 0.11	0.30 ± 0.07
	Savanna	0.03 ± 0.13		0.02 ± 0.06
	Woodland	-0.00 ± 0.06		-0.01 ± 0.01
Temperature	Grassland	0.11 ± 0.12	0.40 ± 0.11	0.11 ± 0.03
	Shrubland	0.16 ± 0.11	0.15 ± 0.10	-0.12 ± 0.03
	Savanna	0.10 ± 0.17		-0.00 ± 0.03
	Woodland	0.10 ± 0.18		0.03 ± 0.07
Temperature^2	Grassland	0.01 ± 0.08	0.23 ± 0.09	-0.02 ± 0.03

Term	Site	RE	SR	GPP
	Shrubland	-0.10 ± 0.05	-0.02 ± 0.07	-0.09 ± 0.03
	Savanna	-0.00 ± 0.19		-0.00 ± 0.02
	Woodland	0.01 ± 0.19		0.0 ± 0.03

Chapter 2: ^{13}C signature of biological soil crusts is depleted next to C_3 plants suggesting mixotrophy

Eva Dettweiler-Robinson[1], Jenn Rudgers[1], Robert Sinsabaugh[1]

1. Department of Biology, MSC03 2020, 1 University of New Mexico, Albuquerque, NM 87131-0001

Abstract

Plants and biological soil crusts (biocrusts) are producers in drylands, but biocrusts seldom show net carbon uptake. We hypothesized that biocrusts augment carbon fixation by incorporating plant-derived carbon. We collected biocrusts located beneath a C_3 forb (*Gutierrezia sarothrae*), a C_4 grass (*Bouteloua gracilis*), and 25 cm from the nearest plant (interspace), and in a mesocosm experiment with a live or removed C_4 grass. We determined biocrust community, isolated cyanobacteria/lichen, and plant leaf ^{13}C values. Communities and isolates under C_3 were depleted by ~2‰ relative to other locations, suggesting C_3 plants contribute ~16% of biocrust C. The biocrust $\delta^{13}C$ did not differ under live versus dead C_4 plants, suggesting that biocrusts are not obtaining significant C from living C_4 plants. Potential mechanisms for C transfer from plants include mixotrophy and fungal translocation. Plant-derived C may constitute a significant resource for biocrusts, coupling activities of primary producers in drylands.

Introduction

Drylands cover 45% of the earth's terrestrial surface (Prăvălie 2016) and are important drivers of interannual variability in global carbon dynamics (Ahlstrom et al. 2015). Primary producers in drylands include vascular plants and biological soil crusts

("biocrusts"). Biocrusts are present in arid and semi-arid communities globally (Belnap et al. 2001) and contain algae, cyanobacteria, mosses, lichens, bacteria, and fungi living at the soil surface. In addition to primary production, biocrusts contribute to ecosystem structure and function by reducing soil erosion, fixing nitrogen, intercepting atmospheric deposition, and affecting infiltration of precipitation (Belnap et al. 2001, Belnap 2002, Elbert et al. 2012). Desert and steppe biocrusts account for an estimated 0.59 Pg yr−1 of annual global terrestrial CO_2 uptake (Elbert et al. 2012). Thus, understanding controls on C cycling through dryland biocrusts has potential to improve estimates of global terrestrial C flux.

Despite the presence of photosynthetic organisms in biocrusts, researchers observed that biocrusted soils typically show a net release of C and only rarely net uptake in field conditions (however, *in situ* collars record fluxes from soil and roots in addition to biocrusts; Wilske et al. 2008, de Guevara et al. 2014, Darrouzet-Nardi et al. 2015), and net release under extremely dry or wet conditions in the lab (Lange et al. 1998, Grote et al. 2010). Biocrusts maximize gross photosynthetic rates at moderate moisture levels and cool to moderate temperatures (Grote et al. 2010). However, in many regions, the majority of moisture arrives during the hottest season (Zhou et al. 2008) and drylands have pulses of precipitation interspersed between long dry periods (Huxman et al. 2004). During these moist periods, autotrophic biocrust components must repair their tissues and initiate activity, so they initially respire before accumulating new C (Sponseller 2007). Thus, the total time available for biocrusts to fix C is often short because small rain events are followed by dry periods. Some organisms are capable of supplementing their photosynthetic C capture by incorporating fixed C from external organic sources. For

example, when grown in culture, some terrestrial cyanobacteria and algae use mixotrophic strategies (Yu et al. 2009, Gustavs et al. 2016). Biocrusts can take up organic and inorganic forms of C *in situ* (Green et al. 2008), but the significance of plant-derived C to biocrust function has not been investigated. Determining the controls on C uptake, exchange, and release in biocrusts will improve understanding of C cycling in drylands.

In this study, we estimated the amount of plant-derived C in biocrusts using the natural abundance of C stable isotopes, which are expressed in parts per thousand (per mil, ‰). Stable isotopes distinguish plant functional groups by photosynthetic pathway: C_3 plants have $\delta^{13}C$ values near -28‰ and C_4 plants have values near -14‰ (O'Leary 1988). Because biocrusts are mixtures of functionally different microbes and macrobes, their $\delta^{13}C$ values vary considerably among dryland ecosystems (estimates range from -15 to -25‰, Aranibar et al. 2003, Zelikova et al. 2012). Cyanobacteria and cyanolichens can have carbon-concentrating mechanisms (Badger and Price 1992), leading to relatively higher $\delta^{13}C$ values than C_3 plants; thus their $\delta^{13}C$ values are typically closer to those of C_4 plants (Raven et al. 2008). However, if biocrusts incorporate plant-derived C predominantly from C_3 or C_4 plants, then those biocrusts should be relatively depleted or relatively enriched, respectively.

We used field samples and a mesocosm experiment to address the following objectives: 1) We determined ^{13}C values of dryland primary producers (C_3 plants, C_4 plants, and biocrust communities in interspaces) to find endpoint values for mixing models (see below). 2) We compared $\delta^{13}C$ values of biocrust communities and isolated biocrust autotrophs from three locations: beneath C_3 plants, beneath C_4 plants, or in interspaces between plants. If biocrust autotrophs use plant C, then their isotopic

signatures should differ among these three locations because more plant C is available to biocrusts near the plants than in the interspace. Previous work has shown that shallow soils next to C_3 shrubs were depleted in ^{13}C compared to bulk soils in the surrounding C_4 grassland (Bai et al. 2012). To estimate the proportion of plant-derived C in biocrust autotrophs, we used a two-source mixing model. Mixing models can determine the relative contributions of isotopically different C sources to target organisms (Peterson and Fry 1987). 3) To determine whether photosynthetically active plants influence biocrust isotopic signatures more strongly than dead plants, we set up a mesocosm experiment in which we paired biocrusts with living plants or dead plants. Living plants produce root-respired CO_2 available for biocrust fixation, but dead plant material could be degraded through microbial and abiotic activity, and thus differences in isotopic signature in biocrusts may suggest which process is more important for biorust uptake of plant C.

Methods

Study sites. We collected biocrusts from two sites in New Mexico. At the Sevilleta National Wildlife Refuge (SNWR) grassland (34.359, -106.736, WGS 84 Web Mercator elevation 1600 m), we collected light cyanobacterial biocrusts (*Microcoleus* spp.; Garcia-Pichel et al. 2013). The grassland is dominated by the C_4 bunchgrasses blue grama (*Bouteloua gracilis* (Willd. ex Kunth) Lag. ex Griffiths) and black grama (*B. eriopoda* (Torr.) Torr.) with some dropseed (*Sporobolus* spp. R. Br.) and C_3 threeawns (*Aristida* spp. L.). Shrubs are uncommon but include C_3 yucca (*Yucca glauca* Nutt.) and Mormon tea (*Ephedra torreyana* S. Watson). Herbaceous C_3 plants include snakeweed (*Gutierrezia sarothrae* (Pursh) Britton & Rusby), fineleaf hymenopappus

(*Hymenopappus filifolius* Hook.), and globe mallows (*Sphaeralcea* spp. A. St.-Hil.). The climate is semi-arid with mean annual temperature of 13C and a summer monsoon season that delivers 60% of the ~250mm mean annual precipitation (Moore 2016). Livestock grazing has been excluded since 1973.

At the La Puebla site (private property, 35.978, -105.995, elevation 1800 m), we collected dark, mature biocrusts. These biocrusts were composed of cyanobacteria (*Microcoleus* spp*., Scytonema* spp., *Nostoc* spp.), with scattered mosses (including *Bryum argenteum, Pterygoneurum ovatum, Syntrichia ruralis*), and lichens (*Collema* spp., *Placidium* spp., *Psora* spp.). This site is a juniper savanna with scattered piñon pine (*Pinus edulis* Engelm.) and one-seed juniper [*Juniperus monosperma* (Engelm.) Sarg.]. The understory is dominated by the C_4 bunchgrass *B. gracilis,* the C_3 bunchgrass Indian rice grass [*Achnatherum hymenoides* (Roem. & Schult.) Barkworth], the C_3 herb *G. sarothrae*, and the C_4 shrub four-wing saltbush [*Atriplex canescens* (Pursh) Nutt.]. Mean annual temperature is 11C and a summer monsoon season delivers 60% of 290mm mean annual precipitation (Western Regional Climate Center 2015). Livestock grazing has been excluded since the 1950s.

Field mesocosm experiment. At the La Puebla site, we set up field mesocosms in August 2013 by transplanting 80 individual *B. gracilis* with their associated soil and biocrusts, collected from nearby natural areas into separate 7.57 L pots. We tried to minimize disturbance to the rhizosphere but some sandier soils fell apart more than the loamier microsites. From half of the pots, we removed the plant aboveground biomass and root crown, killing the plant but leaving roots to decompose without disturbing the soil structure. The plants remained living in the other half of the pots. All pots were drip

irrigated (RBY100MPTX filter, Rainbird, Azusa, CA, USA; 1.9cm hose) with well water via maximum 12.11 L h^{-1} pressure compensating spray stakes (#22500-002030, Netafim USA, Fresno, CA, USA) and 91.4cm dripper assembly (#40201-002020; Netafim USA, Fresno, CA, USA). For the small, frequent treatment, we automated watering once per week for 1min using a timer (Orbit model 62056, Orbit, Bountiful, Utah, USA). Although this design could provide up to 200mL of water per pot, the water output emitted from each sprayer was actually 100mL per event because the hose dried between applications. For the large, infrequent treatment, we hand-watered 400mL with well water once per month. Water additions occurred only during the summer months (May-September). There was no difference between watering treatments in plant size (20.8g ± 1.9 s.e.; $F_{1,8}$ = 0.18, P = 0.68) or biocrust $\delta^{13}C$ (-20.5‰ ± 0.3 s.e., $F_{1,8}$ = 0.06, P = 0.80). We thus ignore differences between watering treatments in the mesocosm experiment but we do not directly compare the mesocosm with the field-collected samples due to the difference in water regime.

Sample collection. Samples were collected in April 2015. Each biocrust sample was collected from the surface to the depth of biological aggregation of the soil (0.5 - 1.0 cm), excluding any visible live plant material or litter. We did not identify biocrust composition by microscopy nor by molecular methods, but level of development (Belnap et al. 2008) was similar within sites. Additionally, we collected ten leaves from five randomly chosen *B. gracilis* and *G. sarothrae* individuals from the Sevilleta site.

Cover type. At each site, we collected 10 samples each at the center of interspaces, under a C_3 plant canopy, or under a C_4 plant canopy. Interspaces were at least 50cm in diameter. Samples were collected within 3 cm of the base of the C_3 *G. sarothrae*

("GUSA2") or C_4 *B. gracilis* ("BOGR2") plants. From the mesocosm experiment, we collected 10 biocrust samples each from pots with no living *B. gracilis* plants ("BOGR2 removal") and from pots with living *B. gracilis* plants ("BOGR2 living").

Sample type. We analyzed three sample types: plant leaves, biocrust communities, and cyanobacteria/lichen isolates. Biocrust communities included substrate material bound by filaments. To obtain cyanobacteria/lichen isolates, we wet community samples with deionized water and removed green filaments and lichens with forceps under a dissecting microscope (20X magnification). Some substrate material was tightly bound to the filaments and could not be separated, thus percentage carbon by weight was not consistent across samples. We isolated cyanobacteria/lichen from five of the GUSA2, BOGR2, and interspace La Puebla field-collected samples and from BOGR2 removal and BOGR2 living mesocosm samples.

Carbon isotope processing and analysis. All samples were dried at 60 C for 3 d. Biocrust community samples and isolate samples were ground using a mortar and pestle, 10 mg of communities and 1-4 mg of isolates were placed into silver capsules (4 × 6 mm, Costech, Valencia, CA), and capsules were left open and acid fumigated with 12M HCl for 30 h to remove carbonates (Ramnarine et al. 2011). Samples were then air dried for 2 h. Silver capsules were placed into tin capsules (4 × 6 mm, Costech, Valencia, CA) to improve combustion. Leaf samples were ground in liquid nitrogen with a mortar and pestle, and 4 mg were placed into tin capsules. All samples were run on an ECS 4010 Elemental Analyzer (Costech, Valencia, CA, USA) and a Delta V Isotope Ratio Mass Spectrometer (Thermo Scientific, Waltham, MA USA) at the University of New Mexico Center for Stable Isotopes to obtain percentage C (Ch. 1 Appendix 1) and $\delta^{13}C$ values for

each sample (relative to standard Vienna Pee Dee Belemnite). Two BOGR2 cover type and one GUSA2 cover type community samples from the Sevilleta site and one cyanobacteria/lichen from BOGR2 living mesocosm and one community sample from BOGR2 removal from the La Puebla site were excluded from $\delta^{13}C$ analyses because the mass spectrometer did not produce reliable values.

Analysis. All analyses were conducted in R (R version 3.1.3, 2015-03-09, R Core Team 2016).

Objective 1. We compared the $\delta^{13}C$ values among primary producers (GUSA2 plants, BOGR2 plants, and the interspace biocrust community), sites (Sevilleta vs. La Puebla), and their interaction using a 2-way ANOVA. Tukey honest significant difference (HSD) post-hoc tests were used to detect pairwise differences between levels for all tests with more than 2 levels. Additionally, we compared the plant $\delta^{13}C$ values collected from the Sevilleta site to the values from the TRY Plant Trait database (Kattge et al. 2011) using a two-tailed t-test to assess whether the Sevilleta plants differed from the average for the species.

Objective 2. To compare the $\delta^{13}C$ values of the biocrust community growing next to plants to those in the interspaces, we analyzed the effects of site (Sevilleta vs. La Puebla), cover type (C_3, C_4, or interspace), and the interaction using a 2-way ANOVA. To determine if the $\delta^{13}C$ values of living autotrophic components of the biocrust vary by cover type, we used only samples from the La Puebla site to compare the effects of cover type (C_3, C_4, or interspace), sample type (biocrust community or cyanobacteria/lichen only), and their interaction using 2-way ANOVA.

We estimated the proportion of cyanobacteria/lichen C derived from plant C using a two-source mixing model (Tiunov 2007). Mixing models estimate the proportional contribution of different resources to the isotopic signature of the samples. Because there was no difference in $\delta^{13}C$ in the interspace and C_4 canopy (see Results), we estimated the proportion of cyanobacteria/lichen C derived from C_3 plants using the TRY database value (we did not have values from the La Puebla plants):

$$\delta^{13}C_{\text{cyanobacteria/lichen near GUSA2}} = (\alpha) \times \delta^{13}C_{\text{GUSA2 plant}} + (1\text{-}\alpha) \times \delta^{13}C_{\text{cyanobacteria/lichen in interspace}} \quad (1)$$

where α is the proportion of the C derived from the C_3 plant.

Objective 3. To determine if removing a C_4 plant would affect the biocrust community or cyanobacteria/lichen $\delta^{13}C$ value, we compared the effects of BOGR2 presence/removal, sample type (community or isolates), and their interaction using ANOVA.

Results

Biocrust community $\delta^{13}C$ values were intermediate between C_3 and C_4 plants. C_3 and C_4 plants in this study had distinctive $\delta^{13}C$ signatures reflecting their different photosynthetic pathways. At the Sevilleta site, the $\delta^{13}C$ value of the C_3 plant *G. sarothrae* was ~13‰ lighter than that of the C_4 plant *B. gracilis* (Ch. 2 Fig. 1, $F_{3, 26} = 120.2$, $P < 0.01$, all Tukey HSD post-hoc pairwise tests $P \leq 0.05$) as expected. The $\delta^{13}C$ values of *B. gracilis* and *G. sarothrae* from the Sevilleta site were not different from the TRY database values for these species (Ch. 2 Fig. 1, *B. gracilis* TRY mean value = -14.76, $t_4 = 1.56$, $P = 0.19$; *G. sarothrae* TRY mean value = -27.92, $t_4 = 0.81$, $P = 0.46$).

The $\delta^{13}C$ values of biocrust community from both sites ranged from -23 to -16.6‰, reflecting the complex contributions of living and dead autotrophic and heterotrophic organisms present in biocrusts. Observed biocrust values were intermediate between C_3 and C_4 plants and significantly non-overlapping with either (Ch. 2 Fig. 1, all Tukey HSD post-hoc pairwise tests $P \leq 0.05$). In addition, the biocrust community from the La Puebla site was depleted by 2.8‰ (Tukey HSD $P \leq 0.05$) compared to that from the Sevilleta site.

Biocrust community under C_3 plants had depleted $\delta^{13}C$ values. The mean $\delta^{13}C$ value of the biocrust community collected from under the C_3 plants was 2.1‰ lower than for biocrusts collected from interspaces, suggesting strong microsite differences in the biocrust C source (Ch. 2 Fig. 1, $F_{2,51} = 15.96$, $P < 0.01$; Tukey HSD $P \leq 0.05$). These differences were consistent across both collection sites (cover type × site interaction: $F_{2,51} = 1.41$, $P = 0.25$; Site: $F_{1,51} = 1.41$, $P = 0.25$). In contrast, there was no significant difference between the biocrust $\delta^{13}C$ values in the interspace versus under C_4 plants (Tukey HSD $P > 0.05$), suggesting little contribution of C_4 C to biocrusts.

In samples from the La Puebla site, the cyanobacteria/lichen isolates collected under C_3 plants had $\delta^{13}C$ values that were 1.4‰ lower than isolates from the interspaces (Ch. 2 Fig. 2, $F_{2,39} = 8.51$, $P < 0.01$, Tukey HSD $P \leq 0.05$; sample type × cover type interaction, $F_{2,39} = 0.11$, $P = 0.89$). Isolate $\delta^{13}C$ values in the interspace did not differ from those collected under C_4 plant canopies (Tukey HSD $P > 0.05$). The isolates had 2.0‰ higher $\delta^{13}C$ values than the community ($F_{1,39} = 34.6$, $P < 0.01$).

Because the biocrust $\delta^{13}C$ values were depleted next to the C_3 plant, we used the mixing model to calculate that the C_3 plant contributed 15.9% of the cyanobacteria/lichen

isolates C at the La Puebla site. It is unclear, however, whether that C is from living C_3 activity or from non-living sources such as degrading litter. We could not determine if biocrusts incorporated C_4 plant-derived C because there were no differences between $\delta^{13}C$ values of cyanobacteria/lichen between interspaces versus under C_4 plants (Tukey HSD $P > 0.05$), or in mesocosm pots with C_4 live vs. removed (see next section). Thus, we did not use a mixing model to estimate the contribution of C_4 C to biocrusts.

Biocrust $\delta^{13}C$ values were not affected by C_4 plant removal. In the C_4 plant removal mesocosm experiment, biocrust community $\delta^{13}C$ values did not significantly differ between the pots with living C_4 plants and pots where the plant had been removed (Ch. 2 Fig. 2; cover type $F_{1,26} = 0.29$, $P = 0.59$; cover type × sample type $F_{1,26} = 2.59$, $P = 0.12$). Cyanobacteria/lichen isolates had 1.5‰ higher $\delta^{13}C$ values than biocrust community ($F_{1,26} = 10.5$, $P < 0.01$).

Discussion

Across two different grasslands and biocrust types, results were consistent with the hypothesis that C_3 plants provide an important C source not only for biocrust community, but also for biocrust autotrophs, suggesting that they rely on a mixotrophic strategy. Biocrusts appear to use C_3 plant-derived C to meet metabolic demands.

Several potential mechanisms could underlie the incorporation of C_3 plant C into biocrusts. Aboveground litter (with $\delta^{13}C$ values similar to living material; Brüggemann et al. 2011) could fall onto the soil surface and degrade due to biotic and abiotic processes (e.g. photodegradation, Brandt et al. 2010), releasing C compounds which could be taken up by biocrust organisms. Here, biocrust $\delta^{13}C$ values were distinct under *G. sarothrae* but not under *B. gracilis*. *G. sarothrae* leaf litter decomposes more rapidly than *B. gracilis*

litter (Murphy et al. 1998), and *G. sarothrae* leaves had higher percentage C by weight than *B. gracilis* (Supplementary material). Thus, C released from decomposing *G. sarothrae* might be taken up by biocrust organisms more readily than carbon from *B. gracilis*. Roots and root litter are relatively enriched in ^{13}C compared to photosynthetic tissue by ~1-2‰ in C_3 plants and by 0.3‰ in C_4 plants (Werth and Kuzyakov 2010, Brüggemann et al. 2011). If the C in the biocrusts is derived exclusively from the root tissue, the mixing model would predict an even higher proportion of plant C in the cyanobacteria/lichen isolates (20.8% using a *G. sarothrae* root value of -25.92). Living roots also produce exudates (Jones et al. 2004) which vary in isotopic signature due to their chemical composition and factors that affect the allocation and processing of those compounds (Brüggemann et al. 2011). Roots also respire CO_2 that could be taken up at the interface of the soil and atmosphere by the biocrust autotrophs (Beck and Mayr 2012). Respired CO_2 from the roots is relatively depleted compared to the root tissue itself (by 2‰ in C_3 plants and by 1.3‰ in C_4 plants; Werth and Kuzyakov 2010). Root exudates vary in isotopic signature due to their chemical composition and factors that affect the allocation and processing of those compounds (Bruggeman et al. 2011). However, root inputs may be relatively unimportant to the biocrusts under the C_3 plant in this study because *G. sarothrae* has a low proportion of roots at shallow (0-10cm) soil depths and a wide radial extent of roots (>20cm radius deeper than 20cm; Milchunas et al. 1992).

Another potential mechanism of C_3 C transfer to biocrusts is that soil fungi directly couple the plant roots with the biocrusts, facilitating exchanges of water and nutrients (Collins et al. 2008). For example, previous work showed that plant C can be

transported to biocrusts over rapid time scales (Green et al. 2008). Root-associated fungi could provide a transfer route. Arbuscular mycorrhizal fungi (Glomeromycota) are present in the roots of most plant species and use up to 20% of plant photosynthate (Willis et al. 2013). Both *B. gracilis* and *G. sarothrae* host root-associated fungi (Kageyama et al. 2008), and similar fungal taxa can be found in the biocrust community (Collins et al. 2008). If C from plants supports nitrogen fixation by biocrusts, which can be transferred to the plants (Green et al. 2008), then resource exchanges in dryland ecosystems may promote the performance both plant and biocrust primary producer communities (Collins et al. 2014).

Alternatively, individual phototroph C dynamics and biocrust communities may account for differences in microsite biocrust $\delta^{13}C$ values. Cyanobacterial $\delta^{13}C$ values can vary by taxa and across seasons in lakes (Vuorio et al. 2006) and with different light conditions in pure culture (Wada et al. 2012). Bacterial communities vary in the top 10cm between interspace and dryland grass species and among species (Kuske et al. 2002) and thus there may also be different communities of autotrophs at the surface. If communities of biocrusts differ in the plant and interspace microsites and the dominant organisms in the biocrusts have strong differences in fractionation of C in their photosynthetic pathway, then we may observe differences in the $\delta^{13}C$ values without biocrusts incorporating plant C. These differences in microsite conditions and communities may account for different $\delta^{13}C$ values independently of plant C incorporation but we do not yet have the data to resolve these differences.

Biocrust $\delta^{13}C$ values were intermediate to C_3 and C_4 plant values and varied considerably (>8‰) between sites and sample locations. Biocrust community values

reported here are similar to the -18‰ and -19.5‰ reported by Thompson et al. (2006) for interspace biocrusts in the Negev Desert grasslands (275mm annual precipitation) and the Chihuahuan Desert in Arizona (rainfall 380mm annual precipitation [1]), and -22‰ reported by Cable and Huxman (2004) for the Sonoran Desert in Arizona (305mm annual precipitation) respectively. Higher isotopic discrimination (i.e., more negative $\delta^{13}C$ values in biocrust community) may occur in locations with higher rainfall (here, the La Puebla site), as has been observed in cyanolichens (Cuna et al. 2007) and in plants (Wang et al. 2016). Additionally, C_3 trees at the La Puebla site may contribute to root respiration and soil organic material, leading to more depleted $\delta^{13}C$ values in soils at this location. The C_4 grassland may retain a C_4 signal for long time periods (Breecker et al. 2009), and thus differences in interspace and C_4 interspaces (living and dead) may be more difficult to detect.

The cyanobacteria/lichen samples had higher $\delta^{13}C$ values than samples of the biocrust consortium, and this trend could be attributed to the inclusion of soil organic material. Lignins from plant litter, for example, are relatively recalcitrant compounds (Mun and Whitford 1998; although they are subject to photodegradation on the surface; Austin and Ballaré 2010) that are depleted in ^{13}C compared to living plant tissue (Benner et al. 1987, Fernandez et al. 2003, Dumig et al. 2013). Lignin in the soil matrix among the biocrust organisms may explain the lower $\delta^{13}C$ values of community compared to cyanobacteria/lichen isolates. However, differential processing of soil organic C during microbial decomposition may result in plant-species and microbial community-specific changes in organic matter $\delta^{13}C$ (Wedin et al. 1995, Connin et al. 2001) which remains to be resolved.

The results of this study are consistent with the hypothesis that nearly 16% of biocrust autotroph C may derive from C_3 plants. Biocrusts are dominant across drylands globally and thus understanding the role of plant-derived C in biocrust function will help refine prediction of the roles of plant-microbe interactions in ecosystem services, such as C storage, nitrogen fixation, and soil stabilization.

Acknowledgements.

Lee Taylor and Matthew Bowker provided manuscript feedback. This project originated as a project funded by Zack Sharp's Stable Isotope Biogeochemistry course and Dettweiler-Robinson received feedback from Dr. Sharp and the other students in the course. Viorel Atudorei and Laura Burkemper provided assistance with sample preparation and processing. The Sevilleta Long Term Ecological Station provided logistic support for sampling. We thank Eva's dad, Creighton Robinson, for letting us sample on his property.

References

Ahlstrom, A., M. R. Raupach, G. Schurgers, B. Smith, A. Arneth, M. Jung, M. Reichstein, J. G. Canadell, P. Friedlingstein, A.K. Jain, E. Kato, B. Pulter, S. Sitch, B. D. Stocker, N. Viovy, Y. P. Wang, A. Wiltshire, S. Zaehle, N. Zeng. 2015. The dominant role of semi-arid ecosystems in the trend and variability of the land CO_2 sink. Science 348:895–899.

Aranibar, J. N., I. C. Anderson, S. Ringrose, and S. A. Macko. 2003. Importance of nitrogen fixation in soil crusts of southern African arid ecosystems: acetylene reduction and stable isotope studies. Journal of Arid Environments 54:345–358.

Austin, A. T., and C. L. Ballaré. 2010. Dual role of lignin in plant litter decomposition in terrestrial ecosystems. Proceedings of the National Academy of Sciences 107:4618–4622.

Badger, M. R., and G. D. Price. 1992. The CO_2 concentrating mechanism in cyanobacteria and microalgae. Physiologia Plantarum 84:606–615.

Bai, E., T. W. Boutton, F. Liu, X. Ben Wu, and S. R. Archer. 2012. Spatial patterns of soil $\delta^{13}C$ reveal grassland-to-woodland successional processes. Organic Geochemistry 42:1512–1518.

Beck, A., and C. Mayr. 2012. Nitrogen and carbon isotope variability in the green-algal lichen *Xanthoria parietina* and their implications on mycobiont-photobiont interactions. Ecology and Evolution 2:3132–3144.

Belnap, J. 2002. Nitrogen fixation in biological soil crusts from southeast Utah, USA. Biology and Fertility of Soils 35:128–135.

Belnap, J., B. Budel, and O. L. Lange. 2001. Biological soil crusts: Characteristics and distribution. in J. Belnap and O. L. Lange, eds. Biological soil crusts: structure, function, and management. Springer Berlin / Heidelberg. 3-30.

Belnap, J., S. L. Phillips, D. L. Witwicki, and M. E. Miller. 2008. Visually assessing the level of development and soil surface stability of cyanobacterially dominated biological soil crusts. Journal of Arid Environments 72:1257–1264.

Benner, R., M. Fogel, E. K. Sprague, and R. E. Hodson. 1987. Depletion of ^{13}C in lignin and its implications for stable carbon isotope studies. Nature 329:708–710.

Brandt, L. A., J. Y. King, S. E. Hobbie, D. G. Milchunas, and R. L. Sinsabaugh. 2010. The role of photodegradation in surface litter decomposition across a grassland ecosystem precipitation gradient. Ecosystems 13: 765–781.

Breecker D. O, Z. D.Sharp, and L. D. McFadden. 2009. Seasonal bias in the formation and stable isotopic composition of pedogenic carbonate in modern soils from central New Mexico, USA. Bull Geol Soc Am 121:630–40.

Brüggemann, N., A. Gessler, Z. Kayler, S. G. Keel, F. Badeck, M. Barthel, P. Boeckx, N. Buchmann, E. Brugnoli, J. Esperschutz, O. Gavrichkova, J. Ghashghaie, N. Gomez-Casanovas, C. Keitel, A. Knohl, D. Kuptz, S. Palacio, Y. Salmon, Y. Uchida, M. Bahn. 2011. Carbon allocation and carbon isotope fluxes in the plant-soil-atmosphere continuum: a review. Biogeosciences 8:3457–3489.

Cable J. M. and T. E. Huxman. 2004. Precipitation pulse size effects on Sonoran Desert soil microbial crusts. Oecologia 141:317–24.

Collins, S. L., R. L. Sinsabaugh, C. Crenshaw, L. Green, A. Porras-Alfaro, M. Stursova, and L. H. Zeglin. 2008. Pulse dynamics and microbial processes in aridland ecosystems. Journal of Ecology 96:413–420.

Collins, S. L., J. Belnap, N. B. Grimm, J. A. Rudgers, C. N. Dahm, P. D. Odorico, M. Litvak, D. O. Natvig, D. C. Peters, W. T. Pockman, R. L. Sinsabaugh, and B. O. Wolf. 2014. A multiscale, hierarchical model of pulse dynamics in arid-land ecosystems. Annual Review of Ecology, Evolution, and Systematics 45:397–419.

Connin, S. L., X. Feng, and R. A. Virginia. 2001. Isotopic discrimination during long-term decomposition in an arid land ecosystem. Soil Biology and Biochemistry 33:41–51.

Cuna, S., G. Balas, and E. Hauer. 2007. Effects of natural environmental factors on $\delta^{13}C$ of lichens. Isotopes in Environmental and Health Studies 43:95–104.

Darrouzet-Nardi, A., S. C. Reed, E. E. Grote, and J. Belnap. 2015. Observations of net soil exchange of CO_2 in a dryland show experimental warming increases carbon losses in biocrust soils. Biogeochemistry 126:363–378.

de Guevara M. L., R. Lázaro, J. L. Quero, V. Ochoa, B. Gozalo, M. Berdugo, O. Uclés, C. Escolar, and F. T. Maestre. 2014. Simulated climate change reduced the capacity of lichen-dominated biocrusts to act as carbon sinks in two semi-arid Mediterranean ecosystems. Biodivers Conserv 23:1787–807.

Dumig, A., C. Rumpel, M. F. Dignac, and I. Kogel-Knabner. 2013. The role of lignin for the $\delta^{13}C$ signature in C_4 grassland and C_3 forest soils. Soil Biology and Biochemistry 57:1–13.

Elbert, W., B. Weber, S. Burrows, J. Steinkamp, B. Büdel, M. O. Andreae, and U. Pöschl. 2012. Contribution of cryptogamic covers to the global cycles of carbon and nitrogen. Nature Geoscience 5:459–462.

Fernandez, I., N. Mahieu, and G. Cadisch. 2003. Carbon isotopic fractionation during decomposition of plant materials of different quality. Global Biogeochemical Cycles 17:1-9.

Garcia-Pichel F., V. Loza, Y. Marusenko, P. Mateo, and R. M. Potrafka. 2013. Temperature drives the continental-scale distribution of key microbes in topsoil communities. Science 340:1574–7.

Green, L. E., A. Porras-Alfaro, and R. L. Sinsabaugh. 2008. Translocation of nitrogen and carbon integrates biotic crust and grass production in desert grassland. Journal of Ecology 96:1076–1085.

Grote, E. E., J. Belnap, D. C. Housman, and J. P. Sparks. 2010. Carbon exchange in biological soil crust communities under differential temperatures and soil water contents: implications for global change. Global Change Biology 16:2763–2774.

Gustavs, L., R. Schumann, U. Karsten, and M. Lorenz. 2016. Mixotrophy in the terrestrial green alga *Apatococcus lobatus* (Trebouxiophyceae, Chlorophyta). Journal of Phycology 52:311–314.

Huxman, T. E., K. A. Snyder, D. Tissue, A. J. Leffler, K. Ogle, W. T. Pockman, D. R. Sandquist, D. L. Potts, and S. Schwinning. 2004. Precipitation pulses and carbon fluxes in semiarid and arid ecosystems. Oecologia 141:254–268.

Jones, D. L., A. Hodge, and Y. Kuzyakov. 2004. Plant and mycorrhizal regulation of rhizodeposition. New Phytologist 163:459–480.

Kageyama, S. A., K. G. Mandayam, and A. Jumponnen. 2008. Diversity, function and potential applications of the root-associated endophytes. A. Varma, ed. Mycorrhiza: State of the art, genetics and molecular biology, eco-function, biotechnology, eco-physiology, structure and systematics. Springer-Verlag, Berlin Heidelberg. 29–57

Kattge, J., S. Diaz, S. Lavorel, I. C. Prentice, P. Leadley, G. Bonisch, E. Garnier, Westoby, M., Reich, P. B., Wright, I. J., Cornelissen, J. H. C., Violle, C., Harrison, S. P., Van Bodegom, P. M., Reichstein, M., Enquist, B. J., Soudzilovskaia, N. A., Ackerly, D. D., Anand, M., Atkin, O., Bahn, M., Baker, T. R., Baldocchi, D., Bekker, R., Blanco, C. C., Blonder, B., Bond, W. J., Bradstock, R., Bunker, D. E., Casanoves, F., Cavender-Bares, J., Chambers, J. Q., Chapin, F. S., Chave, J., Coomes, D., Cornwell, W. K., Craine, J. M., Dobrin, B. H., Duarte, L., Durka, W., Elser, J., Esser, G., Estiarte, M., Fagan, W. F., Fang, J., Fernandez-Mendez, F., Fidelis, A., Finegan, B., Flores, O., Ford, H., Frank, D., Freschet, G. T., Fyllas, N. M., Gallagher, R. V., Green, W. A., Gutierrez, A. G., Hickler, T., Higgins, S. I., Hodgson, J. G., Jalili, A.. Jansen, S., Joly, C. A., Kerkhoff, A. J., Kirkup, D., Kitajima, K., Kleyer, M., Klotz, S., Knops, J. M H, Kramer, K., Kuhn, I., Kurokawa, H., Laughlin, D., Lee, T. D., Leishman, M., Lens, F., Lenz, T., Lewis, S. L., Lloyd, J., Llusia, J., Louault, F., Ma, S., Mahecha, M. D., Manning, P., Massad, T., Medlyn, B. E., Messier, J., Moles, A. T., Muller, S. C., Nadrowski, K., Naeem, S., Niinemets, U., Nollert, S., Nuske, A., Ogaya, R., Oleksyn, J., Onipchenko, V. G., Onoda, Y., Ordonez, J., Overbeck, G., Ozinga, W. A., Patino, S., Paula, S., Pausas, J. G., Penuelas, J., Phillips, O. L., Pillar, V., Poorter, H., Poorter, L., Poschlod, P., Prinzing, A., Proulx, R., Rammig, A., Reinsch, S., Reu, B., Sack, L., Salgado-Negret, B., Sardans, J., Shiodera, S., Shipley,

B., Siefert, A., Sosinski, E., Soussana, J. F., Swaine, E., Swenson, N., Thompson, K., Thornton, P., Waldram, M., Weiher, E., White, M., White, S., Wright, S. J., Yguel, B., Zaehle, S., Zanne, A. E. Wirth, C.2011. TRY - a global database of plant traits. Global Change Biology 17:2905–2935.

Kuske C. R., L. O. Ticknor, M. E. Miller, J. M. Dunbar, J. A. Davis, S. M. Barns, and J. Belnap. 2002. Comparison of soil bacterial communities in rhizospheres of three plant species and the interspaces in an arid grassland. Appl Environ Microbiol 68:1854–63.

Lange O. L., J. Belnap, and H. Reichenberger. 1998. Photosynthesis of the cyanobacterial soil-crust lichen *Collema tenax* from arid lands in southern Utah, USA: role of water content on light and temperature responses of CO_2 exchange. Funct Ecol 12:195–202.

Milchunas, D. G., C. A. Lee, W. K. Laurenroth, and D. P. Coffin. 1992. A comparison of ^{14}C, ^{86}Rb, and total excavation for determination of root distributions of individual plants. Plant and Soil 144:125–132.

Moore, D. I. 2016. Meteorology Data from the Sevilleta National Wildlife Refuge, New Mexico (1988- present) Dataset. Sevilleta Long Term Ecological Research Site Database, Albuquerque, NM.

Mun, H. T., and W. G. Whitford. 1998. Changes in mass and chemistry of plant roots during long-term decomposition on a Chihuahuan Desert watershed. Biology and Fertility of Soils 26:16–22.

Murphy, K. L., J. M. Klopatek, and C. C. Klopatec. 1998. The effects of litter quality and climate on decomposition along an elevational gradient. Ecological Applications 8:1061–1071.

O'Leary, M. H. 1988. Carbon isotopes in photosynthesis. Bioscience 38:328–336.

Peterson, B. J., and B. Fry. 1987. Stable Isotopes in Ecosystem Studies. Annual Review of Ecology and Systematics 18:293–320.

Prăvălie R. 2016. Drylands extent and environmental issues. A global approach. Earth-Science Rev 161:259–78.

R Core Team. 2016. R: a language and environment for statistical computing. R Foundation for Statistical Computing, Vienna, Austria.

Ramnarine, R., R. P. Voroney, C. Wagner-Riddle, and K. E. Dunfield. 2011. Carbonate removal by acid fumigation for measuring the $\delta^{13}C$ of soil organic carbon. Canadian Journal of Soil Science 91:247–250.

Raven, J. A, C. S. Cockell, and C. L. De La Rocha. 2008. The evolution of inorganic carbon concentrating mechanisms in photosynthesis. Philosophical transactions of the Royal Society of London. Series B, Biological sciences 363:2641–2650.

Sponseller, R. A. 2007. Precipitation pulses and soil CO_2 flux in a Sonoran Desert ecosystem. Global Change Biology 13:426–436.

Thompson, T. L., E. Zaady, P. Huancheng, T. B. Wilson, and D. A. Martens. 2006. Soil C and N pools in patchy shrublands of the Negev and Chihuahuan Deserts. Soil Biology and Biochemistry 38:1943–1955.

Tiunov, A. V. 2007. Stable isotopes of carbon and nitrogen in soil ecological studies. Biology Bulletin 34:395–407.

Vuorio K., M. Meili, and J. Sarvala. 2006. Taxon-specific variation in the stable isotopic signatures ($\delta^{13}C$ and $\delta^{15}N$) of lake phytoplankton. Freshw Biol 51:807–22.

Wada E., K. Ohki, S. Yoshikawa, P.L. Parker, C. Van Baalen, G.I. Matsumoto, M.N. Aita, and T. Saino. 2012. Ecological aspects of carbon and nitrogen isotope ratios of cyanobacteria. Plankt Benthos Res 7:135–45.

Wang, C., D. Liu, W. Luo, Y. Fang, X. Wang, X. Lü, Y. Jiang, X. Hang, and E. Bai 2016. Variations in leaf carbon isotope composition along an arid and semi-arid grassland transect in Northern China. Journal of Plant Ecology.

Wedin, D. A., L. L. Tieszen, B. Dewey, and J. Pastor. 1995. Carbon isotope dynamics during grass decomposition and soil organic matter formation. Ecology 76:1383–1392.

Werth, M., and Y. Kuzyakov. 2010. ^{13}C fractionation at the root-microorganisms-soil interface: a review and outlook for partitioning studies. Soil Biology and Biochemistry 42:1372–1384.

Western Regional Climate Center. 2015. Local Climate Data Summaries. Retrieved from http://www.wrcc.dri.edu/cgi-bin/cliMAIN.pl?nm3031. 11/2/2016.

Willis, A., B. F. Rodrigues, and P. J. C. Harris. 2013. The ecology of arbuscular mycorrhizal fungi. Critical Reviews in Plant Sciences 32:1–20.

Wilske B., J. Burgheimer, A. Karnieli, E. Zaady, M. O. Andreae, D. Yakir, J. Kesselmeier. 2008. The CO_2 exchange of biological soil crusts in a semiarid grass-shrubland at the northern transition zone of the Negev desert, Israel. Biogeosciences 5:1411–23.

Yu, H., S. Jia, and Y. Dai. 2009. Growth characteristics of the cyanobacterium *Nostoc flagelliforme* in photoautotrophic, mixotrophic and heterotrophic cultivation. Journal of Applied Phycology 21:127–133.

Zelikova, T. J., D. C. Housman, E. E. Grote, D. A. Neher, and J. Belnap. 2012. Warming and increased precipitation frequency on the Colorado Plateau: implications for biological soil crusts and soil processes. Plant and Soil 355:265–282.

Zhou, T., R. Yu, H. Li, and B. Wang. 2008. Ocean forcing to changes in global monsoon precipitation over the recent half-century. Journal of Climate 21:3833–3852.

Figures

Chapter 2 Figure 1. Natural abundance $\delta^{13}C$ of *Gutierrezia sarothrae* (C_3, GUSA2) and *Bouteloua gracilis* (C_4, BOGR2) plant leaf tissue, the TRY database value for each species, and biocrust community collected from beneath GUSA2, BOGR2, and the interspace at two sites (Sevilleta and La Puebla) in New Mexico. Whiskers extend ±1 s.e. from the mean value. Letters show Tukey HSD post-hoc differences in biocrust community means for cover type across sites at $P \leq 0.05$.

Chapter 2 Figure 2. Natural abundance $\delta^{13}C$ of biocrust community and cyanobacteria/lichen isolates collected from a) beneath naturally-occurring *Gutierrezia sarothrae* (C_3 plant; GUSA2), *Bouteloua gracilis* (C_4 plant, BOGR2), and interspace areas, and b) in mesocosms that had either the *Bouteloua gracilis* removed or living. Whiskers extend ±1 s.e. from the mean value. Different letters within panels show Tukey HSD post-hoc differences in means for cover type across community/isolates at $P \leq 0.05$.

Chapter 2 Figure 1

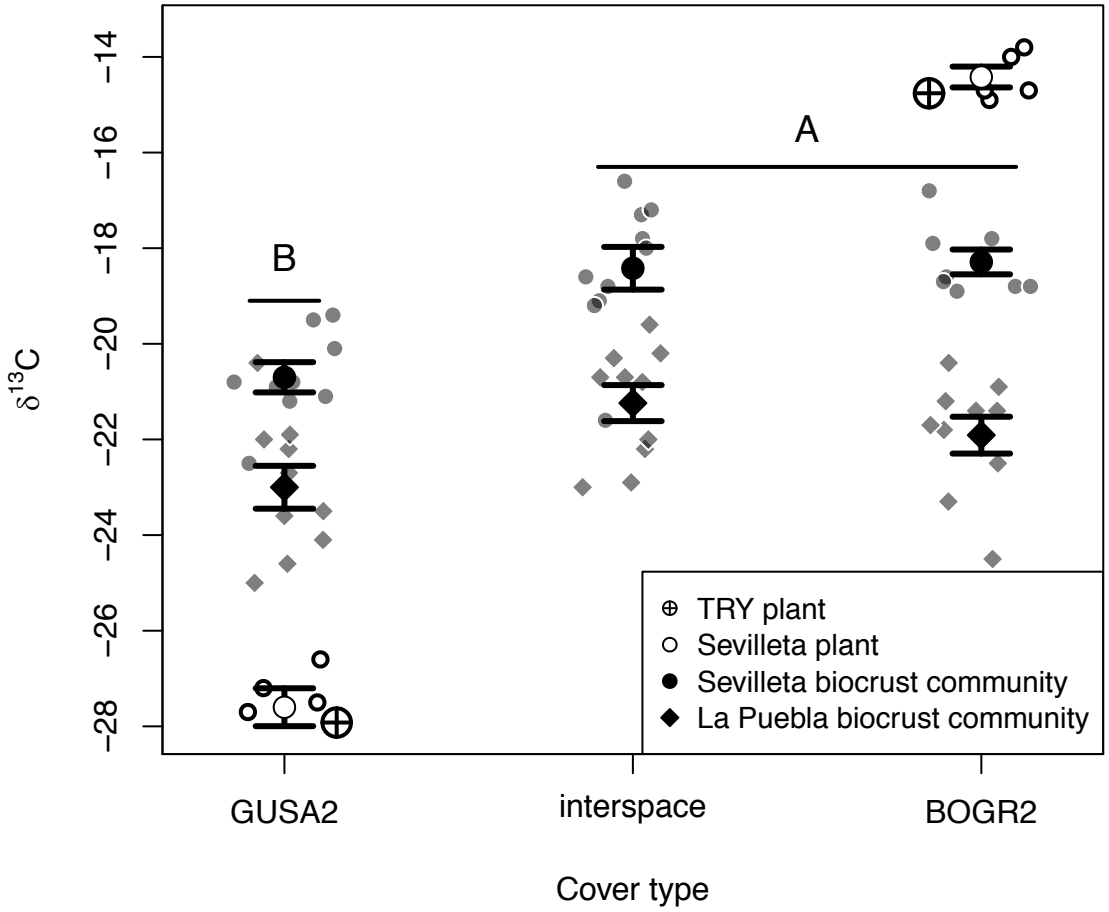

Chapter 2 Figure 2

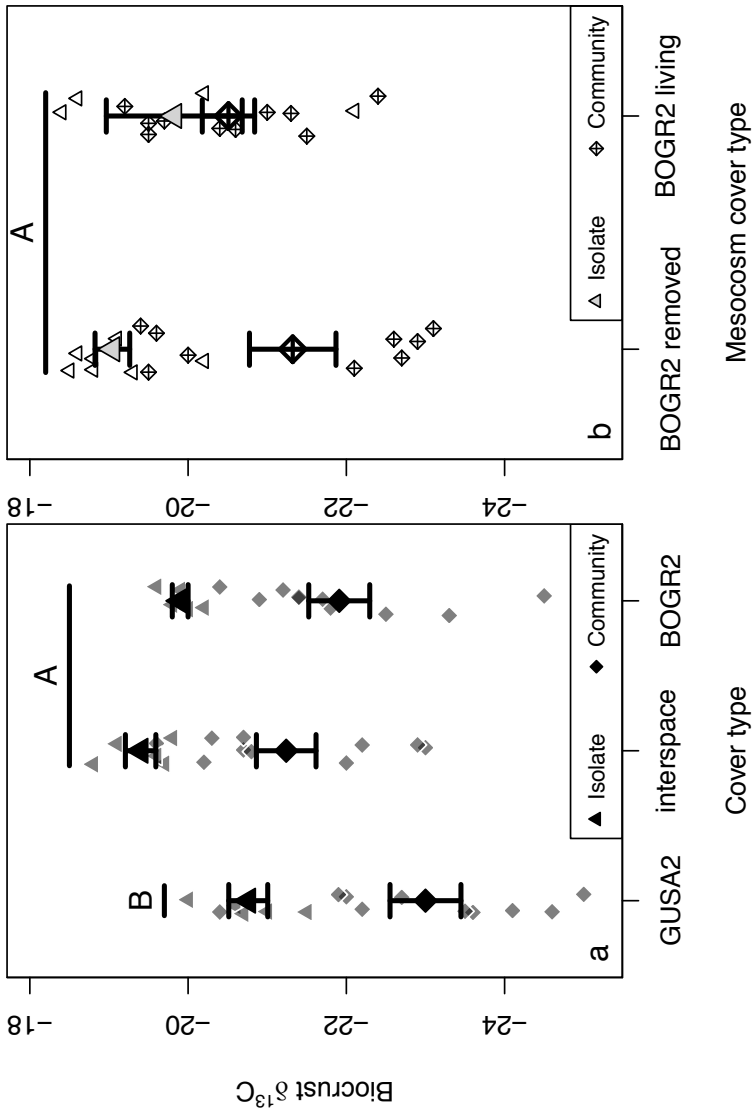

Supplementary Material

Chapter 2 Appendix 1. Percent carbon (mean ± s.e) in plant, biocrust community, and cyanobacteria/lichen isolates by site, cover type (GUSA2 = C_3 forb *Gutierrezia sarothrae*, BOGR2 = C_4 grass *Bouteloua gracilis*, and sample type.

Site	Cover type	Sample type	Percent carbon
Sevilleta	C_3	Plant	49.9 ± 1.2
		Biocrust community	1.2 ± 0.2
	interspace	Biocrust community	1.2 ± 0.2
	C_4	Plant	45.7 ± 0.3
		Biocrust community	1.7 ± 0.2
La Puebla	C_3	Biocrust community	1.2 ± 0.2
		Cyanobacteria/lichen	7.2 ± 1.1
	interspace	Biocrust community	1.4 ± 0.2
		Cyanobacteria/lichen	6.1 ± 0.8
	C_4	Biocrust community	1.5 ± 0.1
		Cyanobacteria/lichen	6.7 ± 0.8
La Puebla mesocosm	C_4 removed	Biocrust community	3.0 ± 0.4
		Cyanobacteria/lichen	6.5 ± 1.1
	C_4 living	Biocrust community	4.6 ± 0.5
		Cyanobacteria/lichen	15.0 ± 9.3

Chapter 3: Fungal connections between plants and biocrusts improve performance and resource content: a test of the fungal loop hypothesis in drylands

Eva Dettweiler-Robinson[1], Jenn Rudgers[1], Robert Sinsabaugh[1]

1. Department of Biology, MSC03 2020, 1 University of New Mexico, Albuquerque, NM 87131-0001

Abstract

Species interactions may couple the resource dynamics of primary producers that are disconnected in space and time. In dryland ecosystems, the primary producers are low density plant species and biological soil crusts. Biocrust activity is rapidly stimulated by rainfall events, but plants require larger events to infiltrate to roots, potentially decoupling their activities in time. Many biocrusts fix nitrogen, but plant roots typically do not extend into the surface soil to intercept it directly, potentially decoupling their activities in space. The fungal loop hypothesis proposes that fungi transport resources between plants and biocrusts, increasing total primary productivity by retaining nutrients in the soil surface and rhizosphere. However, the importance of fungi for plant and biocrust performance has not been investigated. We studied whether fungal connections between plants and biocrusts improve biocrust and plant performance, allocation patterns, or resource content, and whether precipitation regime affects these interactions by decoupling their activities in time. We transplanted a dominant bunchgrass and biocrusts into pots in the field then manipulated the connections between biocrusts and roots using hydrophilic meshes that either impeded or allowed fungal connections, and the precipitation regime (small, frequent vs. large, infrequent water additions). Under the small, frequent regime, biocrust chlorophyll content was 17% higher when fungal connections were intact than impeded. Under the large, infrequent precipitation regime,

plant biomass was >30% higher and the CN of plants and biocrusts were more similar when fungal connections were intact than impeded, suggesting that fungal-mediated resource transfers facilitate stoichiometric convergence. Intact fungal connections enhanced productivity of both primary producers, supporting the fungal loop hypothesis and suggesting that fungi play a major role in biogeochemical cycling in drylands.

Introduction

In ecosystems with low resource availability, the retention of resources in a biotic pool can reduce losses and increase productivity. For example, bacteria in the ocean rapidly mineralize resources from dead higher trophic levels, retaining nutrients in the photic zone rather and preventing loss due to sinking (Azam et al. 1983, Fenchel et al. 2008). Dryland ecosystems have low water and nitrogen availability, constraining productivity (Austin et al. 2004, Ladwig et al. 2012), and resources can be lost via physical and biological processes, such as evaporation, photodegradation (Austin and Vivanco 2006), erosion (Peterjohn and Schlessinger 1990), and denitrification (Marusenko et al. 2013). Species interactions could slow resource loss caused by physical processes by retaining resources in a biotic pool, enabling efficient exchanges, and thereby increasing productivity (Bardgett and Wardle 2010). In arid and semi-arid ecosystems, this process has been hypothesized to occur via soil fungi (Collins et al. 2008). However, this "Fungal Loop Hypothesis" has not been experimentally tested. The existence of a fungal loop would establish a fundamental difference in resource dynamics between drylands and better-studied mesic ecosystems where 1) the source of nutrients for plants is the large pool of soil organic matter processed by microbes (de Deyn et al. 2008), rather than the proposed resource transfers between living primary producers in

drylands and 2) the relative homogeneity of resources in space and time contrasts with the spatial and temporal variability of resources in drylands.

In dryland ecosystems, resource acquisition by different primary producers can be separated in both space and time, potentially accelerating resource losses from the system in the absence of species interactions. The key primary producers in drylands are plants and biological soil crusts (biocrusts). In dry grasslands, plants occur in a patchy distribution and generate the majority of organic matter (Aguilar and Sala 1999). Biocrusts occupy the surface interspaces between plants (separation in space) and consist of cyanobacteria, mosses, lichens, algae, and fungi, some of which fix atmospheric carbon or nitrogen (Belnap 2002). Nitrogen fixed by biocrusts may be a major source of plant N (Barger et al. 2016). For both plants and biocrusts, production is strongly controlled by soil moisture (Thomey et al. 2011). Biocrusts intercept rain events of all sizes, enabling their activity, but insufficient soil moisture can cause net losses of carbon because biocrusts require energy to re-activate after desiccation and they will respire for some time before beginning net photosynthesis (Belnap et al. 2004). Only large rain events will sufficiently increase soil moisture in the rhizospheres of plants to activate plant photosynthesis (Huxman et al. 2004). Thus, nitrogen produced by biocrusts during times that plants are not active may be leached (Veluci et al. 2006) and lost from the system (Belnap 2002).

Species interactions may increase the retention of resources by coupling the resource dynamics of primary producers that are disconnected in space and time. A fungal loop could couple the activities of plants and biocrusts in space by connecting plant patches to the biocrusts in plant interspaces. A fungal loop could couple the activities of plants and

biocrusts in time if fungi take up water or nutrients when they are readily available and transport these resources to primary producers once those producers become active. Prior work showed that fungi can be active at lower soil moistures than plants or bacteria (Allen 2007, Marusenko et al. 2013), supporting their potential role as a resource reserve. Additional evidence supports the hypothesis that fungi connect roots with biocrusts. In a C_4 grassland, plant rhizospheres and biocrusts shared approximately half of their fungal taxa (Porras-Alfaro et al. 2011), and in a creosote shrubland, plant rhizospheres and biocrusts shared 25% of their fungal taxa (Steven et al. 2014). Thus, the possibility exists for these shared fungi to connect plants with biocrusts. In addition, labeled isotope tracer studies have shown that nitrogen and carbon products can be translocated between plants and biocrusts (Hawkes 2003, Green et al. 2008, Zhuang et al. 2015). However, the mechanism of these transfers has not been documented and could involve roots, fungi, other microbes, or physical processes. Fungal hyphae may support more efficient translocation of resources than other potential mechanisms because movement of water and nutrients through hyphae is faster than through dry soil (Frey et al. 2003, Ruth et al. 2011). The ecological consequences of fungal connections for production and resource retention have not been resolved for any dryland ecosystem, and experiments are needed that directly test whether fungal connections between plants and biocrusts improve primary production.

The progression of climate change (IPCC 2013), may affect the ecological consequences of a fungal loop. For example, drought duration (Maloney et al. 2014) and extreme precipitation event sizes (Polley et al. 2013) are predicted to increase in drylands of the southwestern United States and globally (IPCC 2013). The activities of plants and

biocrusts are expected to vary with the precipitation regime, with plants responding only to large (>5mm) rain events, and microbes responding to both small and large events (Huxman et al. 2004). Fungal connections may help to buffer the negative effects of altered precipitation regimes by transferring resources between plants and biocrusts. However, whether the fungal loop shows context-dependency with precipitation regime is unresolved. In particular, it remains unclear whether the effects of fungal connections on plants, biocrusts, and resource retention are stronger under regimes of large, infrequent rain events that activate plants and biocrusts or under small, frequent events that activate only biocrusts.

In this study, we investigated three questions to test the fungal loop and assess its sensitivity to the precipitation regime. 1) Do fungal connections improve the performance of plants and/or biocrusts? We hypothesized that when fungal connections are intact, plant performance should be higher, with higher biomass and more allocation to aboveground and reproductive tissue than when connections are impeded. Biocrust performance should also be higher when fungal connections are intact than impeded, although they may be less responsive than plants because biocrusts can produce both carbon (C) and nitrogen (N), whereas plants require external sources of N. 2) Do fungal connections increase resource content in the plant-soil ecosystem? We expected higher levels of plant and soil N when fungal connections were intact than impeded. We also hypothesized that CN in plants and biocrusts should converge when fungal connections are intact if nutrients are transferred efficiently between them. 3) How much does the fungal loop vary with the precipitation regime? We expected fungal connections to be more important to the performance and nutrient content of primary producers under

precipitation regimes dominated by large rain events than those dominated by small event sizes, because N will become more limiting under higher water availability (Austin et al. 2004, Ladwig et al. 2012).

Methods

We established a mesocosm experiment in La Puebla, NM on private property (35.978, -105.995, WGS 84 Web Mercator). This site was a juniper savanna with scattered piñon pine (*Pinus edulis*) and one-seed juniper (*Juniperus monosperma*) trees and dominated by the bunchgrasses blue grama (*Bouteloua gracilis*) and Indian rice grass (*Achnatherum hymenoides*). Mature biocrusts contained cyanobacteria (*Microcoleus* sp., *Scytonema* sp., *Nostoc* sp.), mosses (including *Bryum argenteum, Syntrichia* sp. *Pterygoneurum* sp.), and lichens (*Collema* sp., *Placidium* sp.). The mean annual temperature is 11C and the site receives an average of 290mm of precipitation annually (Western Region Climate Center 2015), 190mm of which falls in the warm months (average minimum temperature > 0C May-Oct.). Most primary production is driven by summer monsoon rain events that vary in magnitude and frequency (Muldavin et al. 2008). Livestock grazing has been excluded since the 1950s.

Study species. We focused on *Bouteloua gracilis,* a widespread, dominant C_4 bunchgrass (Wynia 2002), which hosts root-endophytic fungi including arbuscular mycorrhizal fungi (Glomeromycota, with typically aseptate hyphae) and dark septate endophytes (Ascomycota) (Herrera et al. 2011, Porras-Alfaro et al. 2008). Root endophytic fungi have been shown to increase water uptake in *B. gracilis* (Allen 1982). Thus, when the system is activated by precipitation, we could potentially observe differences in plant performance caused by fungal-mediated resource transfer.

Mesocosm design. We used a 2 × 2 experimental design to manipulate fungal connections (intact vs. inhibited) in combination with the precipitation regime (large, infrequent vs. small, frequent rain events), with $n = 20$ replicates per treatment combination. We transplanted field-collected *B. gracilis* with intact rhizospheric soil and neighboring biocrusts into plastic pots (7.6L) in July-August 2013. We targeted plants that were 2-3cm in root crown diameter (estimated dry weight of initial aboveground biomass ~5g) to increase transplant survival compared to smaller plants. The pots were sunk into the ground to keep root conditions similar to the field, but the plastic isolated the target plant and biocrusts from the influence of neighbors. The plot was cleared of sparse existing vegetation and fenced to exclude large herbivores. Pots were arranged ~50cm apart in a randomized grid of 15 rows by 20 columns.

*Fungal connection treatment***.** To compare the effects of fungal connections on plant and biocrust performance, hydrophilic mesh was used to inhibit connections between the roots and biocrusts. For the intact fungal connections treatment, we used mesh with 50μm pores (Small Parts, Fort Meade, FL) to inhibit fine roots (Ares 1976), but fungal hyphae could grow through. For the impeded fungal connections treatment, we used mesh with 0.45μm pores (GE Healthcare Life Science, Pittsburg, PA) to inhibit both roots and fungi (Teste et al. 2006) because hyphal diameters range from 2-20μm (Dwivedi and Arora 1978). Bacteria/archaea could pass through both mesh sizes (Reed and Martiny 2007). The mesh was placed horizontally under the biocrust (~0.5-1cm depth) with a small hole (~5 cm diameter) cut in the center to allow the shoots of the bunchgrass to pass through.

In fall 2014, we checked a subsample of ~15 pots for roots occurring above the 0.45μm or 50μm mesh and found none. By the time of harvest in 2015, all plants had produced some roots above the mesh (mean = 27% ± 3.7 s.e. of total root weight across all pots), indicating that our impeded treatment reduced fungal connections, rather than fully impeding them. In Oct. 2015, we collected biocrust samples with a 2.5cm diameter soil core to a depth 0.5-1cm to determine the biomass of roots in the biocrusts. Differences by fungal connection and precipitation regime are presented in Results and Ch. 3 Appendix 2.

*Precipitation regime treatment***.** To assess context-dependency in the action of the fungal loop, we delivered the same volume of water to pots in different frequencies to compare small events that should activate surface microbes to large events that should activate both plants and biocrusts (Collins et al. 2014). The precipitation regime was either small, frequent events (100mL once per week, a 2.5mm event) or large, infrequent events (400mL once per month, a 10mm event). Additions were applied May to November. These size and magnitude patterns are typical for this region during the summer season (Western Regional Climate Center 2015). Pots additionally received natural rainfall. Water additions ensured that the organisms would survive, despite severe drought conditions in the region during the experiment (Helm 2014).

We installed a watering system (RBY100MPTX filter, Rainbird, Azusa, CA, USA; 1.9cm hose) that provided well water to the pots via maximum 12.11 L h^{-1} pressure compensating spray stakes (#22500-002030, Netafim USA, Fresno, CA, USA) and 91.4cm dripper assembly (#40201-002020; Netafim USA, Fresno, CA, USA). For the small, frequent treatment, we automated watering once per week for 1min using a timer

(Orbit model 62056, Orbit, Bountiful, Utah, USA). Although this design could provide up to 200mL of water per pot, the water output emitted from each sprayer was actually 100mL per event because the hose dried between applications. For the large, infrequent treatment, we hand-watered with well water once per month. The well water was higher in calcium, sodium, silicon, potassium, and magnesium (Ch. 3 Appendix 1) than rain water in the southwest US (Carroll 1962).

Response variables. To determine fungal abundance, we stained destructively-harvested roots in Oct. 2015 following Vierheilig et al. (1998), but modified the procedure in several ways: we left roots in KOH at room temperature for 4 days rather than boiling, removed the base by setting roots in 0.1N HCl overnight, then stained with ink (Parker Quink, Parker, Atlanta, GA, USA) and vinegar. We assessed root endophyte colonization of dark septate and aseptate (likely arbuscular mycorrhizal fungi) hyphae via microscopy following scoring methods of McGonigle et al. (1990). We also measured ergosterol in the biocrusts and rooting zone soils to account for fungal abundance of both root-associated and non-root associated fungi (e.g. pathogens, decomposers). We followed methods in Wallander et al. (2001) with the modification that no cyclohexane was added to the KOH-methanol extraction solution, and the solution was heated to 80C for 30 minutes. We created standards with 1- and 10μg ml^{-1} to calculate ergosterol content from area under the curve at 282nm. Ergosterol is not produced by arbuscular mycorrhizal fungi (Olsson et al. 2003). We included metrics for different functional groups of fungi that may interact with the plants, biocrusts, and other microbes in the system.

To determine whether soil moisture was affected by the fungal connection or precipitation regime, we used a TDR probe (Spectrum Technologies, Aurora, IL) with 3.8cm probes. To minimize disruption of the pots, we compared soil moisture a) opportunistically after a natural rain event just prior to the water additions in Aug. 2014 and b) just prior to and 8 hours after the weekly and monthly water additions in Sept. 2014.

To investigate biocrust performance, we sampled chlorophyll *a* in Oct. 2013 and Aug. and Oct. in 2014 and 2015, and scytonemin in Oct. 2015. Chlorophyll *a* increases with photosynthetic potential (Bowker et al. 2002), and scytonemin is a pigment produced by some cyanobacteria for UV protection (Belnap et al. 2004). We randomly sampled biocrusts by aggregating two 11mm diameter × 50mm depth samples into a 1.5mL centrifuge tube for each pot. We weighed each sample then added 1mL of dimethyl sulfoxide (single DMSO extraction with room temperature for 3d, so we captured ~75% of the chlorophyll content; Castle et al. 2011). We measured chlorophyll *a* content by absorbance at 665nm on a plate reader (Castle et al. 2011), and scytonemin content by absorbance at 384, 490, and 663nm (Mushir et al. 2014) with 750nm as a reference. Both pigments were calculated as content per g soil.

We investigated biomass as a metric of plant performance. We harvested plants and washed roots in Oct. 2015, dried them at 60C for 3d, and separately weighed root, aboveground, and total inflorescence (including stems) biomass. We collected seed biomass in 2014 and 2015. We counted the total number of inflorescences, and we removed and weighed seeds from seven random inflorescences. We estimated total seed weight based on the average weight per inflorescence and the total number of

inflorescences. The estimated seed weight was correlated to the total inflorescence biomass (total biomass = 0.732 × estimated seed weight + 0.11; $R^2 = 0.85$).

Additionally, to investigate if performance differed over time, we non-destructively assessed aboveground biomass in Aug. 2013 (~1 month after treatments started) and Aug. and Oct. 2014 and 2015. We created allometric equations to predict aboveground biomass from the largest diameter and the orthogonal diameter (aboveground biomass (g) = 0.5858 × largest dimension (cm) + 0.2734 × orthogonal dimension (cm) + 0.0688 × largest dimension (cm) × orthogonal dimension (cm); $R^2 = 0.88$, $F_{3,180} = 473.4$, $P < 0.001$).

To examine plant allocation patterns, we investigated allocation to roots and seeds, allocation of roots to shallow soils, and allocation patterns in leaves. We divided belowground biomass by total biomass and seed biomass by total (root + aboveground + seed) biomass. To assess root allocation to shallow soil layers, we used a 2.5 cm diameter soil core to collect the soil below the mesh to a depth of 5cm. We dried each core, passed it through 2mm mesh, and weighed the roots. We divided root biomass in the top 5cm sample by total biomass. Rooting depth generally increases with available moisture (van Wilk 2011), and roots can either accumulate to exploit abundant resources or accumulate at sites where scarce resources are likely to be intercepted (Forde and Lorenzo 2001). We determined specific leaf area (SLA) to understand if fungal connection or precipitation regime altered plant investment in thicker, longer-lasting leaves or thinner leaves with higher surface area. We clipped 10 leaves from each plant, rehydrated them in the dark for a minimum of 4 h, scanned the leaf area on a flatbed scanner (HP Photosmart C5180

All-In-One, HP, Palo Alto, CA, USA), and recorded dry weight (after 3d at 60C) (Perez-Harduindeguy et al. 2013).

We determined C and N content of leaves and biocrusts, and resource demand in biocrust and rooting zone soil. We dried samples of each type for 3d at 60C. We estimated molar CN from leaves (4mg) and biocrust (10mg) with the combustion method by elemental analyzer (Carlo Erba NC2100, CE Elantech, Lakewood, NJ, USA) from samples taken during harvest in Oct. 2015. We calculated total N in the mesocosms by summing N in biocrusts and plants. We multiplied percentage N in leaves by the total aboveground biomass and multiplied percentage N in biocrusts by the average mass of biocrust material (250g) in the pots.

We also assessed extracellular enzyme activities in the biocrust and rooting zone soil to assess resource demand and acquisition strategies (Sinsabaugh et al. 2008), because if more N is available, demand for N is hypothesized to be lower. Activities of β-1,4-glucosidase (β-gluc; enabling breakdown of cellulose in plant cell walls), leucine aminopeptidase (LAP, cleaving proteins; useful for acquiring N), and β- 1,4-N-acetylglucosaminidase (NAG, active in degrading chitin produced by fungi) were measured after 1 h on 1g of soil in 125mL bicarbonate buffer following methods in Stursova et al. (2006). We calculated CN_{EEA} = (β-gluc)/(NAG+LAP). To calculate biocrust carbon use efficiency, we used observed CN from combustion, CN_{EEA} from extracellular enzyme activity, and assumed the elemental CN of microbial biomass to be 9, and CUE_{max} of 0.60 with equations from Sinsabaugh et al. (2013).

Analyses. All analyses were run in R version 3.3.1 (2016-06-21; R Core Team 2016). We used qqplots to assess normality of residuals and plotted residuals vs. fitted

values to assess homogeneity of variances. We transformed response variables to best meet model assumptions. All general linear models were run in base R and general linear mixed models were run in package "lme4" (Bates et al. 2015).

Fungal connection treatment effectiveness. Because roots were present above the mesh at harvest in Oct. 2015, we determined if the biomass of roots (natural log transformed), the biomass of roots above the mesh:total root biomass (logit transformed), and the biomass of roots in the biocrust from the soil cores (natural log transformed) differed between fungal connection and precipitation regime. We used general linear mixed effect models to compare the septate and aseptate hyphal colonization (logit transformed) with microsite (above or below the mesh), fungal connection, and precipitation regime fully crossed with pot as a random effect. We also compared each fungal morphotype separately using general linear models.

To determine if the mesh used for the fungal connection treatment affected soil moisture, we used linear models to assess the difference in soil moisture before vs. after a natural rain event in Sept. 2014.

Precipitation regime treatment effectiveness. To assess the efficacy of the precipitation regime, we used general linear models to compare the difference in soil moisture from prior to and 8 hours after the watering event.

Responses to fungal connection and precipitation regime treatments. We constructed general linear models to test hypotheses. All models included the fixed effects of fungal connection, precipitation regime, and the connection × precipitation interaction. Spatial blocking effects representing the row and column of pots within the planting grid were included as potential covariates to account for variation across the

fully randomized grid, but if they were not significant (conservatively, $P > 0.10$), they were dropped from the analyses. We used a more conservative cut-off for removal of covariates to balance their potential contribution to the reduction in error variance with the increase in degrees of freedom when they were removed from the model. For significant or marginally non-significant interactions, we used planned post-hoc comparisons comparing fungal connection treatment within each precipitation regime level rather than all pairwise contrasts because our focus was on the context-dependency of the fungal connection treatments.

Fungal abundance. We measured fungal abundance because fungi may respond to fungal connection and precipitation regime, and in turn, may affect plant and biocrust response. We compared ergosterol content (natural log transformed) between microsites (biocrust vs. rooting zone soil) and below-mesh root colonization (logit transformed) by morphotype (dark septate vs. aseptate) with all interactions using pot as a random effect. We also compared each microsite and morphotype separately by with fungal connection and precipitation regime fully crossed.

To determine if we had captured diverse or redundant fungal characteristics, we also tested pairwise Spearman rank correlations.

Biocrust performance. We used general linear mixed effects models to compare chlorophyll *a* content (square root transformed) across treatments with date (year and month) as a categorical factor as an additional main effect with all interactions, and pot as a random effect to account for repeated measures. We used general linear models to compare scytonemin content (square root transformed) by treatments.

Plant performance. We used multivariate analysis of variance (MANOVA) to assess plant responses that are likely highly correlated. We z-scored all univariate responses, used the response variable as a predictor that did not interact with any treatment, and included pot as a random effect (Jeyabalasingham et al. 2011). We conducted MANOVAs to assess overall plant performance (root biomass, shoot biomass, and seed biomass in Oct. 2015).

Additionally, we used general linear mixed effect models to compare aboveground biomass estimated from allometry (square root transformed) and total seed weight (square root transformed) across treatments over time (see chlorophyll *a* analysis, above).

Resource content. For comparison of plant and biocrust CN and biocrust and rooting zone soil CN_{EEA}, we used general linear mixed effect models with sample type (plant or biocrust, biocrust and rooting zone soil), and all interactions with pot as a random effect. We compared each separately using general linear models. To compare total N in the primary producers, the difference between plant and biocrust CN, and biocrust CUE, we used general linear models.

Fungal abundance as covariates. For all plant and biocrust responses measured in 2015, we used general linear models and compared candidate models with fungal abundance covariates that were allowed to interact fully with all fungal connection × precipitation regime terms. We compared five candidate models using *AICc* for model selection: i) no fungal covariate, or including as a covariate ii) rooting zone ergosterol content, iii) biocrust ergosterol content, iv) dark septate hyphal colonization, or v) aseptate hyphal root colonization. We performed model selection with the following

univariate responses from Oct. 2015: chlorophyll *a* content (square root transformed), scytonemin content (square root transformed), total plant biomass (natural log transformed), root biomass (natural log transformed), aboveground biomass (from destructively sampled data, not allometrically-estimated data; square root transformed), seed biomass (square root transformed), root:total biomass (square root transformed), seed:total biomass (square root transformed), roots in the top 5cm:total biomass (+ 0.01, natural log transformed), SLA, total N in the primary producers, plant CN-biocrust CN, and biocrust CUE.

Results

Effectiveness of fungal connection treatment. The roots above the mesh in 2015 had potential unimpeded fungal and root connections with the biocrust. However, although the root mas and fungal colonization above the mesh differed by treatment combinations, this did not have a great enough effect to override the effects of the imposed treatments on plant and biocrust performance (see below). Root biomass above the mesh and biomass of roots in the biocrust did not differ significantly among fungal connection or precipitation regime treatments (Ch. 3 Appendix 2). Almost no roots above the mesh were in the biocrust (mean 0.002g ± 0.002 s.e., median = 0g) and instead were in a shallow soil layer below the biocrust. Across precipitation regimes, there was 41% higher root biomass above the mesh:root biomass when fungal connections were impeded than intact (t_{46} = -2.73, P = 0.01) which suggests that plants were allocating biomass to seek resources not available when fungal connections were impeded. For hyphal colonization in the roots above the mesh, in the large, infrequent precipitation regime, dark septate hyphal colonization was 86% higher when connections were intact than impeded (t_{49} =

2.53, $P = 0.01$), but in the small, frequent precipitation regime, there was no difference by fungal connections. There was no difference in aseptate colonization by fungal connection or precipitation regime treatments. There was no correlation between the colonization of roots above the mesh vs. below the mesh (aseptate: *rho* = 0.11, $S = 17387$, $P = 0.72$; dark septate: *rho* = 0.06, $S = 18460$, $P = 0.69$). We used colonization below the mesh in our model selection (below) because these fungi were likely present throughout the growth of the plant rather than only in 2015.

The mesh itself did not affect water flow, because one day after a natural rain event, there was no difference in moisture in the top 3.8cm by mesh type ($F_{1,75} = 2.24$, $P = 0.14$; Ch. 3 Appendix 3).

Effectiveness of precipitation regime treatment. The precipitation regime effectively altered soil moisture in the top 3.8cm (Ch. 3 Appendix 4). Eight hours after the watering events, the soil moisture increased 165% more in the large, infrequent regime than in the small, frequent regime ($F_{1,72} = 52.06$, $P < 0.001$). There was no effect of fungal connection ($F_{1,72} = 0.06$, $P = 0.81$) or connection × precipitation regime ($F_{1,72} = 0.17$, $P = 0.67$), suggesting that different mesh pore sizes had no effect on water relations.

Fungal abundance. Fungal abundances and correlations were generally independent of fungal connection treatments (Ch. 3 Table 1, Ch. 3 Appendix 5), indicating that the differences in plant and biocrust performances result from disruption of fungal connections rather than changes in fungal abundance, and we captured distinct fungal communities with the microsite and morphotype sampling. However, in the small, frequent precipitation regime, intact fungal connections increased aseptate colonization by 100% relative to impeded connections ($t_{134} = 2.15$, $P = 0.03$), whereas, in the large,

infrequent regime, the there was no difference between connection treatments. Dark septate hyphal colonization did not differ by fungal connection or precipitation regime.

Fungal abundance metrics did respond to the precipitation regime (Ch. 3 Table 1, Ch. 3 Appendix 5). In the large, infrequent precipitation regime had 44% lower biocrust ergosterol content (t_{73} = 3.10, P = 0.002) and 45% lower aseptate hyphal colonization (t_{72} = 2.67, P = 0.01) than in the small, frequent regime. In contrast, precipitation regime had no effect on rooting zone soil ergosterol. Ergosterol content in the rooting zone soil microsite was 82% lower than in the biocrust, suggesting potential differences in composition between fungal assemblages in biocrust and rooting zone.

Biocrust performance. We detected large differences in chlorophyll *a* across dates (as has been observed previously; Bowker et al. 2002), so we were confident in the ability to detect variability in biocrust performance. After the first year, in the small, frequent precipitation regime, fungal connection intact tended to enhance biocrust performance compared to connections impeded (Ch. 3 Table 2, Ch. 3 Fig. 1, Ch. 3 Appendix 6): in Oct. 2013, chlorophyll *a* content was 24% lower when fungal connections were intact than impeded (t_{312} = 1.78, P = 0.08), but was 20% higher in Oct. 2014 (t_{312} = 1.78, P = 0.08), and 17% higher in Oct. 2015 (t_{312} = -0.77, P = 0.44) when connections were intact than impeded. Scytonemin content in the large, infrequent precipitation regime was 47% lower with fungal connections intact than impeded (t_{42} = -2.08, P = 0.04), but scytonemin content in the small, frequent precipitation regime did not differ by connection (Ch. 3 Fig. 2). Changes in scytonemin content may indicate an increased biocrust stress response when fungal connections are impeded, or alternately may reflect differences in the

biocrust community, such as shifts from *Scytonema*/*Nostoc* to *Microcoleus* which does not produce scytonemin.

Fungal abundance in plant roots was included in the model for scytonemin content in Oct. 2015 (Ch. 3 Table 2, Ch. 3 Appendix 7). Scytonemin content responded positively to dark septate colonization (l.s. slope = 0.84 ± 0.04 s.e.). Dark pigments (melanin in fungi, [Butler and Day 1998] and scytonemin in cyanobacteria) may be a response to stress and may therefore covary.

Plant performance. Differences in plant biomass by fungal connection and precipitation treatments were driven by aboveground and seed biomass with less varation in belowground biomass (Ch. 3 Table 3, Ch. 3 Appendix 8). Throughout their growth, plants in the large, infrequent precipitation regime had higher aboveground biomass (43% in Aug. 2013 $t_{138} = 3.32$, $P = 0.001$; 33% in Oct 2014, $t_{138} = 4.94$, $P < 0.001$; 38% in Oct. 2015, $t_{138} = 4.88$, $P < 0.001$) when fungal connections were intact than impeded (Ch. 3 Fig. 3). Similarly, seed biomass in the large, infrequent precipitation regime was 44% higher in Oct. 2014 ($t_{132} = 1.42$, $P = 0.16$) and 51% higher in Oct. 2015 ($t_{138} = 2.15$, $P = 0.03$) with fungal connections intact than impeded (Ch. 3 Fig. 4).

Total and root biomass in Oct. 2015 were positively related to dark septate colonization (l.s. mean = 3.39 ± 0.05 and 2.87 ± 0.05, respectively), but we cannot resolve if root-associated fungi stimulated biomass production, or if larger plants supported more fungi. Seed biomass in Oct. 2015 was positively related to rooting zone ergosterol content (l.s. mean = 1.07 ± 0.04) suggesting that belowground interactions increase plant fitness.

Allocation patterns of plant biomass responded to treatments (Ch. 3 Table 4, Ch. 3 Appendix 9). In the small, frequent precipitation regime, root:total biomass was 19% higher (t_{57} = 0.85, P = 0.07) and seed:total biomass was 85% lower (t_{57} = 2.04, P = 0.04) with fungal connections intact than impeded, but there was no difference in allocation in the large, infrequent regime. Allocation of roots to the top 5cm was 46% higher when fungal connections were impeded than intact (Ch. 3 Table 4, Ch. 3 Fig. 5). Plants may have allocated less to shallow soil layers when fungi were able to access the surface. Specific leaf area did respond to either fungal connection or precipitation regime treatment (Ch. 3 Appendix 9).

Resource content. Total N content in the plant-biocrust system did not differ by fungal connection or precipitation regime (Ch. 3 Table 5, Ch. 3 Appendix 10). When we compared resource content in plants and biocrusts separately, plant leaf CN in the large, infrequent precipitation regime was 15% lower when fungal connections were intact than impeded (Ch. 3 Fig. 6; t_{109} = -3.38, P = 0.001), but in the small, frequent precipitation regime, leaf CN was 6% higher when fungal connections were intact than impeded (t_{109} = 1.64, P = 0.10; Ch. 3 Fig. 6). Biocrust CN did not differ by fungal connection or precipitation regime treatment. In the large, infrequent regime, the difference between plant and biocrust CN was 32% higher when fungal connections were impeded than intact. This reduced difference was expected if resources were transferred based on a resource gradient from low CN in the biocrusts to high CN in the plants and there was an efficient pathway connecting the two (i.e., fungal hyphae). In the small, frequent precipitation regime, there was no difference in plant - biocrust CN between fungal connection treatments.

In the large, infrequent precipitation regime, CN_{EEA} in rooting zone soil was 86% higher (t_{132} = 3.09, P = 0.002) and in biocrusts was 18% higher (t_{132} = 1.93, P = 0.06) with fungal connections intact than impeded (Ch. 3 Table 5, Ch. 3 Fig. 7, Ch. 3 Appendix 10) suggesting lower N demand with connections intact. In the small, frequent precipitation regime, there were no significant differences between fungal connection. There was no difference in biocrust carbon use efficiency across fungal connection or precipitation regime treatments, suggesting no difference in allocation to microbial growth vs. maintenance/respiration.

Discussion

Do fungal connections improve the performance of plants and/or biocrusts? Plant and biocrust performance was enhanced by fungal connections between the rhizosphere and biocrusts. Plant performance (aboveground biomass and seed weight) was higher with intact fungal connections than with impeded connections, suggesting that fungal connections to the biocrust may have enhanced uptake of limiting resources, allowing plants to maintain higher biomass (Smith and Read 2008, Mandyam and Jumponnen 2005). Plant allocation patterns reflected the allocation to foraging for soil resources (high root:total biomass) when the fungal connections were impeded. Plants have been shown to allocate more to roots in shallow depths under low resource conditions (Ho et al. 2005). However, plants face trade-offs with such allocation, because shallow soils are more subject to wet-dry cycles and thus present harsher conditions for root growth (Schwinning and Ehlringer 2001). Biocrusts showed less response to fungal connection treatments, perhaps because they are able to produce both C and N and did not rely on transport of resources from deeper soil layers. Biocrusts responded to fungal connections

under the small, frequent precipitation regime rather than the large, infrequent regime, supporting the role of fungi as benefiting producers that are active with different temporal patterns. Biocrusts may benefit directly from fungal connections due to resource transfer, or indirectly if fungal connections improve plant performance which in turn ameliorates environmental conditions through shading from a larger, healthier plant.

Several potential mechanisms may underlie enhanced plant and biocrust productivity when fungal connections were intact. First, fungi could provide resources mechanistically through hydraulic redistribution (Allen et al. 2007, Prieto et al. 2012) and C or N translocation (He et al. 2003). We found lower CN in plants when fungal connections were intact, consistent with the hypothesis that fungi can transport N from the biocrusts to the plant roots. Fungi are the best candidates for translocating water and nutrients because their small-diameter, linear networks of hyphae, presence in both the plants and biocrusts (Porras-Alfaro et al. 2011), and rapid cytoplasmic movement in hyphae (Lew et al. 2005). Other potential biotic factors include microarthropods and other microbes. Microarthropods could affect resource cycling (Darby and Neher 2016), and may also have been impeded from traveling between the biocrust and rooting zone soil by the mesh. If bacteria and archaea were the main drivers of the interactions, we would not have seen a difference between the fungal connection treatments because bacteria and archaea could fit through both mesh types. Thus we conclude that these groups did not contribute to the effects observed.

Do fungal connections increase resource content in the plant-soil ecosystem? Although there was not a difference in the total amount of nitrogen in the plant-biocrust system, the CN of plants in mesocosms with intact fungal connection were more similar

to biocrust CN than with connections impeded, suggesting that fungal hyphae could act as conduits that connect the plants and biocrusts to move N along a gradient (biocrust: high N content; plants: low N content; Boberg et al. 2010). Biocrust CN may have responded less strongly to fungal connections than plants because biocrusts are able to fix both carbon and nitrogen and thus may rely less on transport up from deeper soil layers.

How much does the fungal loop depend on the precipitation regime? Plant and biocrust response to fungal connections was context-dependent on precipitation regime. Under the small, frequent precipitation regime, biocrusts responded positively to fungal connections, suggesting connections ameliorated stressful water conditions (as has been observed with arbuscular mycorrhizal plants; Augé et al. 2015). Plants showed little response to fungal connections under the small, frequent regime, suggesting that fungi may enhance performance only when plants have sufficient water resources to support symbiont activity. Fungi have been shown to take up >5% of plant carbon (Jones 2009), and thus plants may need to be robust enough to maintain the interaction with their root-associated fungi. Similar context-dependency on resource availability has been found in other plant-microbe systems (Hoeksema et al. 2010). For example, mesic grasslands, limited P vs. N availability result in mutualistic vs. commensalistic outcomes of plant-arbuscular mycorrhizal interactions (Johnson et al. 2015). With dark septate endophyte interactions, availability of simple sugars and organic nitrogen sources in the environment increased the growth of inoculated plants compared to uninoculated plants (Mayerhofer et al. 2013). Thus precipitation may directly affect interactions based on which species are active at the same times, or may indirectly affect interactions by supporting activity and production which creates resources to be exchanged.

Conclusions

Research on plants and biocrusts, the two primary producers in drylands, has proceeded largely independently, with the assumption that they are functionally isolated (Schlesinger et al. 1990). However, without a mechanism that allows resource transfer (e.g. nitrogen fixed by biocrusts is taken up by plants), resources may be depleted from the ecosystem. The fungal loop provides a mechanism for biotic control of resource retention. Understanding how the fungal loop changes with precipitation regime is important for predicting shifts in resource retention and primary production in drylands under climate change.

Acknowledgements

We acknowledge undergrads Nada Kherbik, Amre Elmauoed, Ryan Sanchez, and others who assisted with lab and field work. We received support from UNM Biology and Biology Graduate Student Association grants. Lee Taylor and Matthew Bowker provided manuscript feedback. We thank Eva's dad, Creighton Robinson, for letting us sample on his property.

References

Aguilar, M.R. & Sala, O.E. (1999). Patch structure, dynamics and implications for the functioning of arid ecosystems. *Trends Ecol. Evol.*, 14, 273–277

Allen, M.F. (1982). Influence of vesicular-arbuscular mycorrhizae on water movement through *Bouteloua gracilis* (H.B.K.) Lag ex steud. *New Phytol.*, 91, 191–196

Allen, M.F. (2007). Mycorrhizal fungi: highways for water and nutrients in arid soils. *Vadose Zo. J.*, 6, 291–297

Ares, J. (1976). Dynamics of the root system of Blue Grama. *J. Range Manag.*, 29, 208–213

Augé, R.M., Toler, H.D. & Saxton, A.M. (2015). Arbuscular mycorrhizal symbiosis alters stomatal conductance of host plants more under drought than under amply watered conditions: a meta-analysis. *Mycorrhiza*, 25, 13–24

Austin, A.T., Yahdjian, L., Stark, J.M., Belnap, J., Porporato, A., Norton, U., D.A. Ravetta & Schaeffer, S. M. (2004). Water pulses and biogeochemical cycles in arid and semiarid ecosystems. *Oecologia*, 6, 221–235

Austin, A.T. & Vivanco, L. (2006). Plant litter decomposition in a semi-arid ecosystem controlled by photodegradation. *Nature*, 442, 555–558

Azam, F., Field, J.G., Graf, J.S., Meyer-Rei, L.A. & Thingstad, F. (1983). The Ecological Role of Water-Column Microbes in the Sea, *Mar. Ecol. Prog. Ser*, 10, 257–263

Bardgett, R.D. & Wardle, D.A. (2010). *Aboveground-belowground linkages: biotic interactions, ecosystem processes, and global change*. Oxford University Press, Oxford

Barger, N.N., Weber, B., Garcia-Pichel, F., Zaady, E. & Belnap, J. (2016). Patterns and controls on nitrogen cycling of biological soil crusts. In: *Biological soil crusts: an organizing principle in drylands* (eds. Webber, B., Budel, B. & Belnap, J.). Springer International Publishing, pp. 257–285

Bates, D. M. Maechler, B. Bolker & S. Walker (2015). Fitting Linear Mixed-Effects Models Using lme4. Journal of Statistical Software, 67(1), 1-48.

Belnap, J. (2002). Nitrogen fixation in biological soil crusts from southeast Utah, USA. *Biol. Fertil. Soils*, 35, 128–135

Belnap, J., Phillips, S.L. & Miller, M.E. (2004). Response of desert biological soil crusts to alterations in precipitation frequency. *Oecologia*, 141, 306–316

Bowker, M.A., Reed, S.C., Belnap, J. & Phillips, S.L. (2002). Temporal variation in community composition, pigmentation , and Fv/Fm of desert cyanobacterial soil crusts. *Microb. Ecol.*, 43, 13–25

Butler, M. J. & A. W. Day. 1998. Fungal melanins: a review. Canad. J. Microb, 44, 1115-1136.

Carroll, D. (1962). *Rainwater as a Chemical Agent of Geologic Processes-A Review*. Geological Survey Water-Supply Paper 1535-G.

Castle, S.C., Morrison, C.D. & Barger, N.N. (2011). Extraction of chlorophyll a from biological soil crusts: a comparison of solvents for spectrophotometric determination. *Soil Biol. Biochem.*, 43, 853–856

Collins, S.L., Sinsabaugh, R.L., Crenshaw, C., Green, L., Porras-Alfaro, A., Stursova, M. & Zeglin, L. (2008). Pulse dynamics and microbial processes in aridland ecosystems. *J. Ecol.*, 96, 413–420

Collins, S.L., Belnap, J., Grimm, N.B., Rudgers, J.A., Dahm, C.N., Odorico, P.D., Litvak, M., Natvig, D.O., Peters, D.C., Pockman, W.T., Sinsabaugh, R.L. & Wolf, B.O. (2014). A multiscale, hierarchical model of pulse dynamics in arid-land ecosystems. *Annu. Rev. Ecol. Evol. Syst.*, 45, 397–419

Darby, B. & D. A. Neher (2016). Microfauna within biological soil crusts. In: *Biological soil crusts: an organizing principle in drylands* (eds. Weber, B., Budel, B. & Belnap, J.). Springer International Publishing, pp. 139–157

De Deyn, G.B., Cornelissen, J.H.C. & Bardgett, R.D. (2008). Plant functional traits and soil carbon sequestration in contrasting biomes. *Ecol. Lett.*, 11, 516–531

Dwivedi, R.S. & Arora, D.K. (1978). Hyphal interaction among some soil fungi. *Plant Soil*, 50, 571–574

Fenchel, T. (2008). The microbial loop – 25 years later. *J. J Exp. Mar. Biol. Ecol.,* 366, 99-103

Frey, S.D., Six, J. & Elliott, E.T. (2003). Reciprocal transfer of carbon and nitrogen by decomposer fungi at the soil–litter interface. *Soil Biol. Biochem.*, 35, 1001–1004

Forde, B. & Lorenzo, H. (2001). The nutritional control of root development. *Plant Soil*, 232, 51–68

Green, L.E., Porras-Alfaro, A. & Sinsabaugh, R.L. (2008). Translocation of nitrogen and carbon integrates biotic crust and grass production in desert grassland. *J. Ecol.*, 96, 1076–1085

Hawkes, C.V. (2003). Nitrogen cycling mediated by biological soil crusts and arbuscular mycorrhizal fungi. *Ecology*, 84, 1553–1562

He, X.-H., Critchley, C. & Bledsoe, C. (2003). Nitrogen transfer within and between plants through common mycorrhizal networks (CMNs). *CRC. Crit. Rev. Plant Sci.*, 22, 531–567

Helm, R. (2014). *U.S. Drought Monitor*. *NOAA*. Available at: http://droughtmonitor.unl.edu/. Last accessed

Herrera, J., Poudel, R., Nebel, K. A. & Collins, S.L. (2011). Precipitation increases the abundance of some groups of root-associated fungal endophytes in a semiarid grassland. *Ecosphere*, 2, art50

Ho, M.D., Rosas, J.C., Brown, K.M. & Lynch, J.P. (2005). Root architectural tradeoffs for water and phosphorus acquisition. *Funct. Plant Biol.*, 32, 737–748

Hoeksema, J.D., Chaudhary, V.B., Gehring, C.A., Johnson, N.C., Karst, J., Koide, R.T. A. Pringle, C. Zabinski, J. D. Bever, J. C. Moore, G. W. T. Wilson, J. N. Klironomos, & J. Umbanhowar (2010). A meta-analysis of context-dependency in plant response to inoculation with mycorrhizal fungi. *Ecol. Lett.*, 13, 394–407

Huxman, T.E., Snyder, K.A., Tissue, D., Leffler, A.J., Ogle, K., Pockman, W.T., Sandquist, D.R., Potts, D.L. & Schwinning, S. (2004). Precipitation pulses and carbon fluxes in semiarid and arid ecosystems. *Oecologia*, 141, 254–268

IPCC 2013. Climate change 2013: the physical science basis. fifth assessment report of the intergovernmental panel on climate change. In: Stocker TF, Qin D, Plattner G-K, Tignor M, Allen SK, Boschung J, Nauels A, Xia Y, Bex V, Midgley PM eds. Cambridge, United Kingdom and New York, NY, USA: Cambridge Press, 1535 pp.

Jeyabalasingham, A. & Ragavan, A.J. (2011). Repeated Measures Analysis of Correlated Data with Multiple Responses using SAS. *SAS Paper.*, 231, 1–10

Johnson, N.C., Wilson, G.W.T., Wilson, J.A., Miller, R.M. & Bowker, M.A. (2015). Mycorrhizal phenotypes and the Law of the Minimum. *New Phytol.*, 205, 1473–1484

Jones, D.L., Kielland, K., Sinclair, F.L., Dahlgren, R.A., Newsham, K.K., Farrar, J.F. & Murphy, D.V. (2009). Soil organic nitrogen mineralization across a global latitudinal gradient. *Global Biogeochem. Cycles*, 23, 1–5

Ladwig, L.M., Collins, S.L., Swann, A.L., Xia, Y., Allen, M.F. & Allen, E.B. (2012). Above- and belowground responses to nitrogen addition in a Chihuahuan Desert grassland. *Oecologia*, 169, 177–85

Lew, R.R. (2005). Mass flow and pressure-driven hyphal extension in Neurospora crassa. *Microbiology*, 151, 2685–2692

Maloney, E.D., Camargo, S.J., Chang, E., Colle, B., Fu, R., Geil, K.L., Hu, Q., Jiang, X., Johnson, N., Karnauskas, K.B., Kinter, J., Kirtman, B., Kumar, S., Langenbrunner, B., Lombardo, K., Long, L.N., Mariotti, A., Meyerson, J.E., Mo, K.C., Neelin, J.D., Zaitao, P., Seager, R., Serra, Y., Seth, A., Sheffield, J., Stroeve, J., Thibeault, J., Xie, S., Wang, C., Wyman, B. & Zhao, M. (2014). North American climate in CMIP5 experiments: Part III: Assessment of twenty-first-century projections. *J. Clim.*, 27, 2230–2270

Mandyam, K. & Jumpponen, A. (2005). Seeking the elusive function of the root-colonising dark septate endophytic fungi. *Stud. Mycol.*, 53, 173–189

Marusenko, Y., Huber, D.P. & Hall, S.J. (2013). Fungi mediate nitrous oxide production but not ammonia oxidation in aridland soils of the southwestern US. *Soil Biol. Biochem.*, 63, 24–36

Mayerhofer, M.S., Kernaghan, G. & Harper, K.A. (2013). The effects of fungal root endophytes on plant growth: A meta-analysis. *Mycorrhiza*, 23, 119–128

McGeehan, S. & Naylor, D. (1988). Automated instrumental analysis of carbon and nitrogen in plant and soil samples. *Commun. Soil Sci. Plant Anal.*, 19, 493–505

McGonigle, T.P., Miller, M.H., Evans, D.G., Fairchild, L. & Swan, J.A. (1990). A new method which gives an objective measure of colonization of roots by vesicular-arbuscular mycorrhizal fungi. *New Phytol.*, 115, 495–501

Muldavin, E.H., Moore, D.I., Collins, S.L., Wetherill, K.R. & Lightfoot, D.C. (2008). Aboveground net primary production dynamics in a northern Chihuahuan Desert ecosystem. *Oecologia*, 155, 123–32

Mushir, S., Deep, S. & Fatma, T. (2014). Screening of cyanobacterial strains for UV screening compound scytonemin - environmental perspectives. *Int. J. Innov. Res. Sci. Eng. Technol.*, 3, 9191–9196

Olsson, P. A., Larsson, L., Bago, B., Wallander, H. & Aarle, I. M. (2003). Ergosterol and fatty acids for biomass estimation of mycorrhizal fungi. *New Phytol*., 159: 7–10.

Pérez-Harguindeguy, N., Diaz, S., Garnier, E., Lavorel, S., Poorter, H., Jaureguiberry, P., Bret-Harte, M.S. S., Cornwell, W.K. K., Craine, J.M. M., Gurvich, D.E. E., Urcelay, C., Veneklaas, E.J. J., Reich, P.B. B., Poorter, L., Wright, I. J. J., Ray, P., , Enrico, L., Pausas, J. G., Vos, A. C. de, Buchmann, N., Funes, G., Quétier, F., Hodgson, J. G., Thompson, K., Morgan, H. D., Steege, H. ter, Heijden, M. G. A. van der, Sack, L., Blonder, B., Poschlod, P., Vaieretti, M. V., Conti, G., Staver, A. C., Aquino, S. & Cornelissen, J. H. C. (2013). New Handbook for standardized measurement of plant functional traits worldwide. *Aust. J. Bot.*, 61, 167–234

Peterjohn, W.T. & Schlesinger, W.H. (1990). Nitrogen loss from deserts in the southwestern United States. *Biogeochemistry*, 10, 67–79

Polley, H.W., Briske, D.D., Morgan, J.A., Wolter, K., Bailey, D.W. & Brown, J.R. (2013). Climate change and North American rangelands: trends, projections, and implications. *Rangel. Ecol. Manag.*, 66, 493–511

Porras-Alfaro, A., Herrera, J., Sinsabaugh, R.L., Odenbach, K.J., Lowrey, T. & Natvig, D.O. (2008). Novel root fungal consortium associated with a dominant desert grass. *Appl. Environ. Microbiol.*, 74, 2805–13

Porras-Alfaro, A. & Bayman, P. (2011). Hidden fungi, emergent properties: endophytes and microbiomes. *Annu. Rev. Phytopathol.*, 49, 291–315

Prieto, I., Armas, C. & Pugnaire, F.I. (2012). Water release through plant roots: new insights into its consequences at the plant and ecosystem level. *New Phytol.*, 193, 830–841

Reed, H. & Martiny, J. (2007). Testing the functional significance of microbial composition in natural communities. *FEMS Microbiol. Ecol.*, 62, 161–170

Ruth, B., Khalvati, M. & Schmidhalter, U. (2011). Quantification of mycorrhizal water uptake via high-resolution on-line water content sensors. *Plant Soil*, 342, 459–468

Schwinning, S. & Ehleringer, J.R. (2001). Water use trade-offs and optimal adaptations to pulse-driven arid ecosystems. *J. Ecol.*, 89, 464–480

Sinsabaugh, R.L., Lauber, C.L., Weintraub, M.N., Ahmed, B., Allison, S.D., Crenshaw, C., Contosta, A. R., Cusack, D., Frey, S., Gallo, M. E., Gartner, T. B., Hobbie, S. E., Holland, K., Keeler, B. L., Powers, J. S., Stursova, M., Takacs-Vesbach, C., Waldrop,

M. P., Wallenstein, M. D., Zak, D. R. & Zeglin, L. H. (2008). Stoichiometry of soil enzyme activity at global scale. *Ecol. Lett.*, 11, 1252–1264

Sinsabaugh, R.L., Manzoni, S., Moorhead, D.L. & Richter, A. (2013). Carbon use efficiency of microbial communities: stoichiometry, methodology and modelling. *Ecol. Lett.*, 16, 930–939

Smith, S. & Read, D. (2008). Mineral nutrition, toxic element accumulation and water relations of arbuscular mycorrhizal plants. In: *Mycorrhizal Symbiosis* (eds. Smith, S. & Read, D.). London, pp. 145–187

Steven, B., Gallegos-Graves, L.V., Yeager, C., Belnap, J. & Kuske, C.R. (2014). Common and distinguishing features of the bacterial and fungal communities in biological soil crusts and shrub root zone soils. *Soil Biol. Biochem.*, 69*,* 302-312

Stursova, M., Crenshaw, C.L. & Sinsabaugh, R.L. (2006). Microbial responses to long-term N deposition in a semiarid grassland. *Microb. Ecol.*, 51, 90–98

Teste, F.P., Karst, J., Jones, M.D., Simard, S.W. & Durall, D.M. (2006). Methods to control ectomycorrhizal colonization: effectiveness of chemical and physical barriers. *Mycorrhiza*, 17, 51–65

Thomey, M.L., Collins, S.L., Vargas, R., Johnson, J.E., Brown, R.F., Natvig, D.O. & Friggens, M. (2011). Effect of precipitation variability on net primary production and soil respiration in a Chihuahuan Desert grassland. *Glob. Chang. Biol.*, 17, 1505–1515

Van Wijk, M.T. (2011). Understanding plant rooting patterns in semi-arid systems: an integrated model analysis of climate, soil type and plant biomass. *Glob. Ecol. Biogeogr.*, 20, 331–342

Veluci, R.M., Neher, D.A. & Weicht, T.R. (2006). Nitrogen fixation and leaching of biological soil crust communities in mesic temperate soils. *Microb. Ecol.*, 51, 189–196

Vierheilig, H., Coughlan, A., Wyss, U. & Piche, Y. (1998). Ink and vinegar, a simple staining technique for arbuscular-mycorrhizal fungi. *Appl. Environ. Microbiol.*, 64, 5004–5007

Wallander, H., Nilsson, L.O., Hagerberg, D. & Bååth, E. (2001). Estimation of the biomass and seasonal growth of external mycelium of ectomycorrhizal fungi in the field. *New Phytol.*, 151, 753–760

Western Regional Climate Center. 2015. Local Climate Data Summaries. Retrieved from http://www.wrcc.dri.edu/cgi-bin/cliMAIN.pl?nm3031. 11/2/2016.

Wynia, R. (2007). Blue Grama Plant Guide. *USDA-NRCS*

Zhuang, W., Downing, A. & Zhang, Y. (2015). The influence of biological soil crusts on ^{15}N translocation in soil and vascular plant in a temperate desert of northwestern China. *J. Plant Ecol.*, 8, 420–428

Figures

Chapter 3 Figure 1. Biocrust chlorophyll *a* content means ± 95% *CI* by fungal connection (intact = gray symbol; impeded = black symbol) and precipitation regime (small, frequent *vs*. large, infrequent) from 2013-2015. Different letters within each level of precipitation regime (small, frequent = lowercase; large, infrequent = uppercase) indicate significant differences between fungal connection treatments at $P \leq 0.05$ (false discovery rate), and ´ following the letter indicates differences at $P \leq 0.10$.

Chapter 3 Figure 2. Biocrust scytonemin content means ± 95% *CI* by fungal connection (intact = gray symbol; impeded = black symbol) and precipitation regime (small, frequent *vs*. large, infrequent). Different letters within each level of precipitation regime (small, frequent = lowercase; large, infrequent = uppercase) indicate significant differences between fungal connection treatments at $P \leq 0.05$ (false discovery rate).

Chapter 3 Figure 3. Plant aboveground biomass 2013-2015 means ± 95% *CI* by fungal connection (intact = gray symbol; impeded = black symbol) and precipitation regime (small, frequent *vs*. large, infrequent). Different letters within each level of precipitation regime (small, frequent = lowercase; large, infrequent = uppercase) indicate significant differences between fungal connection treatments at $P \leq 0.05$ (false discovery rate).

Chapter 3 Figure 4. Total seed biomass 2014-2015 means ± 95% *CI* by fungal connection (intact = gray symbol; impeded = black symbol) and precipitation regime (small, frequent *vs*. large, infrequent). Different letters within each level of precipitation regime (small, frequent =

lowercase; large, infrequent = uppercase) indicate significant differences between fungal connection treatments at $P \leq 0.05$ (false discovery rate).

Chapter 3 Figure 5. Plant allocation patterns means ± 95% *CI* by fungal connection (intact = gray symbol; impeded = black symbol) and precipitation regime (small, frequent *vs*. large, infrequent) for A) root:total biomass and B) seed:total biomass. Different letters within each level of precipitation regime (small, frequent = lowercase; large, infrequent = uppercase) indicate significant differences between fungal connection treatments at $P \leq 0.05$ (false discovery rate), and ´ following the letter indicates differences at $P \leq 0.10$. For C) roots in the top 5cm sample:total biomass, different letters above bars indicate significant differences between fungal connection treatments across precipitation regime at $P \leq 0.05$ (false discovery rate).

Chapter 3 Figure 6. CN means ± 95% *CI* by fungal connection (intact = gray symbol; impeded = black symbol) and precipitation regime (small, frequent *vs*. large, infrequent) for plants and biocrusts. Different letters within each level of precipitation regime (small, frequent = lowercase; large, infrequent = uppercase) indicate significant differences between fungal connection treatments at $P \leq 0.05$ (false discovery rate), and ´ following the letter indicates differences at $P \leq 0.10$.

Chapter 3 Figure 7. CN_{EEA} means ± 95% *CI* by fungal connection (intact = gray symbol; impeded = black symbol) and precipitation regime (small, frequent *vs*. large, infrequent) as a measure of resource demand in microbial communities in the biocrust and rooting zone soil microsites. Different letters within each level of precipitation regime (small, frequent = lowercase; large, infrequent = uppercase) indicate significant differences between fungal connection treatments at $P \leq 0.05$ (false discovery rate).

Chapter 3 Figure 1

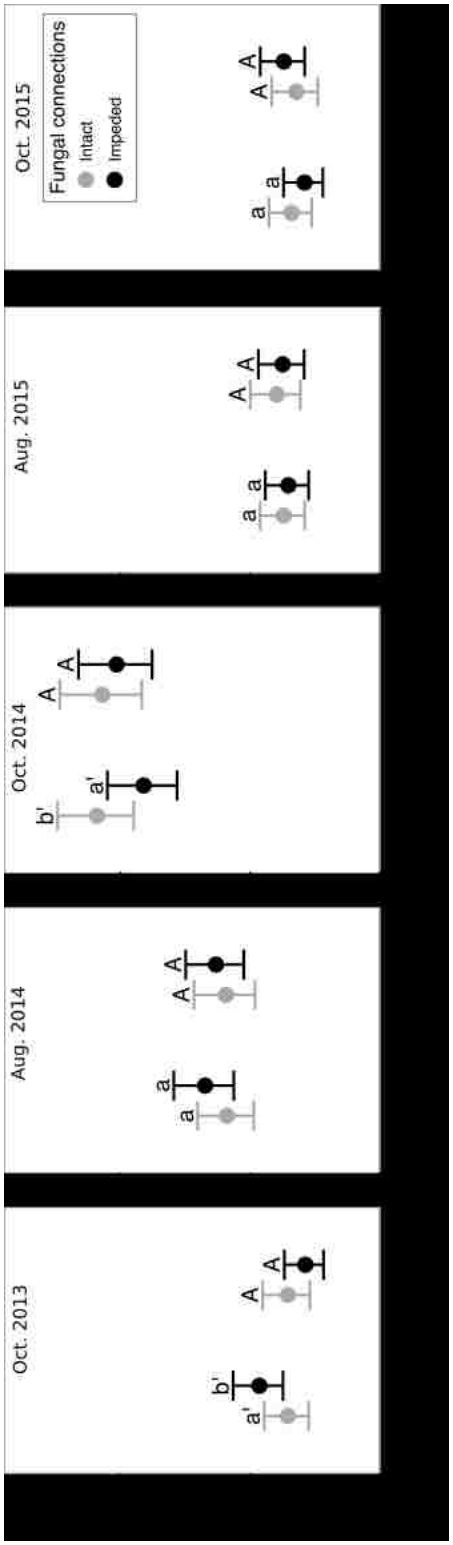

Chapter 3 Figure 2

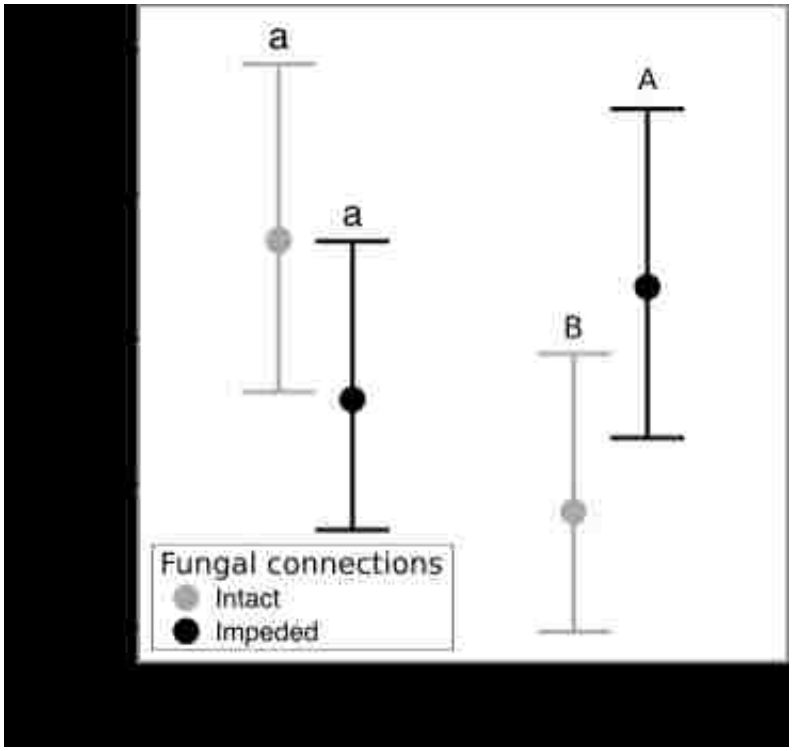

Chapter 3 Figure 3

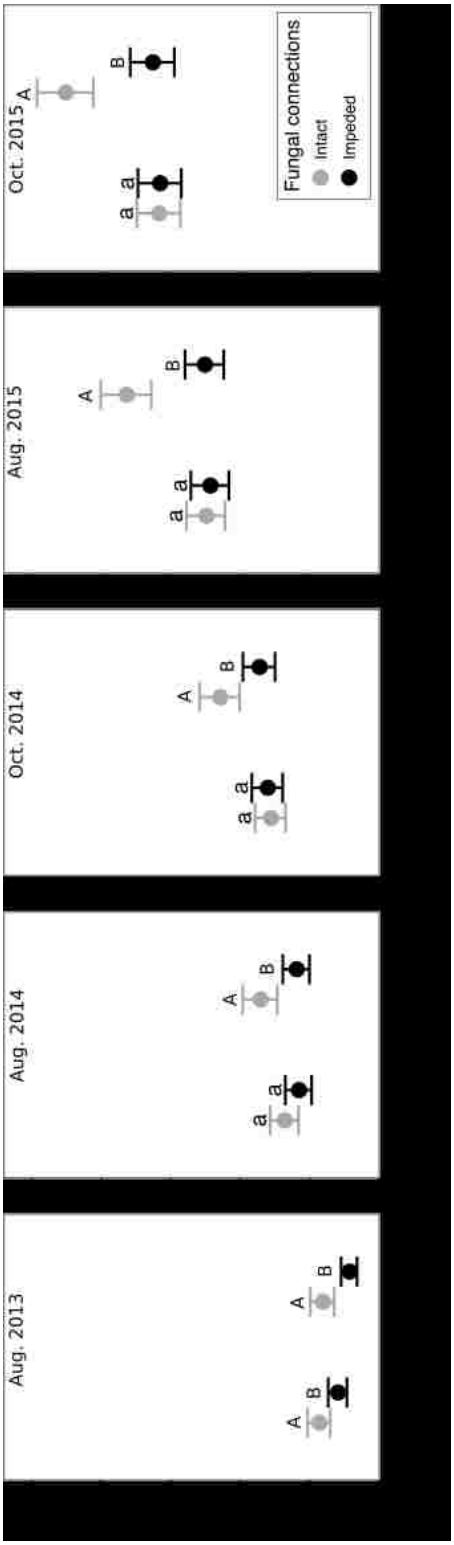

Chapter 3 Figure 4

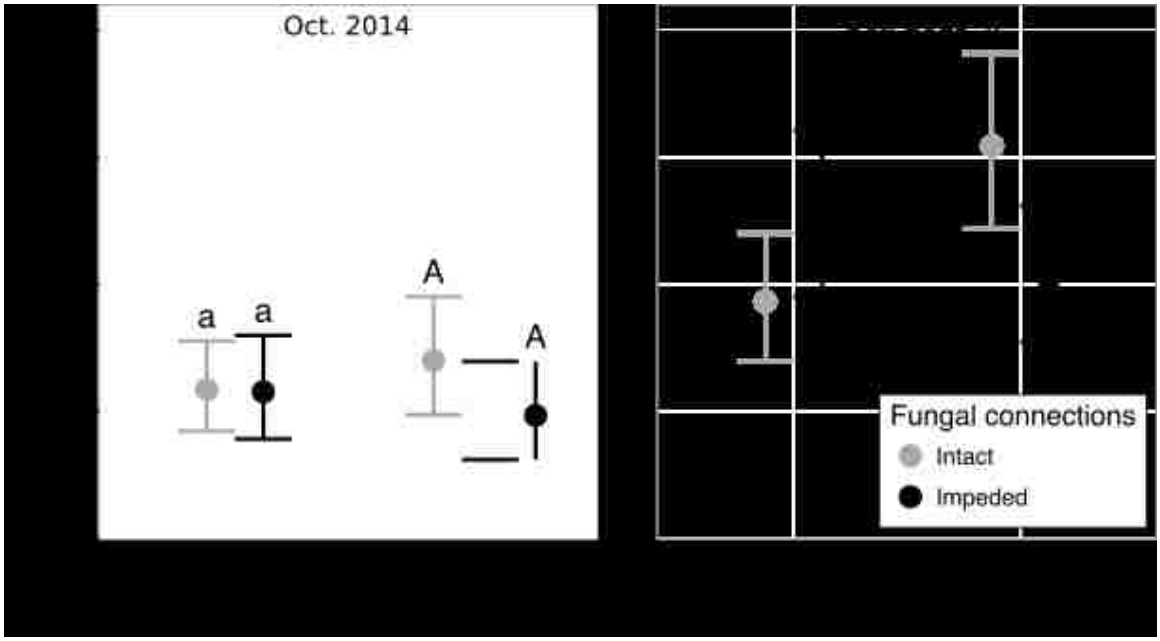

Chapter 3 Figure 5

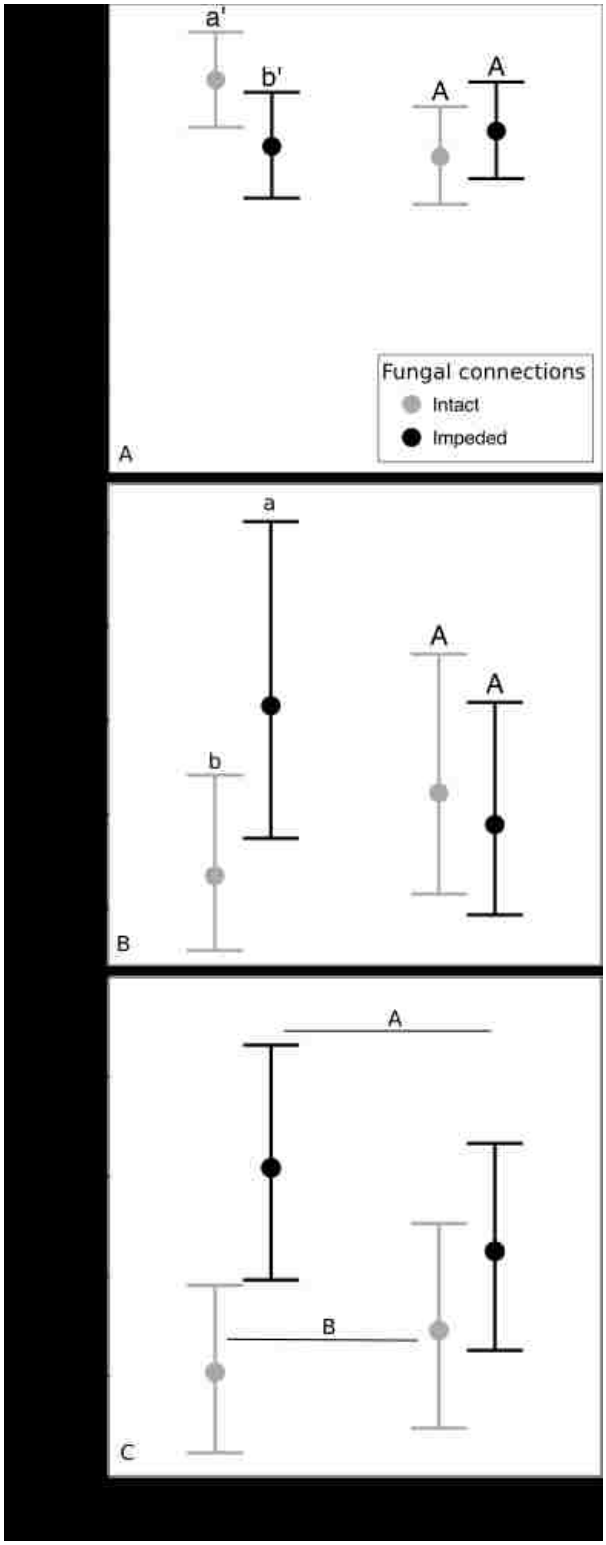

Chapter 3 Figure 6

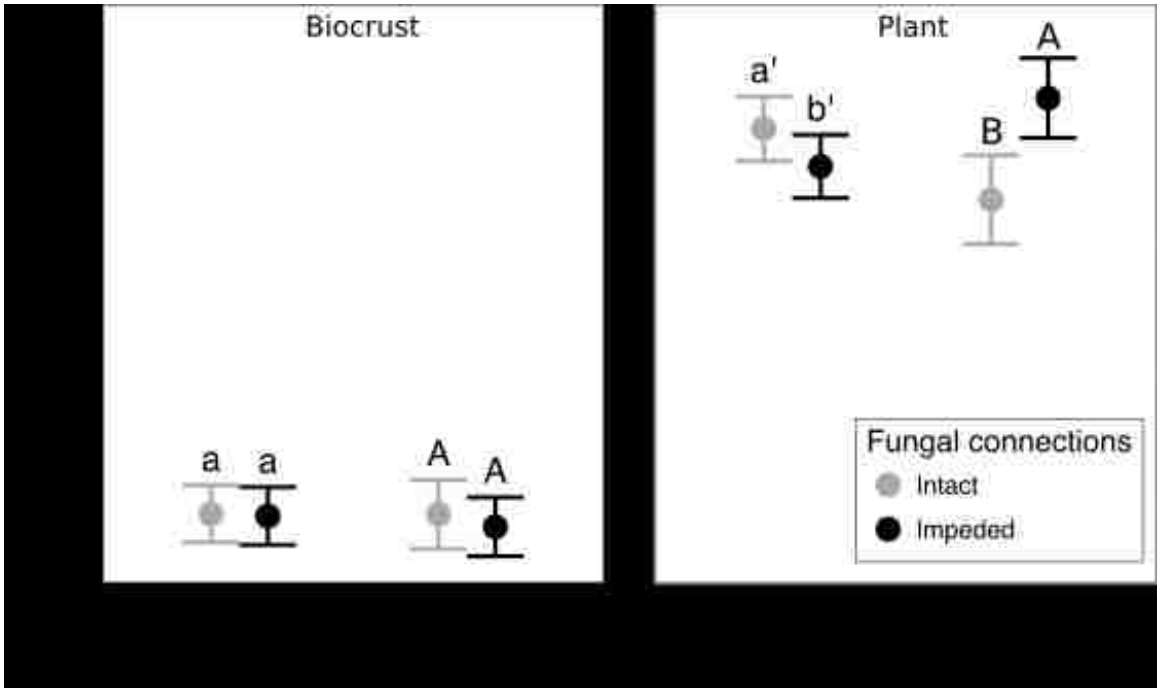

Chapter 3 Figure 7

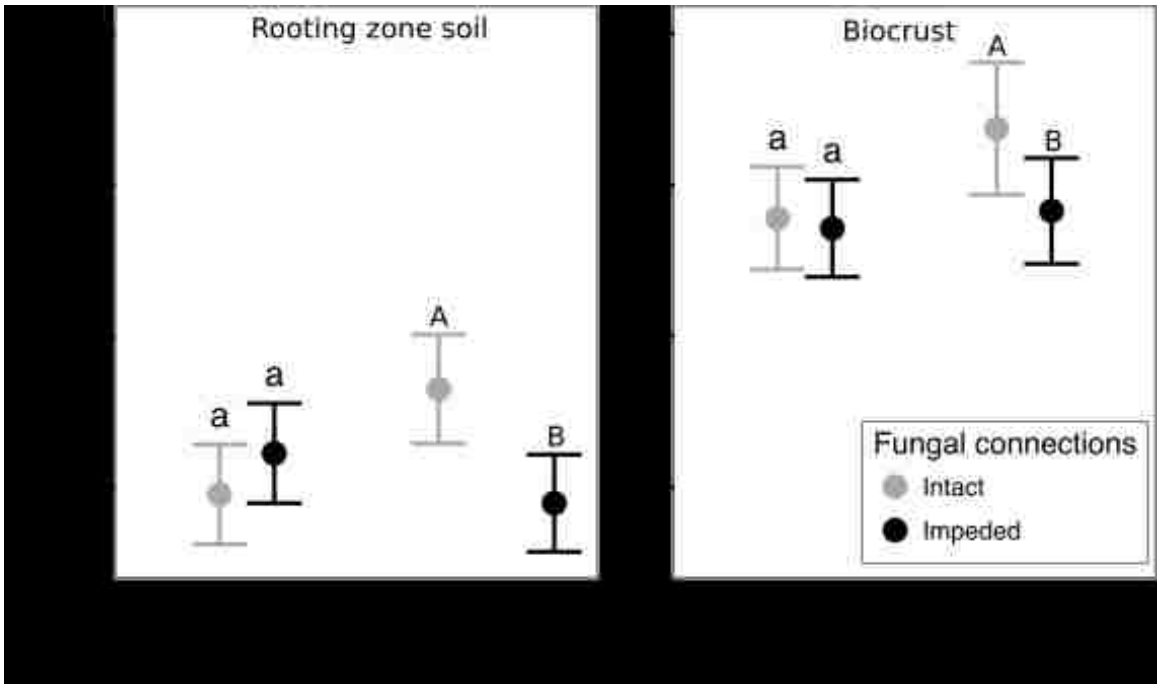

Tables

Chapter 3 Table 1. Results from general linear mixed effects and general linear models of fungal abundance by fungal connection and precipitation regime. Ergosterol was compared between two microsites, biocrust or rooting zone soil ($N = 154$) and each were run separately. Root colonization represented two morphotypes: dark septate or aseptate hyphae ($N = 142$), and each were run separately. Position in the planting grid (row, column) was retained in the model if $P \leq 0.1$. P-values ≤ 0.05 are shown in bold.

Chapter 3 Table 2. Results from general linear mixed effects and general linear models of biocrust performance by fungal connection and precipitation regime. Chlorophyll *a* was compared across five dates ($N = 382$) between 2014-2015. Oct. 2015 chlorophyll *a* and scytonemin results include any fungal abundance covariate retain after model selection. Position in the planting grid (row, column) was retained in the model if $P \leq 0.1$. P-values ≤ 0.05 are shown in bold.

Chapter 3 Table 3. Results from general linear mixed effects and general linear models of plant performance by fungal connection and precipitation regime. Multivariate ANOVA for root, aboveground, and seed biomass (centered and scaled) were run with pot as a random factor ($N = 212$). Aboveground biomass was compared across five dates (Aug. 2013, Aug. and Oct. 2014, Aug. and Oct. 2015, $N = 385$) and seed biomass was compared across two dates (Oct. 2014 and Oct. 2015, $N = 135$). Oct. 2015 results of total, root, and seed biomass included any fungal abundance covariate retained after model selection. Aboveground biomass (destructive) did not include a fungal abundance metric and thus we report the results of aboveground biomass (allometry). Position in the planting grid (row, column) was retained in the model if $P \leq 0.1$. P-values ≤ 0.05 are shown in bold.

Chapter 3 Table 4. Results from general linear models of plant allocation by fungal connection and precipitation regime. We analyzed root:total biomass, seed:total biomass, and root biomass in the top 5cm sample:total biomass. No fungal abundance covariates were included in the final models. Position in the planting grid (row, column) was retained in the model if $P \leq 0.1$. *P*-values ≤ 0.05 are shown in bold.

Chapter 3 Table 5. Results from general linear mixed effects and general linear models of resource content by fungal connection and precipitation regime. CN ($N = 118$) and CN_{EEA} (N = 140) were compared across microsites (biocrust, leaf, or rooting zone soil) and each were run separately. No fungal abundance covariates were retained after model selection for total nitrogen by mass in the plant + biocrust, biocrust or root CN, the difference in CN between plants and biocrusts, rooting zone soil or biocrust CN_{EEA}, or biocrust CUE. Position in the planting grid (row, column) was retained in the model if $P \leq 0.1$. *P*-values ≤ 0.05 are shown in bold.

Factor	*ln*(Ergosterol, µg g^{-1})		*ln*(Biocrust ergosterol + 0.1, µg g^{-1})		*ln*(Rooting zone soil ergosterol + 0.1, µg g^{-1})		*logit*(Root colonization)		*logit*(Aseptate hyphae)		*logit*(Dark septate hyphae)	
	X^2	*P*	$F_{1,73}$	*P*	$F_{1,72}$	*P*	X^2	*P*	$F_{1,66}$	*P*	$F_{1,67}$	*P*
Connection	0.01	0.92	0.007	0.93	0.32	0.57	4.61	**0.03**	2.16	0.15	0.65	0.42
Precipitation	7.84	**0.005**	4.53	**0.04**	0.14	0.71	7.97	**0.004**	5.38	**0.02**	0.54	0.46
Connection × Precipitation	0.005	0.94	0.001	0.97	0.004	0.95	4.44	**0.04**	1.92	0.17	0.04	0.84
Row	3.00	0.08			8.06	0.**006**						
Column									3.57	0.06		
	Microsite						Morphotype					
X = Additional factor	61.23	**<0.001**					0.60	0.44				
X × Connection	0.02	0.88					3.82	**0.05**				
X × Precipitation	4.50	**0.03**					2.96	0.08				
X × Connection × Precipitation	0.006	0.94					2.88	0.09				

Chapter 3 Table 2

	Performance		Fungal abundance covariance analyses			
	sqrt(Chl. *a* 2014-2015, μg g^{-1} soil)		*sqrt*(Chl. *a*, μg g^{-1} soil)		*sqrt*(Scytonemin, mg g^{-1} soil)	
Factor	X^2	*P*	$F_{1,72}$	*P*	$F_{1,42}$	*P*
Connection	2.96	0.08	1.12	0.29	5.18	**0.03**
Precipitation	0.00	0.99	0.31	0.58	2.81	0.10
Connection × Precipitation	4.10	**0.04**	2.41	0.12	7.46	**0.01**
	Date				Dark septate hyphae	
X = Additional factor	173.1	**<0.001**			0.87	0.36
X × Connection	11.41	**0.02**			3.45	0.07
X × Precipitation	0.42	0.98			0.16	0.69
X × Connection × Precipitation	8.80	0.07			3.40	0.07

	Performance						Fungal abundance covariance analyses					
	MANOVA (scaled root, aboveground, and seed biomass)		*sqrt*(Aboveground biomass 2013-2015, g)		*sqrt*(Seed biomass. 2014-2015, g)		*ln*(Total biomass, g)		*ln*(Root biomass, g)		*sqrt*(Seed biomass, g)	
Factor	X^2	*P*	X^2	*P*	X^2	*P*	$F_{1,47}$	*P*	$F_{1,59}$	*P*	$F_{1,54}$	*P*
Connection	0.62	0.43	6.71	0.01	0.004	0.95	0.08	0.77	1.03	0.31	0.04	0.85
Precipitation	9.92	**0.002**	0.18	0.67	0.65	0.42	1.29	0.26	0.05	0.82	1.57	0.22
Connection × Precipitation	8.01	**0.005**	1.02	0.31	1.07	0.30	2.76	0.10	0.003	0.95	0.14	0.71
Row			2.96	0.08								
Column					4.04	**0.04**			3.23	0.08	5.61	**0.02**
	Response variable		Date		Year		Dark septate hyphae		Dark septate hyphae		Rooting zone ergosterol	
X = Additional factor	0.04	0.98	481.57	**<0.001**	8.51	0.003	3.69	0.06	5.81	**0.02**	5.61	**0.02**
X × Connection			11.04	0.03	2.38	0.12	0.12	0.72	0.51	0.48	0.74	0.39
X × Precipitation			46.26	**<0.001**	3.95	**0.05**	0.07	0.80	0.75	0.39	12.71	**0.001**
X × Connection × Precipitation			10.42	**0.03**	2.76	0.10	0.69	0.41	0.22	0.64	3.14	0.08

Chapter 3 Table 4

Factor	Fungal abundance covariance analyses					
	logit(Root:total biomass)		*logit*(Seed: total biomass)		*ln*(Roots in top 5cm sample:total biomass + 0.01)	
	$F_{1,57}$	P	$F_{1,57}$	P	$F_{1,41}$	P
Connection	3.43	0.07	4.18	**0.04**	8.35	**0.006**
Precipitation	4.98	**0.03**	1.34	0.25	0.05	0.82
Connection × Precipitation	3.40	0.07	3.06	0.08	1.44	0.24
Row					7.85	**0.01**
Column					10.75	**0.002**

	Resource Content				Fungal abundance covariance analyses													
	Plant & biocrust CN		Biocrust & rooting zone soil CN_{EEA}		Total N		Biocrust CN		*Plant CN*		Plant CN-biocrust CN		Rooting zone soil CN_{EEA}		Biocrust CN_{EEA}		CUE	
Factor	X^2	*P*	X^2	*P*	$F_{1,39}$	*P*	$F_{1,65}$	*P*	$F_{1,44}$	*P*	$F_{1,39}$	*P*	$F_{1,64}$	*P*	$F_{1,55}$	*P*	$F_{1,60}$	*P*
Connection	0.01	0.91	1.33	0.25	1.35	0.25	0.15	0.70	1.89	0.17	0.99	0.32	1.86	0.18	0.02	0.88	0.04	0.84
Precipitation	0.001	0.98	7.96	**0.005**	1.48	0.23	0.001	0.98	3.71	0.06	1.34	0.25	5.80	**0.02**	6.60	**0.01**	2.62	0.11
Connection × Precipitation	0.11	0.74	9.15	**0.002**	0.16	0.69	1.24	0.27	7.98	**0.01**	5.26	**0.03**	7.00	0.01	4.25	**0.04**	2.01	0.16
Column	5.03	**0.02**							3.73	0.06					5.01	**0.03**		
	Microsite		Microsite															
X = Additional factor	356.06	**<0.001**	58.25	**<0.001**														
X × Connection	1.55	0.21	1.03	0.31														
X × Precipitation	4.27	**0.04**	0.08	0.78														
X × Connection × Precipitation	10.57	**0.001**	1.20	0.27														

Supplementary Material

Chapter 3 Appendix 1. Water chemistry of well water used for precipitation regime treatments (from University of New Mexico Analytical Chemistry Laboratory).

Analyte	Concentration (ppm)
Al	0.017
As	-0.012
B	0.54
Ba	0.025
Be	-0.044
Ca	43.64
Cd	-0.046
Co	0.95
Cr	-0.021
Cu	0.008
Fe	-0.034
K	10.38
Li	0.18
Mg	4.22
Mn	-0.041
Mo	-0.002
Na	163.20
Ni	-0.034
Pb	-0.017
Se	-0.13
Si	30.05
Sr	0.84

Analyte	Concentration (ppm)
V	-0.009
Zn	-0.044

Chapter 3 Appendix 2. Analyses for roots above the mesh in 2015.

Chapter 3 Appendix 2 Table 1. Results from general linear mixed effects and general linear models of root biomass and fungal abundance that grew above the mesh in 2015 by fungal connection and precipitation regime. Total root biomass above the mesh, root biomass above the mesh/total root biomass, and root biomass in biocrust soil core (2.54cm diameter) was compared. Colonization of root above the mesh was compared by two morphotypes: dark septate or aseptate hyphae ($N = 110$) and each response is analyzed separately. Position in the planting grid (row, column) is included in all models. P-values ≤ 0.05 are shown in bold.

Factor	*ln*(Root biomass above mesh, g)		*logit*(Roots above mesh:root biomass)		*ln*(Root biomass in biocrust, g + 0.01)		*logit*(Hyphal colonization above mesh)		*logit*(Aseptate hyphae)		*logit*(Dark septate hyphae)	
	$F_{1,47}$	P	$F_{1,46}$	P	$F_{1,54}$	P	X^2	P	$F_{1,49}$	P	$F_{1,49}$	P
Connection	0.14	0.71	5.11	**0.03**	0.16	0.69	1.95	0.16	2.71	0.11	1.23	0.27
Precipitation	2.40	0.13	2.07	0.16	0.01	0.92	0.23	0.63	0.37	0.54	4.32	**0.04**
Connection × Precipitation	0.24	0.62	0.13	0.72	0.44	0.51	0.02	0.89	0.008	0.92	6.52	**0.01**
Row	3.25	0.08	8.45	0.55	0.39	0.53	0.06	0.81	0.22	0.64	0.004	0.95
Column	2.05	0.16	0.13	0.72	1.81	0.18	0.05	0.83	0.03	0.86	0.18	0.67
							Morphotype					
X = Additional factor							48.4	**<0.001**				
X × Connection							3.45	0.06				
X × Precipitation							3.97	**0.05**				
X × Connection × Precipitation							3.85	**0.05**				

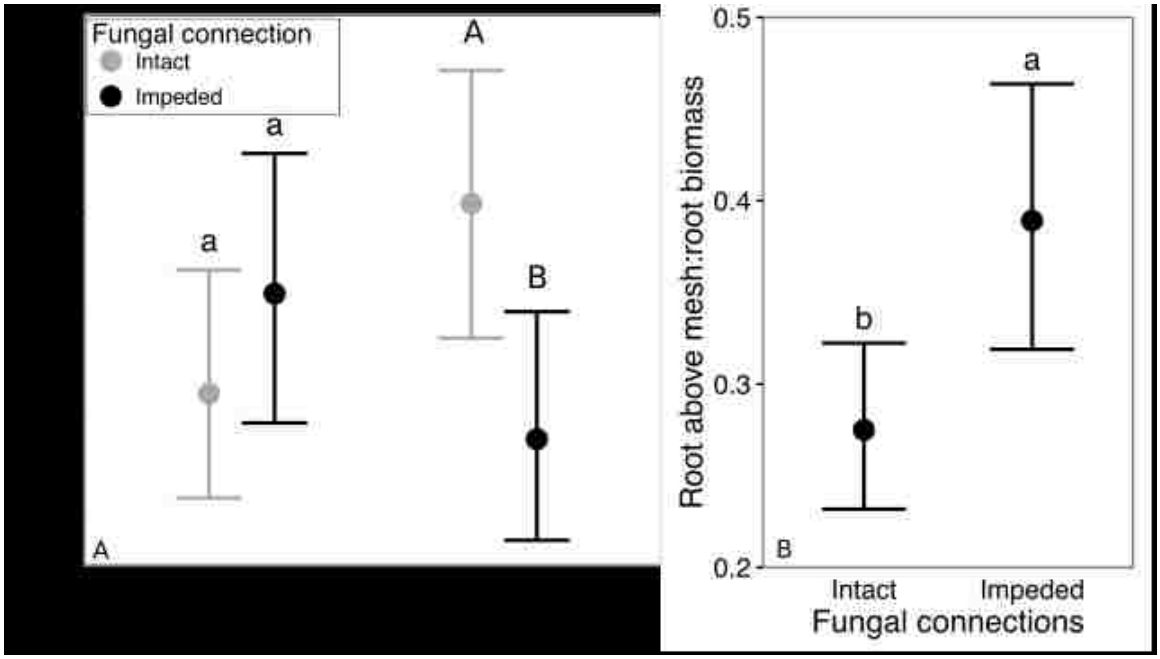

Chapter 3 Appendix 2 Figure 1. A) Dark septate hyphal colonization in roots above mesh by precipitation regime and fungal connection. Different letters within each level of precipitation regime (small, frequent = lowercase; large, infrequent = uppercase) indicate significant differences between fungal connection treatments at $P \leq 0.05$ (false discovery rate). B) Proportion of roots above mesh to total root biomass by fungal connection. Different letters indicate significant differences between fungal connection treatments at $P \leq 0.05$ (false discovery rate).

Chapter 3 Appendix 3. Results from general linear models of soil moisture following natural rain event by fungal connection. Position in the planting grid (row, column) is included in all models. *P*-values ≤ 0.05 are shown in bold.

Factor	*ln*(Soil moisture after natural rain event, %)	
	$F_{1,73}$	*P*
Connection	2.39	0.13
Row	1.55	0.22
Column	1.25	0.27

Chapter 3 Appendix 4. Results from general linear models of difference in soil moisture (8 hours after-before) watering event by fungal connection and precipitation regime. Position in the planting grid (row, column) is included in all models. *P*-values ≤ 0.05 are shown in bold.

Factor	*sqrt*(Soil moisture after watering, %)	
	$F_{1,71}$	*P*
Connection	0.05	0.82
Precipitation	51.6	**<0.001**
Connection × Precipitation	0.18	0.67
Row	0.67	0.41
Column	3.87	**0.05**

Chapter 3 Appendix 5. Fungal abundance by treatments and correlations among metrics.

Chapter 3 Appendix 5 Table 1. Results from general linear mixed effects and general linear models of fungal abundance by fungal connection and precipitation regime. Ergosterol was compared between two microsites, biocrust or rooting zone soil ($N = 154$) and each were run separately. Root colonization represented two morphotypes: dark septate or aseptate hyphae ($N = 142$) and each were run separately. Position in the planting grid (row, column) is included in all models. P-values ≤ 0.05 are shown in bold.

Factor	*ln*(Ergosterol, µg g^{-1} soil)		*ln*(Biocrust ergosterol + 0.1, µg g^{-1} soil)		*ln*(Rooting zone soil ergosterol +0.1, µg g^{-1} soil)		*logit*(Root colonization)		*logit*(Aseptate hyphae)		*logit*(Dark septate hyphae)	
	X^2	*P*	$F_{1,71}$	*P*	$F_{1,71}$	*P*	X^2	*P*	$F_{1,65}$	*P*	$F_{1,65}$	*P*
Connection	0.01	0.90	0.004	0.95	0.45	0.50	3.84	**0.05**	2.14	0.15	0.55	0.46
Precipitation	7.81	**0.005**	4.43	**0.04**	0.10	0.75	7.73	**0.005**	5.30	**0.02**	0.55	0.46
Connection × Precipitation	0.002	0.97	0.004	0.95	0.04	0.84	3.58	0.06	1.90	0.17	0.02	0.88
Row	3.01	0.08	0.48	0.49	8.34	0.005	0.01	0.91	0.008	0.93	0.04	0.85
Column	0.03	0.85	0.004	0.95	0.41	0.52	1.92	0.17	3.46	0.07	0.04	0.84
	Microsite						Morphotype					
X = Additional factor	136.2	**<0.001**					0.60	0.44				
X × connection	0.02	0.87					3.82	**0.05**				
X × precipitation	4.47	**0.03**					2.95	0.08				
X × connection × precipitation	0.006	0.94					2.88	0.09				

Chapter 3 Appendix 5 Table 2. Spearman correlations between fungal abundance metrics.

	Biocrust ergosterol			Dark septate hyphae			Aseptate hyphae		
	rho	*S*	*P*	*rho*	*S*	*P*	*rho*	*S*	*P*
Rooting zone ergosterol	0.01	75435	0.94	0.08	54933	0.51	-0.005	59944	0.97
Dark septate hyphae	0.03	58078	0.83				-0.04	62072	0.74
Aseptate hyphae	-0.01	60160	0.94						

Chapter 3 Appendix 5 Figure 1. Fungal abundance means ± 95% *CI* by fungal connection (intact = gray symbol; impeded = black symbol) and precipitation regime (small, frequent *vs*. large, infrequent). A) Ergosterol content by microsite (biocrust vs. rooting zone soil). B) Root colonization by morphotype. Different letters within each level of precipitation regime (small, frequent = lowercase; large, infrequent = uppercase) indicate significant differences between fungal connection treatments at $P \leq 0.05$ (false discovery rate).

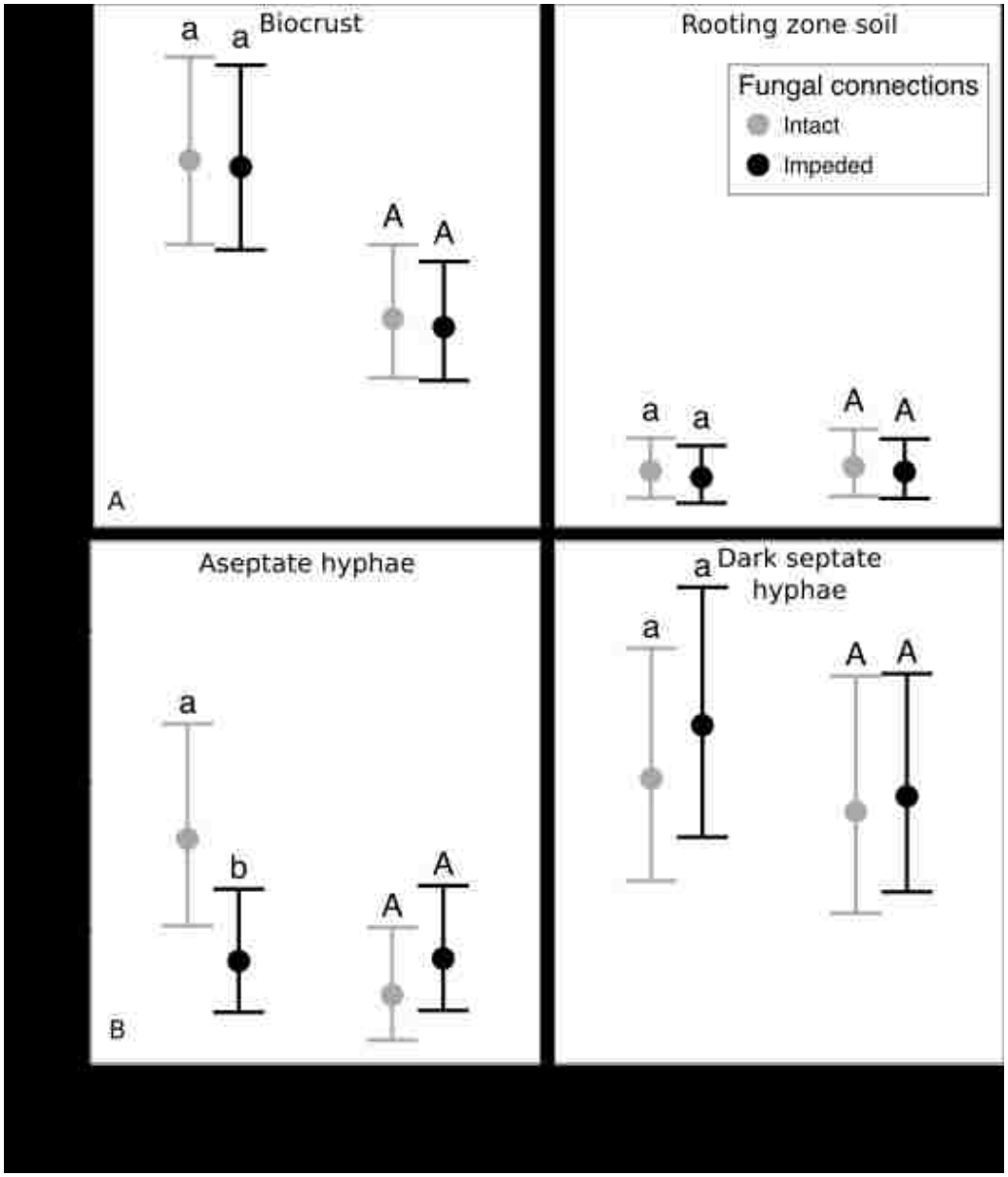

Chapter 3 Appendix 6. Biocrust performance.

Chlorophyll *a* content varied considerably year-to-year and in 2014 was ~120% higher than in 2013 or 2015. Within 2014, chlorophyll *a* content was 60% higher in Oct. than Aug. Biocrust chlorophyll *a* content did not differ between Aug. and Oct. 2015 (t_{322} = 1.5, P = 0.43).

Chapter 3 Appendix 6 Table 1. Results from general linear mixed effects and general linear models of biocrust performance by fungal connection and precipitation regime treatments. Chlorophyll *a* was compared across five dates (N = 382). Additional factors include fungal abundance covariates for chlorophyll *a* and scytonemin in 2015. Position in the planting grid (row, column) was retained in all models. P-values ≤ 0.05 are shown in bold.

	Performance		Fungal abundance covariance analyses			
	sqrt(Chlorophyll *a* 2013-2015, µg g^{-1})		*sqrt*(Chlorophyll *a*, µg g^{-1})		*sqrt*(Scytonemin, mg g^{-1})	
Factor	X^2	P	$F_{1,70}$	P	$F_{1,41}$	P
Connection	3.25	0.07	1.05	0.31	3.90	0.06
Precipitation	0.003	0.99	0.30	0.59	2.42	0.13
Connection × Precipitation	4.51	**0.03**	2.25	0.14	5.48	**0.02**
Row	1.15	0.28	0.17	0.68	4.26	**0.04**
Column	0.47	0.49	0.000	0.99	0.08	0.78
	Date				Dark septate hyphae	
X = Additional factor	173.1	**<0.001**			0.92	0.34
X × Connection	11.40	**0.02**			2.61	0.11
X × Precipitation	0.42	0.98			0.10	0.75
X × Connection × Precipitation	8.81	0.07			2.45	0.12

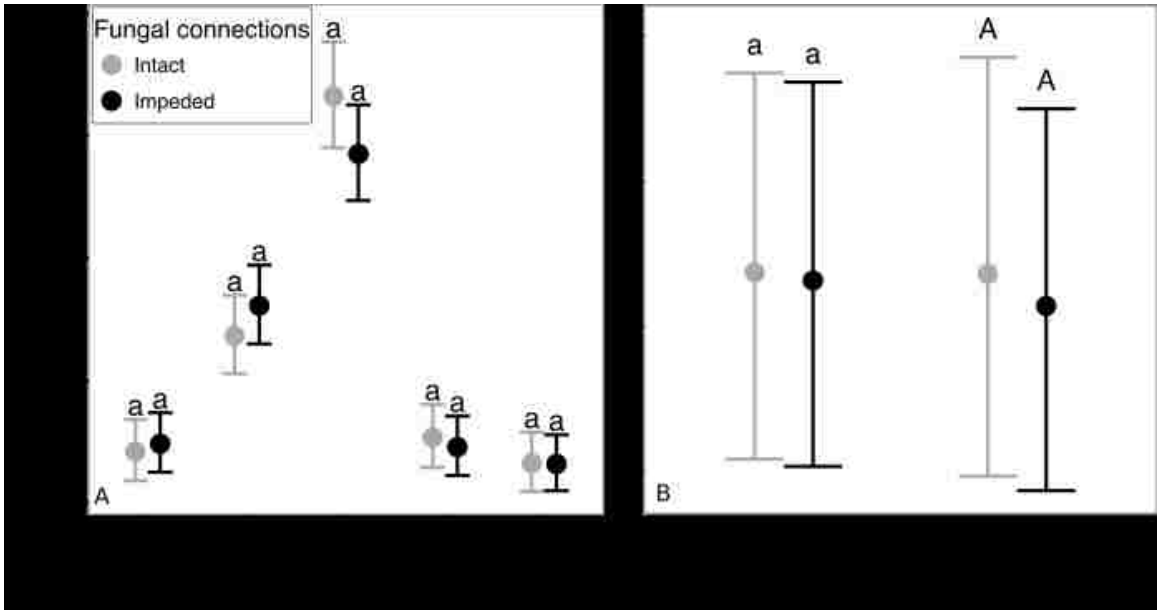

Chapter 3 Appendix 6 Figure 1. Biocrust chlorophyll *a* means ± 95% *CI* by fungal connection (intact = gray symbol; impeded = black symbol). A) Chlorophyll *a* by date (October 2013-October 2015) and connection. Different letters indicate differences between fungal connection treatments within dates at $P \leq 0.05$ (false discovery rate). B) Chlorophyll *a* by connection and precipitation averaged across dates. Different letters within each level of precipitation regime (small, frequent = lowercase; large, infrequent = uppercase) indicate significant differences between fungal connection treatments at $P \leq 0.05$ (false discovery rate).

Chapter 3 Appendix 7. Model selection results (*K* and *AICc* values) alternative models with no fungal abundance metrics (*k* = 7) or fungal abundance metrics fulling interacting with fungal connection and precipitation regime (k = 11) in biocrust performance, plant performance and allocation, and resource content models. The lowest *AICc* value for each response variable are shown in bold and values with delta = 2 of lowest value are shown in italics.

		None	Rooting zone ergosterol	Biocrust ergosterol	Dark septate hyphae	Aseptate hyphae
Biocrust performance	*sqrt*(Chlorophyll *a,* µg g^{-1})	**139.6**	142.4	145.1	141.1	149.5
	sqrt(Scytonemin, mg g^{-1})	35.1	44.5	42.9	**32.9**	44.3
Plant performance	*ln*(Total biomass, g)	**62.9**	*61.6*	68.2	*61.2*	72.7
	sqrt(Aboveground biomass g)	**186.4**	194.7	193.8	192.2	194.5
	n(Root biomass, g)	97.9	104.1	102.2	**95.0**	106.4
	sqrt(Seed biomass, g)	44.4	**40.4**	46.6	47.0	53.4
Plant allocation	*sqrt*(Root:total biomass)	**86.1**	95.7	96.0	93.8	96.0
	sqrt(Seed:total biomass)	**122.5**	123.7	122.6	131.0	132.2
	ln(Roots in top 5cm sample:total biomass + 0.01)	**-33.3**	-21.3	-26.0	-27.9	-21.4
	SLA (g cm^{-2})	**-358.8**	-349.5	-353.8	-352.3	-350.1
Resource content	Total N	**-10.3**	1.4	-1.0	0.9	-0.5
	Plant CN	**223.1**	233.4	232.1	225.1	231.1
	Biocrust CN	**243.3**	250.2	250.0	250.4	253.1
	Plant CN – Biocrust CN	**210.5**	220.1	217.5	222.1	222.3
	Rooting zone soil CN_{EEA}	**-36.7**	-27.3	-27.1	-28.2	-26.7
	Biocrust CN_{EEA}	**-26.1**	-20.2	-20.1	-15.5	-20.2
	CUE	**-246.1**	-241.8	-240.3	-212.6	-219.5

Chapter 3 Appendix 8. Results from general linear mixed effects and general linear models of plant performance by fungal connection and precipitation regime. Total biomass includes roots, aboveground, and seeds. Repeated measures analysis of variance with pot as a random effect was used for root, aboveground, and seed biomass (centered and scaled) because they were expected to be correlated (N = 212), and each response was also analyzed separately. Finally, we analyzed aboveground biomass across multiple dates (N = 385) and seed biomass between 2014 and 2015 (N = 135). Position in the planting grid (row, column) were retained in all models. P-values ≤ 0.05 are shown in bold.

	Performance						Fungal abundance covariance analyses							
	MANOVA (scaled root, aboveground, and seed biomass)		*sqrt*(Aboveground biomass 2013-2015, g)		*sqrt*(Seed biomass 2014-2015, g)		*ln*(Total, g)		*sqrt*(Aboveground biomass, g)		*ln*(Root biomass, g)		*sqrt*(Seed biomass, g)	
Factor	X^2	*P*	X^2	*P*	X^2	*P*	$F_{1,45}$	*P*	$F_{1,69}$	*P*	$F_{1,58}$	*P*	$F_{1,53}$	*P*
Connection	0.29	0.59	7.37	0.007	0.003	0.96	0.03	0.85	1.16	0.28	1.12	0.30	0.01	0.93
Precipitation	9.77	**0.002**	0.22	0.63	0.70	0.40	0.39	0.54	13.66	**0.004**	0.17	0.68	1.70	0.20
Connection × Precipitation	6.70	**0.01**	0.70	0.40	1.05	0.30	0.84	0.36	8.86	**0.004**	0.02	0.88	6.97	**0.01**
Row	2.58	0.11	3.40	0.06	2.57	0.11	2.00	0.16	3.34	0.07	1.31	0.26	1.59	0.21
Column	2.19	0.13	0.96	0.34	4.89	**0.03**	2.42	0.13	0.11	0.73	3.53	0.06	4.00	0.05
	Response Variable		Date		Year		Dark septate hyphae				Dark septate hyphae		Rooting zone ergosterol	
X = Additional factor	0.07	0.96	481.6	**<0.001**	8.77	0.003	5.24	**0.03**			6.18	**0.01**	6.97	**0.01**
X × Connection			11.04	**0.03**	2.63	0.10	0.01	0.94			0.54	0.46	0.63	0.43
X × Precipitation			46.25	**<0.001**	3.87	**0.05**	0.61	0.44			1.05	0.31	13.35	**<0.001**
X × Connection × Precipitation			10.42	**0.03**	3.07	0.08	0.02	0.88			0.32	0.57	2.79	0.10

Chapter 3 Appendix 9. Results from general linear models of plant allocation by fungal connection and precipitation regime. We analyzed root:total biomass, seed:total biomass, and roots in top 5cm sample:total biomass. No fungal covariates were included in the final models. Position in the planting grid (row, column) was retained in all models. *P*-values ≤ 0.05 are shown in bold.

	Fungal abundance covariance analyses							
	logit(Root:total biomass)		*sqrt*(Seed biomass:total biomass)		*ln*(Roots in top 5cm sample:total biomass + 0.01)		SLA (g cm^{-2})	
Factor	$F_{1,55}$	*P*	$F_{1,55}$	*P*	$F_{1,41}$	*P*	$F_{1,65}$	*P*
Connection	5.26	**0.03**	3.99	**0.05**	8.35	**0.006**	0.26	0.61
Precipitation	5.45	**0.02**	1.36	0.25	0.05	0.82	0.02	0.88
Connection × Precipitation	5.29	**0.03**	2.90	0.09	1.44	0.24	0.79	0.38
Row	1.99	0.16	0.35	0.55	7.85	**0.01**	0.004	0.95
Column	1.47	0.23	0.30	0.58	10.75	**0.002**	0.67	0.42

Chapter 3 Appendix 10. Results from general linear mixed effects and general linear models of resource content by fungal connection and precipitation regime. In the plant and biocrust microsites, total nitrogen by mass in the plant + biocrust, CN ratio by microsite ($N = 118$), and the difference in CN between plants and biocrusts were compared. In the biocrust and rooting zone microsites, resource demand (CN_{EEA}) was compared by microsite ($N = 140$). In the biocrust microsite, carbon use efficiency was compared by treatments. Position in the planting grid (row, column) was retained in the model if $P \leq 0.1$. *P*-values ≤ 0.05 are shown in bold.

	Resource Content				Fungal abundance covariance analyses													
	Plant & biocrust CN		Biocrust & rooting zone soil CN_{EEA}		Total N (g)		Biocrust CN		Plant CN		Plant CN-biocrust CN		Rooting zone soil CN_{EEA}		Biocrust CN_{EEA}		CUE	
Factor	X^2	P	X^2	P	$F_{1,37}$	P	$F_{1,63}$	P	$F_{1,43}$	P	$F_{1,37}$	P	$F_{1,54}$	P	$F_{1,62}$	P	$F_{1,58}$	P
Connection	0.01	0.91	1.45	0.23	0.69	0.41	0.01	0.91	1.72	0.20	1.31	0.26	0.01	0.93	1.44	0.23	0.001	0.97
Precipitation	0.001	0.97	8.02	**0.005**	1.35	0.25	0.0004	0.98	3.28	0.08	1.15	0.29	6.24	**0.02**	5.62	**0.02**	2.86	0.10
Connection × Precipitation	0.09	0.76	9.35	**0.002**	0.43	0.51	0.67	0.42	8.10	**0.01**	5.99	**0.02**	4.13	**0.05**	5.98	**0.02**	2.58	0.11
Row	0.67	0.41	0.29	0.59	0.27	0.60	0.08	0.78	0.97	0.33	0.83	0.36	1.38	0.25	0.01	0.92	0.89	0.35
Column	4.50	0.03	0.20	0.65	1.86	0.18	2.68	0.11	3.47	0.07	0.61	0.44	4.30	0.04	0.41	0.52	0.44	0.51
	Microsite		Microsite															
X = Additional factor	349.4	**<0.001**	57.70	**<0.001**														
X × Connection	1.43	0.23	1.02	0.31														
X × Precipitation	4.03	**0.04**	0.07	0.78														
X × Connection × Precipitation	10.39	**0.001**	1.15	0.28														